ASSESSMENT OF EFFECTIVE R-VALUE OF BUILDING ENVELOPE USING HIGH DEFINITION THERMAL IMAGING TECHNIQUE

BY

MOHAMMED ABDUL WAHEED KHAN

A Thesis Presented to the

DEANSHIP OF GRADUATE STUDIES

KING FAHD UNIVERSITY OF PETROLEUM & MINERALS

DHAHRAN, SAUDI ARABIA

In Partial Fulfillment of the
Requirements for the Degree of

MASTER OF SCIENCE

In

ARCHITECTURAL ENGINEERING

May 2011

KING FAHD UNIVERSITY OF PETROLEUM & MINERALS

DHAHRAN, SAUDI ARABIA

DEANSHIP OF GRADUATE STUDIES

This thesis, written by ***MOHAMMED ABDUL WAHEED KHAN*** under the direction of his thesis advisor and approved by his thesis committee, has been presented to and accepted by the Dean of Graduate Studies, in partial fulfilment of the requirements for the degree of **MASTER OF SCIENCE in ARCHITECTURAL ENGINEERING.**

Thesis Committee

Adel Abdou 16/05/2011

.....

Dr. Adel. A. Abdou (Thesis Advisor)

.....

Dr. Ismail M. Budaiwi (Member)

16/5/11

.....

Dr. Mohammed S. Al-Homoud (Member)

7/11

.....

Dr. Naser A. Al-Shayea

(Department Chairman)

.....

Dr. Salam A. Zummo

(Dean of Graduate Studies)

28/5/11

.....

Date

عمادة الدراسات العليا

DEANSHIP OF GRADUATE STUDIES

ACKNOWLEDGMENT

In the name of Allah, the Most Gracious and the Most Merciful

All praise and glory are due to Almighty Allah (SWT), to him belongs the sovereignty of the heavens and the earth. I am grateful to Allah for all his favors on me since my birth, these blessings are indeed innumerable, and the greatest of His bounties on me is being a Muslim. Peace and blessings of Allah be upon the noblest of mankind, Muhammad (Peace Be upon Him), his household, his companions and the generality of the true believers to the last day.

I would like to thank my beloved parents, beloved grandparents, aunties, uncles, my brothers, cousins and all my family members for their moral support throughout my academic career. I would never have been able to pursue this without their prayers, cooperation, understanding, patience, guidance, and support.

I would like to express my profound gratitude and appreciation to my thesis committee chairman Dr. Adel A. Abdou for his support, intellectual guidance, suggestions, advice, and readiness to assist during this research. His extensive knowledge, patience, and experience made it possible to shape the thesis. He was always available when I needed him and he answered all my questions, at any time of the day. I am also grateful to my thesis committee members, Dr. Ismail M. Budaiwi and Dr Mohammed S. Al-Homoud for their support, guidance, suggestions, and advice. Thanks are also due to the department's chairman Dr. Naser Al –Shayea and his secretary Mr. Iqbal ghani for their support and to the staff members of the department who has helped me directly or indirectly during this work, specially to Er Sardar sharieff.

I would like to acknowledge the support and facilities provided by King Fahd University of Petroleum and Minerals. I would like also to acknowledge the staff members for their kind support and continuous cooperation. Moreover, I would like to express my deepest thanks to every instructor who contributed in building my knowledge and experience. Thanks are also due to faculty and staff members of the Architectural Engineering Department for their cooperation.

Special thanks are due to my friends and colleagues who made my stay at the university a precious and an unforgettable era. I would like to make special thanks to my brother Mohammed Abdul Khadir Khan Asif and my friends Kareem bhai, Malik bhai, Najid bhai, Riyaz bhai, Ibrahim, Khadar bhai, Touseef, Rizwan bhai, Zubair, Thabreez, Minhaj, Aqeel, Afzal, Jibran, Rizwan, Fasi, Subhan, Ashraf, Zabi, Waseem bhai, Sarfaraz bhai, Khalil bhai, Nasar bhai, Faizan bhai, Safdar bhai, Naseer, Moin and Masood. Last but not least I would like to thank everybody who contributed to this achievement in a direct or an indirect way.

TABLE OF CONTENT

LIST OF TABLES

LIST OF FIGURES

THESIS ABSTRACT

NAME: MOHAMMED ABDUL WAHEED KHAN
TITLE: ASSESSMENT OF EFFECTIVE R-VALUE OF BUILDING ENVELOPE USING HIGH DEFINITION THERMAL IMAGING TECHNIQUE
DEPARTMENT: ARCHITECTURAL ENGINEERING
DATE: May 2011

Infrared thermography is an important and powerful technique for diagnostics and evaluation of building envelope, in terms of locating thermal bridges, damaged thermal insulation, air leakage, moisture damage, and cracks, all of which contribute to an increase in the energy consumption of the buildings. This is because typically the thermal gains or losses in practice are greater than those estimated during the design stage. Accurate and detailed information of where a problem occurs can reveal the source of the problem thus avoiding extensive renovation work and hence decreasing the cost of repair work and potential energy savings can be achieved. The present study is aimed at assessing the effective R-value of building envelope, using high definition thermal imaging technique.

It focuses on the investigation of the thermal performance of building envelope of residential building under hot-humid climate represented by Dhahran, Saudi Arabia. A residential building on KFUPM campus is selected to conduct both thermographic and heat flux measurements. The building envelope is modified by installing three different types of insulation with intentionally introduced envelope defects (Test Wall). Data obtained by heat flux measurements about the building envelope thermal characteristics have being processed following methods of the ISO standard 9869:1994. To solve the required algorithm a MATLAB Program was developed. Simultaneously thermal imaging technique is used to record the surface temperature of the test wall. Recorded thermal images (IRT) are analyzed to detect missing and damaged thermal insulation, and thermal bridging. A method for quantification of the impact of thermal insulation defects is developed to improve the prediction of the actual thermal resistance of building envelope using infrared thermography. As a result of analysis of R-value calculation for the test wall it is found that R-values determined using IRT on average are varying from the R-value measured using dynamic method by 7.3% when R-value is determined based on reference R-value measured using dynamic method. The IRT method described in the study can be used to obtain the effective R-value of the envelope considering the total defective area rather than measuring the R-values at single point using the dynamic method. Energy simulation program Visual DOE is then used to evaluate the impact of thermal bridging on cooling energy, compared to when the building envelope is properly designed and well constructed.

ARABIC ABSTRACT

الاسم: **محمد عبد الواحد خان**
العنوان: **تقييم معامل المقاومة الحرارية "الفعلى" لغلاف المباني باستخدام تقنية التصوير الحراري عالية الجودة**
التخصص: **الهندسة المعمارية**
التاريخ: **مايو 2011**

ملخص البحث:

يعتبر التصوير الحراري بالأشعة تحت الحمراء تقنية هامة وفعالة لتشخيص وتقييم غلاف المباني، من حيث التعرف على أماكن الجسور الحرارية، والعوازل الحرارية التالفة والشقوق، وتسرب الهواء والأضرار الناتجة عن تسرب الرطوبة. وكلها من الأمور التي تسهم في زيادة استهلاك الطاقة في المباني وذلك لكون فقدان أو اكتساب الحرارة غالبا ما يكون أكبر من ما يتم تقديره أثناء مرحلة تصميم المبنى. ويمّكن التصوير الحراري من الحصول على معلومات دقيقة ومفصلة عن مكان حدوث المشكلة ومصدرها وبالتالي تجنب الأعمال الواسعة للإصلاح أو التجديد ومن ثَم توفير التكاليف واستهلاك الطاقة.

وتركز الدراسة على التحقق من الأداء الحراري للمبنى في ظل المناخ الحار الرطب الممثل في الظهران بالمملكة العربية السعودية وذلك بهدف تقييم معامل المقاومة الحرارية "الفعلى" لغلاف المبنى باستخدام تقنية التصوير الحراري. وقد تم تحديد مبنى سكني في الحرم الجامعي لجامعة الملك فهد للبترول والمعادن وتعديل جزء من غلاف المبنى عن طريق تركيب ثلاثة أنواع مختلفة من العزل الحراري وإحداث بعض العيوب بها لغرض الدراسة ومن ثَم قياس الانسياب الحراري عبر غلاف المبنى ودرجات الحرارة على الأسطح والفراغات الداخلية والخارجية باستخدام طرق الحساب الـ ISO 9869:1994 . كالطريقة البسيطة والطريقة الديناميكية . وفي نفس الوقت استخدام تقنية التصوير الحراري لقياس التغيرات في دراجات الحرارة لسطح غلاف المبنى ثم معالجة الصورة الحرارية لتشخيص وتحديد أماكن العوازل الحرارية التالفة أو الغير موجودة، والجسور الحرارية. وقد خلصت الدراسة بتطوير طريقة لتحديد معامل المقاومة الحرارية الفعلي لغلاف المبنى باستخدام تقنية التصوير الحراري آخذاً في الاعتبار العيوب الموجودة ومساحتها واختلاف توزيع الحرارة بها، وتشير النتائج أن تقدير معامل المقاومة الحرارية باستخدام تقنية التصوير الحراري تختلف بحوالي 7.3% في المتوسط مقارنة بقياسها باستخدام الطريقة الديناميكية عند نقطة قياس واحدة. وهذا بطبيعة الحال يؤدي إلى تقييم أفضل لمعامل المقاومة الحرارية وتأثيره على استهلاك طاقة التبريد عند دراسة المباني باستخدام برامج النمذجة والمحاكاة للطاقة مقارنة باستخدام معاملات المقاومة الحرارية النظرية والتي تستخدم المعرفة التفصيلية بتكوين وعناصر الغلاف الخارجي للمبنى.

CHAPTER ONE

1 INTRODUCTION

1.1 Background

This chapter presents the background for the research subject along with problem statements, significance of study, the objectives, research methodology used, scope and limitation and the structure of the thesis.

Energy requirements are increasing in line with population growth and globalization effects. Electricity generation facility development is not in pace with demand. So, efforts are being made world-wide to conserve energy resources and optimize the utilization of energy. One such direction is to use thermally efficient building materials in the construction industry so as to minimize the consumption of energy (M. Al-Hadhrami, and A. Ahmad, 2009). Residential buildings in Saudi Arabia consumed 53.4% of energy used in the year 2008 as shown in **Figure 1.1**, compared to 52.9% in the Year 2007 (SEC, 2008) and 51% in the year 2002 (N. Saleh, 2006), indicating that there is an increasing trend in the energy consumption in the residential buildings. A distribution of Sold Energy in terms of percentage for the kingdom of Saudi Arabia (KSA) in Years 2007 and 2008 is shown in **Figure 1.2.**

In KSA residential buildings air-conditioning requires about 73% of total energy consumption (A. Elhadidy et. al, 2000). In KSA the climate is hot and in some places also hot and humid, thus, knowledge of the thermal properties of building materials is essential in building design and in selecting air-conditioning systems; heat transfer through a building envelope constitutes an appreciable percent of the total thermal load. Proper selection of building materials could reduce considerably this thermal transmission load (M. Al-Hadhrami, and A. Ahmad, 2009).

The building envelope determines the energy exchange between outdoor environment and indoor spaces and hence governs the overall energy performance of the building. Appropriate selection of thermal insulation, glazing type, shading elements and proper construction, can reduce the heat transfer through the building envelope (Hatice Sozer, 2010). Thus building envelope and operation period of the heating ventilation and air conditioning (HVAC) system are important parameters affecting total energy consumption in the building, especially in envelope dominant residential building.

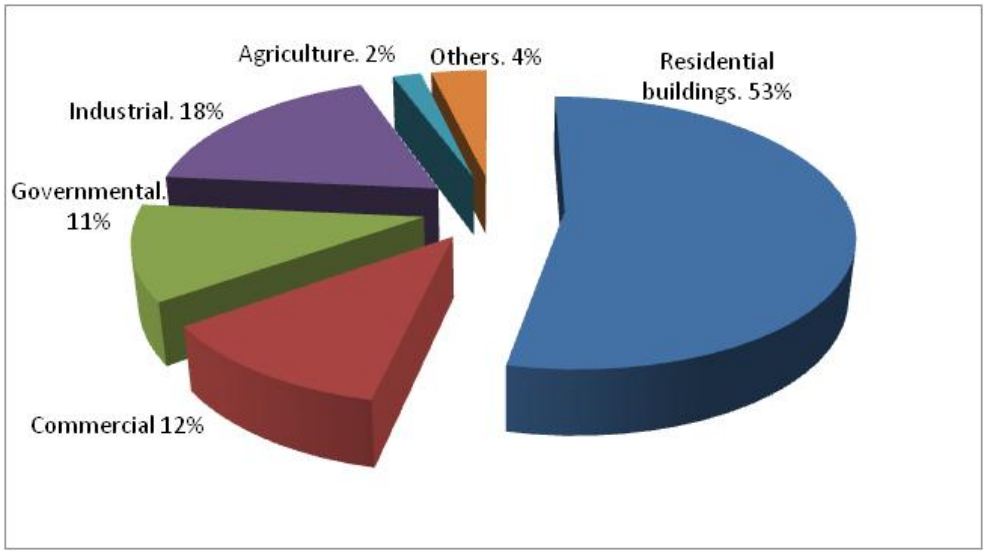

Figure 1.1 Distribution of Sold Energy in KSA in the Year 2008 (SEC, 2008)

The demand for energy efficient constructions has increased significantly in recent times. Development in the field of energy, together with the demand for pleasant indoor environments, have resulted in ever greater significance having to be attached to both the function of buildings thermal insulation, air tightness and the HVAC system (FLIR System, 2009). Infrared can easily detect building abnormalities that result into energy losses. By repairing these areas energy can be saved (FLIR System, 2004).

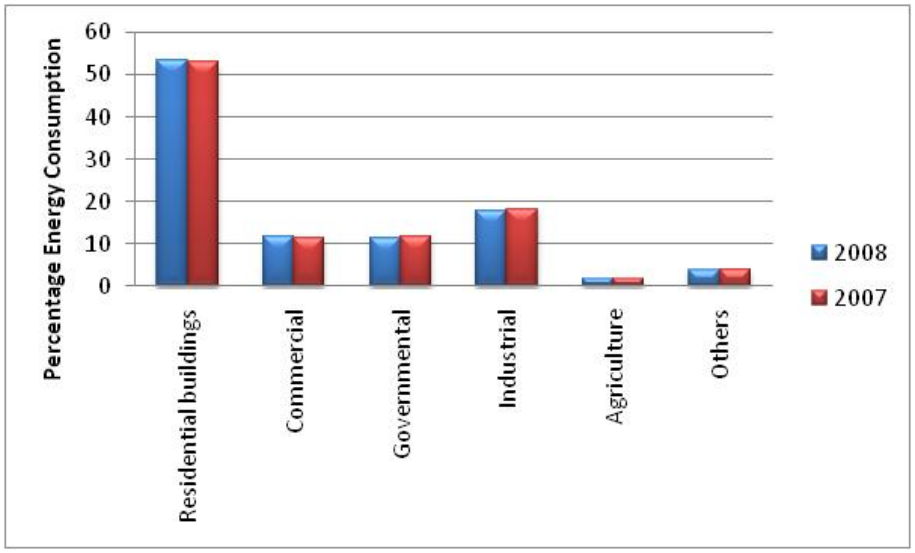

Figure 1.2 Distribution of Sold Energy in Percentage in the kingdom in Year 2007 and 2008 (SEC, 2008)

The human eye can detect light waves or visible radiation of the electromagnetic spectrum (0.39-0.77 Microns) that is result of solar radiation or artificial lights. The eye cannot detect the infrared (IR) radiation that typically falls between wavelengths of 2-15 Microns. IR thermography is a powerful tool for fast and accurate diagnostics of building envelope. The use of IR imaging is a valuable tool for inspecting and performing non destructive testing of building elements, detecting where and how energy is leaking from a buildings envelope. IR inspections can also be used for preventive maintenance. It is a device that makes an image of the thermal pattern and

is calibrated to measure the emissive power of surface in an area at various temperatures, it uses a lens to focus the emitted IR radiation on to a detector and the electrical response signal is converted into visual display in which the different colors correspond to various temperatures (C. Balaras and A. Arguiriou, 2002, B. Raj et. al; 2007). This process of IR scanning to produce thermal images is known as thermography (AIT, 1990).

The surface temperature is influenced by air flow within or through the building envelope, the surface temperature distribution can be used to detect thermal irregularities due to thermal bridging, insulation defects, and moisture or air leakage. (AIT, 1990 and H. Wiggenhauser, 2002). Infrared thermography is a measuring and visualization process that allows obtaining, in real time, very useful images to the understanding of flow topology and temperature field distribution (L. Neto et. al; 2006).

Infrared thermography is a well established tool for non destructive testing of materials and commonly used for investigating aspects of the building envelope- wall and roofs (D. Titman, 2001). Detection, verification, remediation can be easily and effectively carried out with the utilization of infrared thermography. (A. Colantonio, 98)

A new momentum to broaden IR thermography building applications is strongly supported by an increasing demand for low energy consumption and predictive maintenance of constructions (E. Grinzato et al. 1998).

1.2 Statement of Research Problem

As envelope thermal load dominates in residential buildings, residential buildings on average consume more than 53.4% of total consumed energy in Saudi Arabia (SEC, 2008). Heating ventilation and air conditioning system (HVAC) consumes about 73% of total electricity consumed in residential buildings (A. Elhadidy et. al, 2000). The thermal load can significantly be reduced by considering climatic thermal design strategies. It might not be possible to completely avoid using mechanical systems in harsh climates of Saudi Arabia but the thermal load could be minimized by determining the energy leakage spots in the building envelope with the help of infrared thermography.

Thermography can be used to detect insulation defect, air leakage, heat loss through windows, thermal bridges, moisture damages, examination of heating and cooling systems and for preventive maintenance. Despite thermography potential uses to buildings, its application to building materials has not been greatly studied yet (E. Barreira and P. Vasco, 2005).

Despite the general awareness about the importance and relevance of envelope thermal design, practical guidelines on envelope thermal design to avoid thermal bridging and damaging of insulation are not always available especially for a country such as Saudi Arabia that has variations of climatic conditions. Despite the potential of infrared thermography there is little published work about quantitative studies of building envelope air tightness using thermograms (Dufour et al. 2009).

Building envelope often contains numerous highly conductive heat flow paths, called thermal bridges, which are major sources of heat loss and deterioration of building materials due to moisture condensation. The detection of moisture problems before

causing serious damage has usually been carried out by means of time consuming testing procedures such as electronic moisture meters. IR techniques provide an efficient way of detecting, verifying and evaluating moisture damage at low cost (M. Lyberg, 1990).

1.3 Objectives of the Study

1 To develop a method for quantification of thermal characteristics (i.e. R-value) in terms of change in heat transfer based on the measurements with infrared thermography, the aim is

- To improve the prediction of actual thermal resistance ($R_{actual)}$ of building envelope. and
- To examine the subsequent impact on energy consumption.

2 To devise a systematic procedure for assessing the R-Value of building envelope using infrared thermography

1.4 Significance of the Study

The high energy consumption is mostly related to poor thermal performance of building envelope. Therefore, this study focuses on investigating the thermal performance of building envelope under hot-humid climates in Saudi Arabia using infrared thermography, in terms of identification of the thermal deficiency in building envelope, and finding its impact on energy consumption by developing a method for quantification of thermal bridging, and missing thermal insulation. This study is beneficial to those who design residential buildings, the study provides a method of

quantification for thermal bridging, and missing insulation to improve the energy efficiency of a typical residential building in Saudi Arabia.

1.5 Scope and Limitations

The scope of the study will be limited to:

1. The building envelope of residential building.
2. Quantification of thermal bridging, damaged insulation and missing insulation in the building envelope due to bad workmanship or construction.
3. A residential building in hot-humid climate represented by Dhahran will be considered.

1.6 Research Methodology

To achieve the stated objectives three main phases are found necessary to be carried out as follows and as shown in **Figure 1.3**.

Phase I: Literature review

1.1 A comprehensive literature review is conducted to study the infrared thermography concept and techniques, building diagnosis procedure and measurements utilizing infrared thermography.

1.2 The study of various defects in building envelope such as thermal bridging damaged thermal insulation, air leakage, moisture damage and cracks.

Phase II: Procedure and Measurements

2.1 Procedure for conducting infrared thermography measurements

2.2 Selection of residential building and construction of test wall

2.3 Conducting thermographic and heat flux measurements.

Phase III: Data Analysis and Simulations

3.1 Analysis of heat flux measurement.

3.2 Developing a method for thermographic image analysis.

3.3 Developing a method to estimate in-situ resistance (R) value using IR thermography.

3.4 Simulation analysis utilizing a modeling and simulation program, to find the impact of thermal deficiencies on energy consumption.

3.5 Systematic procedure for assessing the R- value of building envelope using infrared thermography.

3.6 Conclusion and Recommendations.

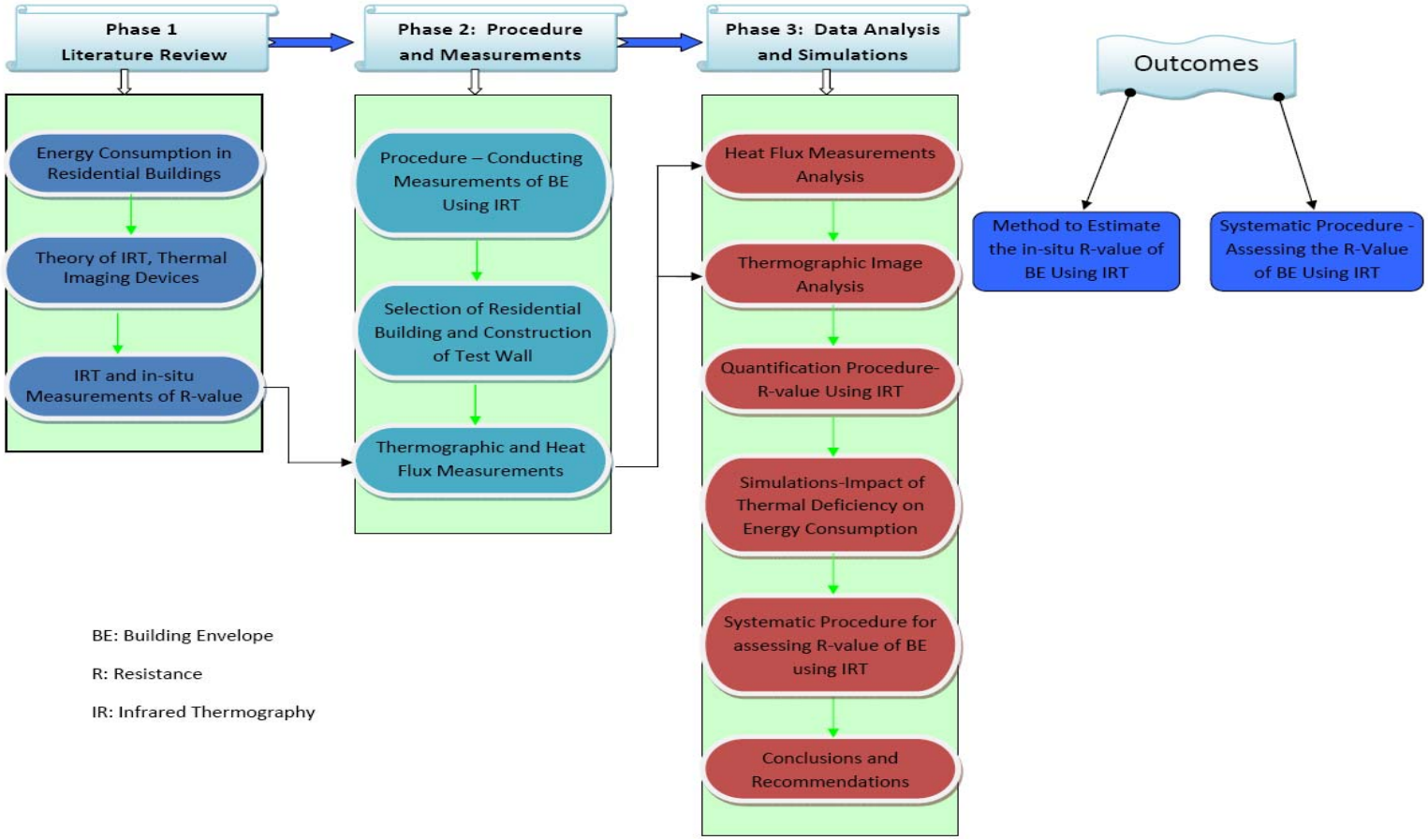

Figure 1.3 Research Methodology

CHAPTER TWO

2 LITERATURE REVIEW

2.1 Impact of Envelope Thermal Design on Energy Consumption

With the increasing population and living standards, energy issue is becoming more and more important, because of a possible energy shortage in the future (Y. Jinghua, 2009).The application of surface treatments such as light coatings, light color tiles on exterior surface of building envelope and low-emissive sheets on exterior/interior surfaces have significantly improved the overall thermal performance of buildings in hot climates (N. Saleh, 2006). Infiltration causes about 15-30% of the energy use of space heating including ventilation in the typical finished detached house (J. Jokisalo et al. 2008).

Thermal, visual and acoustical comfort in the building with minimum energy consumption is of great importance for the health of the users and for the energy conservation. As a result building envelope has to be designed as an element of passive system with optimal performance in its control of heat, light and sound (G. Oral et al. 2003). The most important design parameters affecting indoor thermal comfort and energy consumption in buildings are orientation of building, building form, thermal properties of building envelope. Among these building envelope is the

most important parameter as it separates the outdoor and indoor environment (Z. Yilmaz, 2006).

The measure of building envelope thermal insulation remains a prerequisite towards the improvement of building energy efficiency. Thermal bridges in the building envelope remain a weak spot in the construction, causing thermal losses in practice more than the predicted (T. Theodosiou and A. Papadopoulos, 2008). The energy consumption of buildings can be reduced with proper selection of envelope designs. Energy studies have investigated the impact of orientation on the energy consumption of buildings. (N. Saleh, 2006)

2.2 Energy Analysis Using Simulation Methods and Techniques

The thermal performance of a building should better be evaluated at the early design stage when many vital decisions related to building physics are taken (N. Saleh, 2006). Simulation tools for determining building thermal characteristics have become more and more exciting in the building industry. This is partly because computer resources have increased enormously during the past two decades (P. Tuomaala and Rahola, 1995). Many of the popular building energy simulation programs around the world are reaching maturity, some use simulation methods (and even code) that originated in the 1960s. BLAST and DOE-2 are two mainly used energy simulation software's in USA. The 50 years (1960-2010) have seen significant advances in analysis and computational methods, providing an opportunity for significant improvement in these tools. The main difference between the two programs is load calculation method. DOE-2 uses a room weighting factor approach while BLAST uses a heat balance approach. Both programs are widely used throughout the world. The other program is EnergyPlus which is an all-new program, based on the most

popular features and capabilities of BLAST and DOE-2 (B. Crawley et. al; 2001). EnergyPlus is an energy analysis and thermal load simulation program. EnergyPlus calculates heating and cooling loads necessary to maintain thermal control set points, conditions throughout a secondary HVAC system and coil loads, and the energy consumption of primary plant equipment and simultaneous integration of these utilizing a heat balance approach. (http://apps1.eere.energy.gov/buildings/ energyplus/energyplus_about.cfm).

For energy simulations building case studies can also be modeled using computer simulation program TRNSYS, which requires specific input parameters, such as size of floor, wall area, roof area, window area, building volume etc (A. Farraj and V. Hanby, 2008). Energy modeling is utilized on buildings more often for two main purposes, modeling for building and HVAC system design, and associated design optimization. In order to achieve energy cost savings, multiple energy efficiency strategies are employed for design proposed building, encompassing high performance building envelope, lighting system, and HVAC system, through energy modeling. (Y. Pan and Z. Huang 2008)

2.3 Brief History of Thermography

Less than 200 years ago the existence of the infrared portion of the electromagnetic spectrum wasn't even suspected. The discovery was made accidentally during the search for a new optical material (FLIR systems, 2009). Sir William Herschel (Astronomer) was first to discover that transmission of infrared radiation is different from material to material (X. Maldague 2001).

The first heat picture became possible in 1840, the result of work by Sir John Herschel (Astronomer), Based upon the differential evaporation of a thin film of oil when

exposed to heat pattern focused upon it, the thermal image could be seen by reflected light where the interference effects of the oil film made the image visible to the eye. He had managed to obtain a primitive record of the thermal image on paper, which he called a thermograph. Between the years 1900 and 1920, the inventors of the world discovered the infrared. Many patterns were issued for devices to detect personnel, artillery, aircraft, ships and even ice bergs. Image converter received the greatest attention by the military because it enabled an observer for the first time in history to literally see in dark. (FLIR systems, 2009)

2.4 Theory and Significance of Thermography

The subjects of infrared radiation and the related techniques of thermography are still new to many who will use an infrared camera. In this section the theory behind thermography will be presented.

An increase in temperature causing an increase in heat transfer is directly proportional to the surface temperature differences between the defective and non-defective areas. When there is a higher rate of heat transfer, defects will appear to be more apparent. (M. Chew, 1998)

Thermography is one of the many techniques used to “see the unseen”. It uses a distribution (Graphy) of the surface temperatures (Thermo) to assess the structure or behavior of what is under the surface. On the whole thermography is a contact technique to record a distribution of surface temperatures and infrared thermography is a (contact-less) technique with many distinct advantages (X. Maldague 2001).

The application of infrared thermography has provided a reliable and accurate assessment method for the inspection of buildings and structures. Infrared

thermography technique detects the energy by an infrared scanner and mapping the temperature contour over the surface of a target area to provide appropriate measure of the damaged part of the building. (Y. Tommy and W. Choi, 2004).

The Electromagnetic Spectrum: The electromagnetic spectrum is divided arbitrarily into a number of wavelength regions called bands. Distinguished by the methods used to produce and detect the radiation. There is no fundamental difference between radiations in the different bands of the electromagnetic spectrum. They are all governed by same law and the only differences are those due to difference in wavelengths. Thermography makes use of the infrared spectral band. The infrared band is often further subdivided into four smaller bands and they include:

- ✓ The near infrared (0.75-3.0 Microns)
- ✓ The middle infrared (3.0-6.0 Microns)
- ✓ The far infrared (6.0-15.0 Microns)
- ✓ The extreme infrared (15-100 Microns). (FLIR systems, 2009)

2.5 Thermal Insulations

Thermal insulation is the material that retards or offers resistance to flow of heat. Heat flows from a higher temperature region to one at a lower level of temperature. Hence there is continuous flow of heat from surroundings to the air-conditioned space, there by increasing the space temperature (heat gain) or decreasing the space temperature (heat loss). Thermal insulation however cannot stop the heat flow completely, but it can reduce the rate of heat flow and contributes in reducing the required air-conditioning system size hence reducing the annual energy cost (P N Ananthanarayanan, 2007).

Thermal insulation is a major contributor and obvious practical and logical first step towards achieving energy efficiency especially in envelope-load dominated buildings located in sites with harsh climatic conditions. The amount of energy required to cool/heat a building depends on how well the envelope of that building is treated thermally, especially in envelope-dominated structures such as residences. Insulating the building very well is not enough if it is not airtight. Infiltration can have significant contribution to energy waste especially in residences with loose construction. Building type has its role in determining the effectiveness of envelope thermal insulation on the thermal performance of buildings. The use of more thermal insulation is more critical in the envelope-load dominated buildings compared to those buildings with more internal-load dominance. Although wall and roof insulation are important, roof insulation is generally more critical than walls as it is continuously exposed to the direct summer solar radiation during daylight hours, **Table 2.1** describes the various types of insulations with their thermal conductivity and **Figure 2.1** shows the steps to be considered in selection of insulation material. (Al-Homoud, 2005). From an economic and environment conservation point of view, it is more beneficial to design buildings with high thermal insulation characteristics than the practice currently followed in the construction of buildings. This will result in long-term benefit of reducing the cost of cooling as well as reducing the pollution of the environment due to heavy use of fuel. K.S. Al-Jabri et.al (2005).

Table 2.1 Common building insulation materials (Al-Homoud, 2005)

Form	Material	Density (Kg/m3)	Thermal conductivity (W/m-K)
Blankets : Batts or Rolls	Fiberglass (sand & recycled glass)	12–56	0.04–0.033
	Rock wool (natural rocks)	40–200	0.037
	Polyethylene	35–40	0.041
Loose-fill blown-in or poured-in	Fiberglass (open cell structure)	10-48	0.038–0.030
	Rock wool (open cell structure)	-	0.040
	Cellulose (ground-up waste paper)	24–36	0.054–0.046
	Perlite (natural glassy volcanic rock)	32–176	0.06–0.04
	Vermiculite	64–130	0.068–0.063
Rigid Board	Fiberglass (open cell structure)	24–112	0.035–0.032
	Expanded Polystyrene (closed cell foam)	16–35	0.038–0.037
	Extruded Polystyrene (closed cell foam)	26–45	0.032–0.030
Polyurethane	Perlite (natural glassy volcanic rock)	32–176	0.06–0.04
	Vermiculite (natural mineral)	64–130	0.068–0.063
	Cellulose (waste paper)	24–36	0.054–0.046

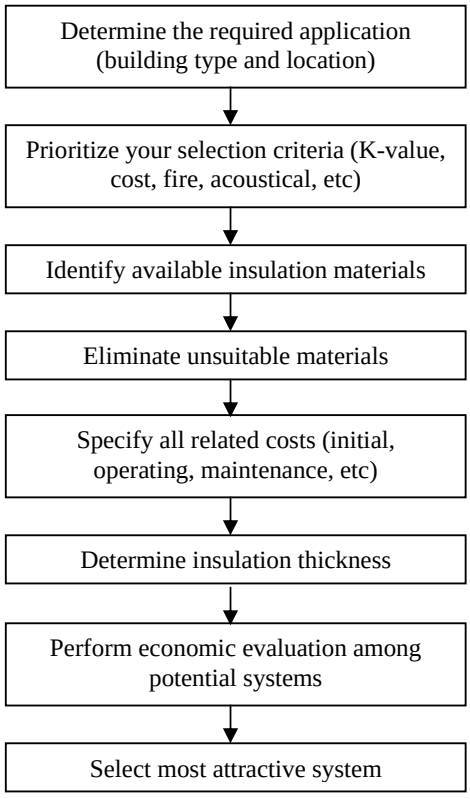

Figure 2.1 Thermal insulation selection Procedure (Al-Homoud, 2005)

2.6 Diagnosis of Buildings – Using infrared Thermography

Thermography works in the wavelength band of infrared radiation that for building materials ranges between 2 and 14 Microns (Italo and Valter, 1998). The use of IR imaging is a valuable tool for inspecting and performing non destructive testing of building elements, detecting where and how energy is leaking from the building envelope. The ambient air temperature influences the temperature of the equipment and its performance. High winds will enhance heat transfer from the surface of the buildings and higher convective heat losses can reduce the surface temperatures, accordingly outdoor inspections must be avoided during windy conditions. On the other hand, for identifying air infiltration problems, relatively high winds will make it easier to detect during the inspection of the interior windows and doors. Distance effects and angle of vision are also factors that affect data collection and may play a role in the interpretation of the results. Improperly installed or damaged insulation appears on a thermograph as a light colored patch with distinct edges, which generally outlined the non-insulated area. Air leakage through windows and doors allows unwanted outdoor air to enter inside the building (infiltration) or indoor air to escape (exfiltration) causing discomfort for occupants. An air inspection around a window or a door frame can easily pinpoint the leaking areas. IR can locate water damaged areas with a good accuracy. Water can cause serious damages to roofs by reducing the thermal effectiveness of insulation (C. Balaras and A. Arguiriou, 2002), through infrared imaging, thermal bridges, moisture absorbed by buildings' materials as well as other parameters related to a building's thermal and energy behavior can be determined. G.Fivos sargentis et.al (2009) and Will Decker (2009).

With the development of testing technology, the infrared thermography is applied in the building industry. It has the virtues of great speed and a large range of tested

temperature, and has non-contact surface temperature measurement. It is specially adapted for testing the building envelope surface temperature distribution. According to the testing result, building envelope defects can be observed. For the building envelope, the heat flow takes place when there is noticeable temperature difference between indoor and outdoor conditions (Yogzheng et.al, 2006). IR thermography of walls/ roofs provides the data for making appropriate decisions, because IR thermography can accurately detect and locate the defective areas quickly. IR expedites the identification of building envelope defects and thermal boundary areas of concern. IR is a particularly important tool to find the primary sources of energy loss. David L. Jakovac (2010).

2.7 Factors Impacting Thermographic Measurements

To measure temperature variation precisely, it is necessary to compensate for the effect of number of different radiation sources. This is done on-line automatically by the camera, by providing the following information;

- The emissivity of object
- The reflected apparent temperature (using a pre described procedure)
- The distance between the object and the camera
- The relative humidity and air temperature of indoor and outdoor environment. (FLIR Systems Manual, 2009 and C. Balaras and A. Arguiriou, 2002)

A. Factors affecting the IR thermography inspection of a Wall System

1. Climate/ Weather: wind, rain, ambient temperature
2. Wetting of wall surface or moisture content within the wall
3. Building: Orientation to the path of sunshine during the survey, existence of any heat generating equipment inside the building.

4. Wall Surface: - emissivity, dryness, reflectivity, texture, roughness, color, stains, wall finish.
5. Angle of vision and survey distance
6. Building in shade of eaves or adjacent building, or screening objects (e.g. trees).

B. Factors affecting the IR thermography inspection of a roof system

1. Dryness of the roof surface and water films
2. Climate/ Weather:- wind (low speed winds are preferred), rain, ambient temperature
3. Building in shade of eaves or adjacent building, or screening objects (e.g. trees),
4. Difference in thickness of the roof membrane
5. Equipments below or above (e.g. AC machine) the roof area, existence of hot air exhaust onto a roof from fans or vents
6. Surface texture (e.g. multi-layer membranes)
7. Survey distance from object (Tommy and Choi, 2004).

2.8 Application of Infrared Thermography Technique- Inspection and Diagnosis

The following section describes applications of infrared thermography in identifying various defects in the building envelope.

A. Damaged insulation and thermal bridging

The Primary purpose of thermal insulation is to reduce conductive heat flow through the building envelope. Thermal bridging plays a relatively large role in heat loss. Thermal bridging can be divided into two groups:

- ✓ Thermal bridging within the building components
- ✓ Thermal bridging at joints between the building components.

They have two important consequences compared with those of the unbridged structure

- ✓ A change in heat flow rate; and
- ✓ A change in internal surface temperature. (G. Mao and G. Johannesson, 1997).

Insulation deficiencies do not necessarily lead to air infiltration. Areas with insulation deficiencies typically have higher temperatures than where there is only an air infiltration (FLIR Systems Manual, 2009). Thermal bridging is created mostly by structural elements such as supports, panels, reinforcements, hooks etc (E. Grinzato et al. 1998). **Figure 2.2 (a)** illustrates an Example for thermal bridging and **Figure 2.2 (b)** illustrates an example for damaged insulation.

B. Moisture defects

Moisture penetration and condensation could cause a lot of physical damage to the building envelope (Al-Homoud, 2005). Insulation materials lose their heat retaining properties if they become moist (Al-Homoud, 2005 and Christopher, 2009).

Building defects related to moisture and water damages may only show up when heat has been applied to the surface example from the sun, the presence of water changes the thermal conductivity and the thermal mass of the building material. It may also change the surface temperature of building material due to evaporative cooling. **Figure 2.2 (c)** illustrates an example for moisture defect.

C. Air leakage

Air leakage can be through infiltration, exfiltration and cracks in the building envelope. Infiltration means the uncontrolled penetration of air into the building through the openings. Exfiltration occurs when air escapes the building envelope, and is the opposite of infiltration. On an infrared image air infiltration can be identified by its typical ray pattern, which proceed from the exit in the building structure for example from the skirting strip. Furthermore the areas of air infiltration have a lower detected temperature than areas where there is only an insulation deficiency (FLIR Systems Manual, 2009).

Airtightness defects are the most frequent building envelope failures with a significant impact on the energy efficiency, The most used evaluation method of the overall airtightness of the building envelope of a house, considered as a single zone building, is the fan pressurization or depressurization method, also known as the blower door test. The overall airtightness is given in terms of one of the following indices: the air change per hour at 50 Pa pressure difference (ACH50), or the effective leakage area (ELA). The ACH50 or ELA values can be used to compare the building air tightness

with prescriptions of energy-related guidelines or standards, or with measurements from other houses. These indices can also be used as input to building energy analysis programs. The combined use of infrared thermography and fan depressurization test in situ would be used to quantify the dimensions of crack. Dufour et al. (2009) presented an approach towards such quantification and estimating the dimensions of cracks in walls. **Figure 2.2 (d)** illustrates an Example for Air.

(a) THERMAL BRIDGING

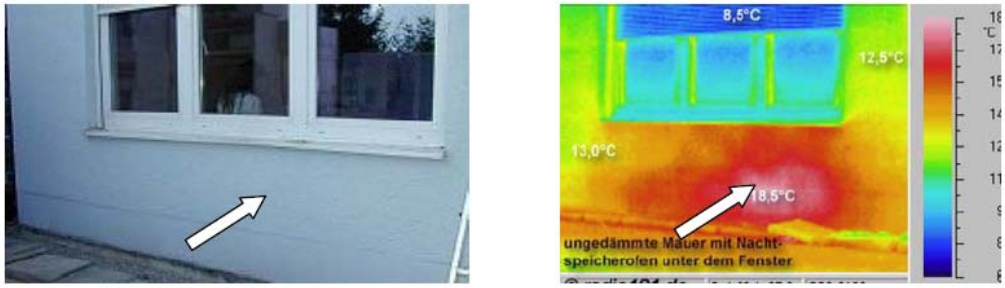

(b) DAMAGED INSULATION

(c) MOISTURE DAMAGE

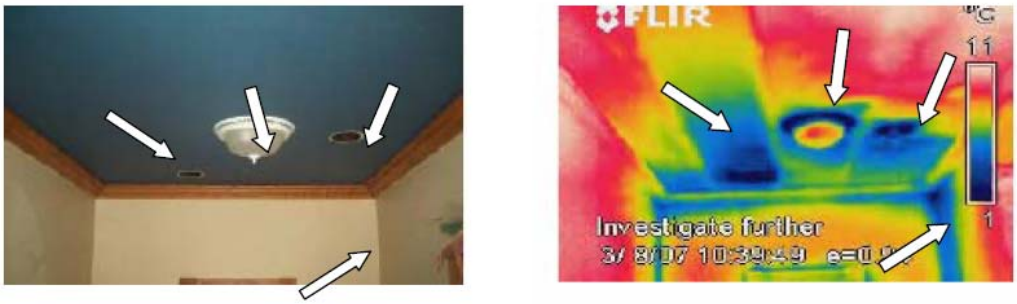

(d) AIR LEAKAGE

Figure 2.2 Various types of defects in the building envelope

2.9 In-Situ Measurement of Thermal Resistance

Two methods can be used for analysis of the data of heat flow meter (HFM) measurements in accordance with the International Standard: ISO 9869:1994, one is called the average method, which is simple, and second is the dynamic method, which is more sophisticated but gives a quality criterion of the measurement and may shorten the test duration for medium to heavy elements exposed to variable indoor and outdoor temperatures. **Figure 2.3** illustrates the methods for in-situ measurements of R-value of building envelope utilizing heat flux instrument. Changhai Peng, Zhishen Wua (2008) has used three different types of methods for in-situ measurements of R-values, one of them is the synthetic temperature method which requires measuring the heat flow rate on the inside surface of the building construction and both the synthetic indoor and outdoor temperatures, and the second, a surface temperature method, just requires testing the heat flow rate on the inside surface of building envelopes and both the inside and outside surface temperatures of building construction. However, the frequency response method introduced in the study only relates to the mean synthetic indoor and outdoor temperatures and the average inside surface temperatures of the building envelopes.

2.10 Simple Method

This method assumes that the conductance or transmittance can be obtained by dividing the mean density of heat flow rate by the mean temperature difference, the average being taken over a long period of time.

Estimate of Resistance (R) is obtained by:

$$R = \sum_{j=1}^{n} (T_{sij} - T_{sej}) / \sum_{j=1}^{n} q_j$$

Estimate of Conductance (Λ) is obtained by:

$$\Lambda = \sum_{j=1}^{n} q_j / \sum_{j=1}^{n} (T_{sij} - T_{sej})$$

Estimate of Transmittance (U) is obtained by:

$$U = \sum_{j=1}^{n} q_j / \sum_{j=1}^{n} (T_{ij} - T_{ej})$$

Where,

index j enumerates the individual measurements

R, Thermal resistance of construction element, $m^2.^oC/W$

Λ, Thermal conductance of construction element, $W/ m^2.^oC$

U, Thermal transmittance of construction element, $W/ m^2.^oC$

T_{si}, Interior surface temperature of the construction element, ^oC

T_{se}, Exterior surface temperature of the construction element, ^oC

T_e, Exterior air temperature of the construction element, ^oC

T_i, Interior air temperature of the construction element, ^oC

q, Density of heat flow rate, W/m^2

When the estimate is computed after each measurement, a convergence to an asymptotical value is observed. This asymptotical value is close to the real value if the following conditions are met.

The HFM should not be exposed to direct solar radiation. It should be noted that a false result can be obtained when there is solar radiation on the exterior surface. The external ambient temperature in the U-value measurement generally takes no account of the solar flux to the exterior surface of the element.

The thermal conductance of the element is constant during the test, if the following below conditions are not fulfilled, misleading results can be obtained.

1. For light elements, which have a specific heat capacity per unit area of less than 20 kJ/ (m^2.K), it is recommended that the analysis is carried out only on data acquired at night (from 1 h after sunset until sunrise), to avoid the effects of solar radiation. The test may be stopped when the results after three subsequent nights do not differ by more than ± 5 %. Otherwise, it shall be continued.

2. For heavier elements, which have a specific heat per unit area of more than 20 kJ/ (m^2.K), the analysis shall be carried out over a period which is an integer multiple of 24 h.

The test shall be ended only when the following conditions are fulfilled:

a) The duration of the test exceeds 72 h
b) The R-value obtained at the end of the test does not deviate by more than ± 5 % from the value obtained 24 h before
c) The R-value obtained by analyzing the data from the first time period during INT (2 x D_T/3) d does not deviate by more than ±5 % from the values obtained from the data of the last time period of the same duration. Where D_T is the duration of the test in days; INT is the integer part
d) If the change in heat stored in the wall is more than 5 % of the heat passing through the wall over the test period, dynamic method shall be used.

Figure 2.3 illustrates the conditions to be met to end the measurements for the test duration of 4 days.

A. Storage effects

The following procedure, relevant for structures of high R-value and high thermal mass, shall be applied in cases where the (simple method) criteria which determine sufficient data have been recorded but are not fulfilled. The use of this correction procedure often permits a shorter measurement time than would otherwise be required to meet these criteria. The procedure involves calculation of internal and external thermal mass factors (Fi and Fe, respectively) for the structure concerned, and an adjustment, involving these factors, to the measured flux at each data point

B. Calculation of the thermal mass factors

The factors shall be obtained for a structure consisting of N plane parallel layers, numbered from 1 to N with layer 1 at the interior surface, for heat flux measured at the interior surface, as follows.

For each layer k, estimate its thermal resistance R_k (m^2.K/W) (thickness divided by thermal conductivity or thermal resistance of airspace) and its thermal capacity [J/m^2.K] [product of specific heat capacity [J/kgK], density (kg/m^3). R is total thermal resistance of the wall, i.e. the sum of all R_ks.

Then for each layer k calculate the inner (R_{ik}) and outer (R_{ek}):

$$R_{ik} = \sum_{j=1}^{k-1} R_j$$

$$R_{ek} = \sum_{j=k+1}^{N} R_j$$

And the factors,

$$F_{ek} = C_k \left[\frac{R_k}{R} \left\{ \frac{1}{6} + \frac{R_{ik}+R_{ek}}{3R} \right\} + \frac{R_{ik} \,.\, R_{ek}}{R^2} \right]$$

$$F_{ik}=C_k \left\{ \frac{R_{ek}}{R} + \frac{R_k^2}{3R^2} - \frac{R_{ik} \cdot R_{ek}}{R^2} \right\}$$

The thermal mass factors for the structure are

$$F_i = \sum_{k=1}^{N} F_{ik}$$

And

$$F_e = \sum_{k=1}^{N} F_{ek}$$

Where,

index j enumerates the individual measurements

R, Estimated total thermal resistance of the wall, m2.K/W

R_k, Thermal resistance for each layer of the structure, m2.K/W

For the interior layer (j=k=1), R_{ik}=0. For the exterior layer (j=k=N), $_{Rek}$= 0.

N= Number of layers

F_i, Internal thermal mass factor

F_e, External thermal mass factor

C. Correction to measured heat flux:

No correction is applied to the data during the first 24 h. Thereafter, Σq_j in calculations of R, Λ, U is replaced by

$$\Sigma q_j = \Sigma q_j - \frac{F_i \, \delta T_i + F_e \, \delta T_e}{\Delta t}$$

Where,

Σq_j, Sum of density of heat flow rate, W/m2

Δt, the interval between readings, in seconds.

δTi, the difference between internal averaged temperature over the 24 h prior to the reading j and internal averaged temperature averaged over the first 24 h of the analysis period.

δTe, the difference between external averaged temperature averaged over the 24 h prior to the reading j and external averaged temperature averaged over the first 24 h of the analysis period.

D. Interpretation of the result

The R, Λ or U-value of the structure shall be taken as the value corresponding to corrected heat flux at the end of the measurement, provided that each of the following conditions holds:

a. The analysis period is not less than 96 h;

b. The analysis period is an integer multiple of 24 h;

c. The R-value so obtained is equal to the value of R used to derive the correction factors, to within 5%.

d. The value of the corrected curve

1. at the end of the test.
2. 24h before the end of the test
3. 48 hours before the end of the test

are all the same within 5%

e) The same results to within 5 % are obtained if the first 12 h of data are discarded.

If condition c) above is not met, the thermal resistance chosen for each layer of the structure shall be reviewed and if alternative values can be justified (so as to make R

consistent with the measured value), the data shall be re-analyzed and new correction factors calculated using the revised thermal resistances.

If conditions d) or e) above are not met, the first few hours of data should be discarded and the remaining data examined and judged against all five of the above conditions. This will be possible only if more than 4 d of data are available.

If the above conditions are not met, the result of the test is subject to a greater uncertainty.

E. When composition of wall is not known

When the composition of the structure is unknown but an estimate of its thermal mass can still be made, it can be of assistance in interpreting results to use the correction factors for a single layer structure. These are

$$F_i = \frac{C}{3} \quad \text{And} \quad F_e = \frac{C}{6}$$

Where C is the product of specific heat capacity [approximately 1, 000 J/ (kg K) for most materials], density and thickness of the element, the use of these factors will not give a valid result if the element contains an insulation layer.

Figure 2.3 illustrates conditions to meet in order to end the measurements considering the storage effect.

2.11 Dynamic Method

The dynamic analysis method is a sophisticated method which may be used to obtain the steady-state properties of a building element from heat flow meter measurements when large variations occur in temperatures and heat flow rates. It takes into account the thermal variations by the use of the heat equation.

The building element is represented in the model by its thermal conductance Λ and several time constants τ. The unknown parameters (Λ, τ_1, τ_2, τ_3...) are obtained by an identification technique using the measured densities of heat flow rates and temperatures.

A. Algorithm of the dynamic method

The measurements give N sets of data of the density of heat flow rate (q_i), indoor and outdoor surface temperatures (T_{Ii}, T_{Ei}) taken at the times t_i (i ranges from 1 to N). The time interval between two measurements is Δt, defined as,

$$\Delta t = t_{i+1} - t_i$$

The heat flow rate at time t_i is a function of the temperatures at that time and at all of the preceding times

$$q_i = A(T_{Ii} - T_{Ei}) + K_1 \dot{T}_{I\,i} - K_2 \dot{T}_{E\,i}$$
$$+ \sum_n P_n \sum_{j=i-p}^{i-1} (T_{Ii})(1-\beta_n)\beta_n(i-j)$$
$$+ \sum_n Q_n \sum_{j=i-p}^{i-1} (T_{Ej})(1-\beta_n)\beta_n(i-j)$$

Where

Derivative of the indoor surface temperature is

$$\dot{T}_{Ii} = (T_{Ii} - T_{I,i-1}) / \Delta t$$

Derivative of the Exterior surface temperature is

$$\dot{T}_{Ei} = (T_{Ei} - T_{E,i-1}) / \Delta t$$

K_1, K_2 as well as P_n and Q_n are dynamic characteristics of the wall without any particular significance. They depend on the time constant τ_n.

The variables β_n, are exponential functions of the time constant τ_n,

$$\beta_n = \exp(-\Delta t / \tau_n)$$

Assuming that 3 time constants (τ_1, τ_2, τ_3) are chosen, and then there will be 9 unknown parameters, which are Λ, K_1, K_2, P_1, Q_1, P_2, Q_2, P_3, Q_4.

Writing equations 2m+3 times for 2m+3 sets of data at various times, a system of linear equations can be solved to determine these parameters, and hence conductance is computed.

The set of 9 equations can be written in matrix form as

$$q = (X)\, Z$$

Where,

q is a vector, the M components of which are the last M heat flow density data, qi. The value of M is then greater than 2m+3 and goes from N - M + 1 to N; (N is number of data sets, m = 3)

Z is a vector, the 2m + 3 components are the unknown parameters

X is a rectangular with M lines (i=N-M+ 1) to N, and 2m+3 columns (1 to 2m + 3). The matrix elements are (p = N-M, where N is large enough)

$$X_{i1} = T_{Ii} - T_{Ei}$$

$$X_{i2} = \dot{T}_I = (T_{Ii} - T_{I,i-1})/\Delta t$$

$$X_{i3} = \dot{T}_E = (T_{Ei} - T_{E,i-1})/\Delta t$$

$$X_{i4} = \sum_{j=i-p}^{i-1} (\dot{T}_{Ii})(1-\beta_1)\beta_1(i-j)$$

$$X_{i5} = \sum_{j=i-p}^{i-1} (\dot{T}_{Ej})(1-\beta_1)\beta_1(i-j)$$

.

.

.

$$X_{i,2m+2} = \sum_{j=i-p}^{i-1} (\dot{T}_{Ii})(1-\beta_m)\beta_m(i-j)$$

$$X_{i,2m+3} = \sum_{j=i-p}^{i-1} (\dot{T}_{Ej})(1-\beta_m)\beta_m(i-j).....$$

The set of equations gives an estimate of Z^* of the Vector Z.

$$Z^* = [(X)' (X)]\text{-}1 (X)'q$$

In fact, the time constants τ_n are unknown. They are found by looking for the best estimate of Z by varying the time constants.

This is done in the following manner:

a) The number of time constants, m, to be used is chosen. Usually, this number is not more than 3.

b) A constant ratio r between these time constants is chosen (usually between 3 and 10) in such a way that $\tau_1 = r\tau_2 = r^2\tau_3$

c) The number of equations M for the set of equations is selected; this number must be larger than 2m + 3 but smaller than the number of data sets. Usually, 15 to 40 equations are enough. That means that at least 30 to 100 data points are needed.

d) The minimum and maximum values of the time constants are determined. Since the computer has a limited accuracy, there is no sense in handling time constants smaller than $\Delta t/10$. On the other hand, p = N - M points are needed for integration. This integration will not be terminated if the time constant is larger than p Δt. It is best to choose the largest time constant lying between $\Delta t/10 < \tau 1 < p\ \Delta t/2$

e) In this interval, estimates Z*of the vector Z for several time constant values are computed. For each value of z*, the estimate q* of the heat flow vector will be computed by

$$q_* = (X)\ Z^*$$

f) The total square deviation between this estimate and the measured values is computed by

$$S^2 = (q - q^*)^2 = \Sigma (qi - qi^*)^2$$

g) The best time constant set is the one giving the smallest square deviation, can be found by repeating steps e) and f) above.

h) The best estimate, Z*, of the vector Z is found in this way. Its first component, Z1 is the best estimate of the conductance (or the transmittance if air temperature is used).

If the largest time constant found for the best estimate is equal to (or greater than) the maximum value, ($p\ \Delta t/2$), the number of equations or the measurement time are not large enough to give a reliable result with this data set and this ratio between time constants. Changing the number of equations or the ratio of increasing (sometimes also by decreasing) the number of data sets may overcome this difficulty.

Quality criteria are needed to indicate confidence in the results when a single measurement is used to estimate the U-value. They have to be such that, if they are fulfilled for a given, unique measurement, there is good confidence (e.g. 90 % probability) that the result will be close enough to the actual value (e.g. within ± 10 %).

In the case of the simple analysis method, the only criterion is that the measurement time is long enough. Of course, if the recorded data show a quasi-steady state, the measurements have a high probability of giving a good result. However, if the temperatures of heat flow varied substantially just before the beginning of measurements, the final result would be erroneous, if the measurement time is not long enough to ignore the preliminary measurements. A criterion exists in the case of

the dynamic interpretation method. The confidence interval for the estimate of the conductance described above is

$$I = \sqrt{.}\left[\frac{S^2 Y(1,1)}{M - 2m - 4}\right] F\,(P, M - 2m - 5)$$

Where,

S^2 is the total deviation obtained by equation.

Y (l, l) is the first element of the inverted X Matrix.

$$(y) = [(X)'(X)]^{-1}$$

M is the number of equations in system and m the number of time constants;

F is the significance limit of the student t-distribution, where P is the probability and (M - 2m – 5) is the degree of freedom.

If this confidence interval for P = 0.9 is smaller than, for example, 5 % of the conductance, the computed conductance is generally very close to the actual value, which is in this case the value obtained under good conditions (night-time steady state for light elements, long measurements for heavy ones), for a given measurement time, the smaller the confidence interval, the narrower the distribution of the results of several measurements.

Figure 2.3 illustrates the procedure involved in dynamic method calculations.

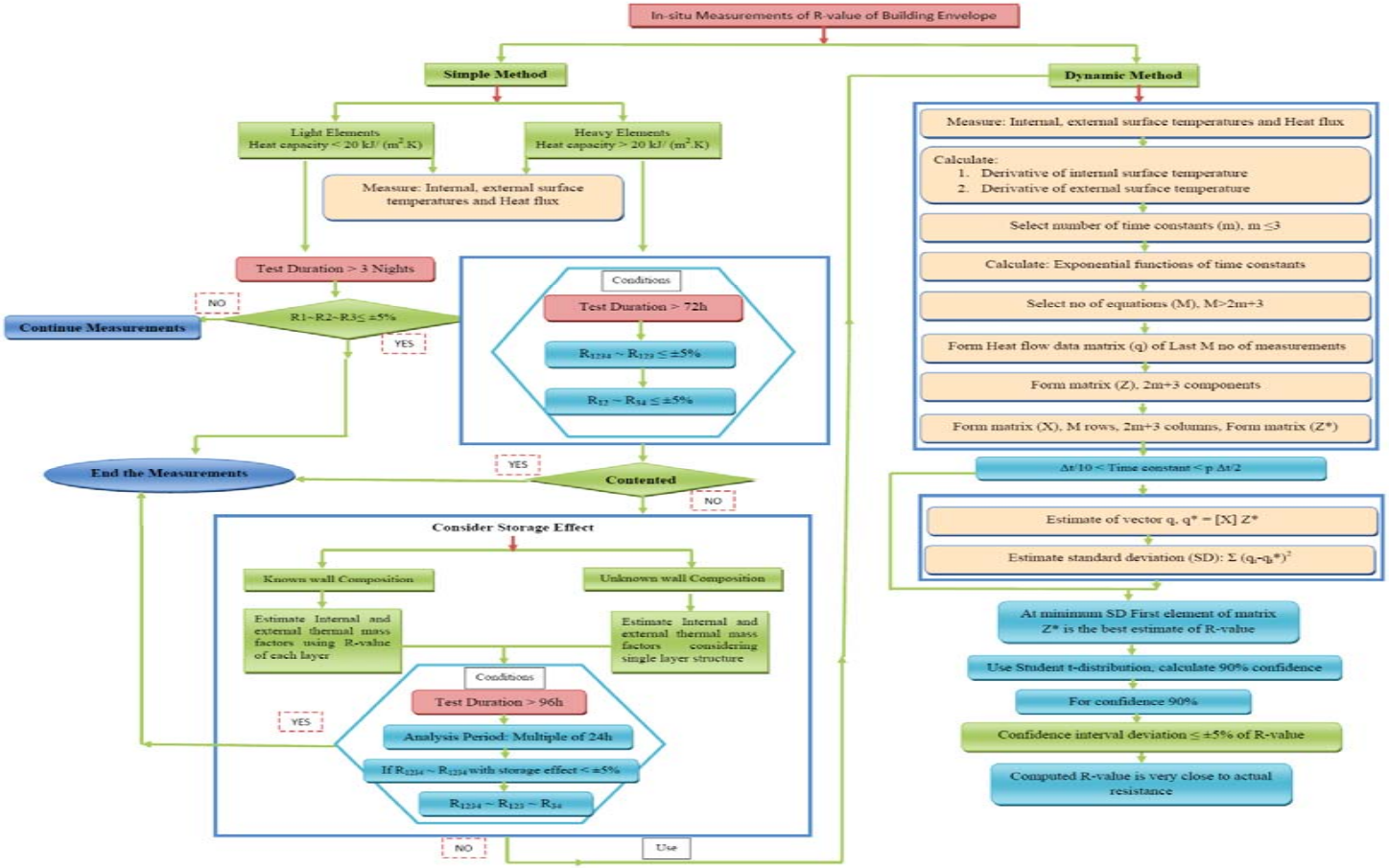

R, Resistance
R1234, R first 4 days
R123, R first 3 days
R12, R first 2 days
R34, R last 2 days
Z*, Estimate of Vector Z
Δt, Time interval between two measurements in seconds
P, N-M
N, number of data sets

Figure 2.3 In-situ Measurements of R-value of Building Envelope

CHAPTER THREE

3 INSTRUMENTS, PROCEDURE AND MEASUREMENTS

This chapter includes the essential features and characteristics required in thermal imaging device, features various available ThermaCam, and also describes the various heat flux measurement instruments, features, and measurement procedures. It also describes the systematic procedure for conducting thermographic measurements of building envelope using infrared thermography.

3.1 Infrared Device Selection and Characteristics

There are wide ranges of infrared devices available for various applications such as buildings, military, maritime night vision, gas detection and automation etc. However, the following are the required few essential and basic characteristics needed to be considered for the selection of the infrared device suitable for building envelope IR investigations. These are

- High resolution/ Image quality
- Wide temperature (-10 to +55 ^{o}C) with sensitivity less the 0.1^{o}C
- Intelligent battery system, easily chargeable and long life battery
- Text and voice annotations
- Output standard JPEG format
- Light weight and ergonomic
- Built in laser pointer

- Incorporated emissivity tables
- Automatic maximum temperature difference calculation
- Temperature sound, image alarms
- Software compatibility and upgrade potential
- Direct access buttons
- Large LCD screen
- Upgrade potential
- Panorama support: Take images in a sequence and automatically combine them to one large image using the FLIR BuildIR
- Flexible interface: Easy access to composite video connection, USB, FireWire, and a direct connection to charge the battery inside the camera.
- Dew point alarm or insulation alarm
- Strong post sale technical support and certified training

3.2 Infrared Devices

There are various infrared devices available such as Flir i3, Flir i5, Flir i7, Flir B series, Flir b series, Flir B620, Flir B20, Flir B250/425 and Flir B660 etc. some of them for example Flir B250 have almost all the features stated above including panorama support, Flir B20 does not have feature like panorama support, and flexible interface. **Figure 3.1** illustrates various examples of thermal imaging devices. However for this case study infrared device selected is ThermaCam B20, due to its availability within the university. It is specially developed by FLIR Systems for demanding and professional building inspections. It has all the features that are indispensable for performing building inspections, and the necessary software to make professional inspection reports. The ThermaCam B20 measures temperatures in the range of -40°C to +120°C. ThermaCam B20 incorporates emissivity tables to make

correct temperature measurements, provides extraordinary image quality with the built in state-of-the-art micro bolometer detector with 0.08°C temperature differences accuracy. Equipped with intelligent Li-Ion battery, it gives autonomy of over 2 hours (FLIR Systems Manual, 2009). During the investigations a tripod must be utilized to fix the camera, which helps the investigator to take the thermal images with better accuracy. Figure 3.2 illustrates a generic setup for conducting infrared measurements.

Figure 3.1 Various types of thermal imaging devices

3.3 Infrared Device Setting

Following are basic camera settings need to be performed before conducting the measurements.

a) The camera on a Tripod need to be fixed for better and accurate measurement, when the display provided with the camera is very small and not enough for normal human eyes to find tiny defects in the envelope, an LCD monitor is preferably required to be connected to the camera for large display, it also provides better and accurate measurement of defective areas. For long time measurements an extra battery of the camera is required.

b) Temperature Range Settings: Two types of temperature measurement ranges are available with ThermaCam B20. One is -40oC to 55oC, and second is from -40^{o}C to 120^{o}C, we must select the appropriate range depending on the

climatic conditions, for example in the peak summer (Dhahran City) the outside surface temperature of the building envelop can go beyond 55^{o}C, This can be found by doing dummy measurements- Take an thermal image of the surface of the building envelope, if the average temperature on any selected area on the surface of the envelope is more than 50^{o}C, (Average temperature for selection can be computed using ThermaCam Softwares) select the higher temperature range of -40^{o}C to 120^{o}C and for all other seasons the lower range can be selected for better accuracy.

c) Focus control settings: Auto focusing the camera, the camera needs to kept steady while auto focusing.

d) Emissivity settings: the appropriate emissivity value for the building surface is to be selected based on the color and surface finish. It is possible to set an approximate emissivity value in advance before measurements, although emissivity value is not correct, it does not affect the last test result. Because emissivity value can be modified by means of software and the correct test result can be obtained after inserting the accurate emissivity value in the software, this can economize in-field work time.

e) Emissivity settings: the appropriate emissivity value for the building surface is to be selected based on the color and surface finish.

f) When conducting measurements for same building, the camera settings need not to be changed, as this makes comparison easier for the various similar surfaces.

3.4 Infrared Measurements Procedure and Requirements

A. Measurement conditions (indoor and influence of the environment)

Information concerning to Environmental conditions such as outside air temperature, relative humidity, cloudiness and any moisture on the outside of the building, together with wind conditions, shall be recorded.

The temperature drop across the building envelope should be sufficiently large to permit the detection of thermal irregularities, for ease of interpretation, the thermographic examination should preferably be carried out with constant temperature- and pressure drops across the envelope. (The interpretation of Thermograms taken under non-steady state conditions requires a higher degree of expertise and knowledge of building physics.) This implies that

- The measurement should not be carried out when the outside or inside air temperature is liable to vary considerably
- The measurement should not be carried when the wall/roof system is exposed to direct solar radiation
- The measurement should not be carried when the wind varies noticeably (ISO 6781- 1983).

The actual pressure condition inside a building is usually caused by a combination of wind condition, ventilation system, thermal differential pressure (temperature difference between air inside and outside). Wind conditions can vary substantially over time and between relatively closely situated locations, thus such variations can have a clear affect on thermographic measurements. It has been demonstrated experimentally that the differential pressure on a façade exposed to an average wind force of about 5m/s will be about 10pa.

The following requirements are likely to ensure approximate steady state conditions for a light weight building structure (e.g. residential buildings), when the thermographic measurements are to be carried out from the inside:

a) For at least 24 hrs before the start of the thermographic measurements the indoor conditions are to be constantly maintained at suitable temperature, and during the measurements, the air temperature drop across the building envelope is required to be at least 10^{o}C. During the same period, the air temperature drop shall not vary more than + 30 % from its value at the start of the measurements. During the examination, the indoor air temperature shall not vary by more than 2^{O}C (ISO 6781- 1983).

b) For residential buildings thermographic measurements should be conducted during uniform outdoor temperature, and make sure that building envelope is not directly exposed to direct solar radiation.

If possible, heat sources that might interfere with the measurements should be shut off before the start of the measurements. Lights directed at or placed near the surface being measured should be shut off during the measurements in order avoid their reflection on the thermographic image. Furniture, picture frames, etc., that might influence the result, should be removed so that the test areas are free. Also be aware of the water piping inside the walls, and electrical installation inside the wall.

Measurement surface (Wall/Roof) must be free of pictures, furniture, clocks or other objects that prevent a direct view of the walls surface. If these must be removed, do it 2 to 4 hours prior to measurement. Avoid measuring wall surfaces with conditioned air blowing directly on them. Avoid measuring solar loaded walls. Do them before the sun hits them or wait several hours after the sun is off the wall. Avoid rainy and windy conditions.

B. Steady state conditions

Measurements must be conducted during steady state conditions. Here steady state condition means when the inside to outside temperature difference is reasonably constant for at least 3 to 4 hours for the measurement.

The examination shall be started by performing a preliminary test over the surface of the envelope. Parts of the surface of special interest, or parts exhibiting anomalies, shall be studied in detail. Thermograms shall be taken of selected parts of the envelope under investigation (parts which are free from defects as well as parts where it is suspected that construction defects.

C. Date and time of measurement

Date and time of the measurement is to be noted for future reference The measurements were conducted during the period 18th July to 11th August, and for Dhahran climate it is recommended to conduct measurements between 5pm and 12pm. to avoid the effect direct solar radiation on the measurement surface and during this time the temperature does not vary rapidly indicating a steady state outside temperature and, the difference in temperature between indoor and outdoor conditions in this time temperature difference will be about 10^{o}C or higher, which is essential for better and accurate measurements.

D. Temperature

At the start and end of the measurements, one needs to determine the inside and outside air temperature to an accuracy of ±1^{O}C, and input to the camera. It also helps in selecting the temperature range in the camera. In the thermal image the temperature scale is displayed on the right hand side of the screen, the scale shows the colors distribution along the various temperatures in the image, with high temperatures at the

upper and the low temperature at the lower end. For accurate measurement of thermal resistance values for this study three indoor and three outdoor temperature sensors were installed, the average of the three were used for calculation purpose.

E. Relative humidity (RH)

At the start and end of the measurements, one needs to determine the inside and outside relative humidity, the camera also compensates of relative humidity for the fact that transmittance is also dependant on the relative humidity of the atmosphere. For short distance and normal humidity the RH can normally be left at a default value of 50% (FLIR Systems Manual, 2009).

F. Pressure

At the start and end of the measurements, one needs to determine accurately the inside and outside pressure difference to make sure that steady state condition was there during the measurement because the differential pressure variations can have a clear affect on thermographic measurements. The recommended negative pressure across the building for thermographic measurement is 10-50pa. When the pressure drop across the envelope is to be determined, it is recommended that this be measured to an accuracy of ±5 Pa (for a low pressure drop ±2 Pa) over the leeward and windward side for each storey. The pressure drop across the building envelope was found to be varying between 11-16pa during the measurement time.

G. Air velocity

Measure the indoor and outdoor air velocity before and after the measurements. Air velocity can be used to find the rate of convective heat transfer under forced convection. Also it is needed to confirm the steady state conditions. For indoor

measurements avoid the direct flow of air from the ac duct on the measurement wall for better and reliable measurements.

H. Emissivity of building material

Emissivity is a very important parameter to be set correctly. It is a measure of how much radiation is emitted from the object, compared to that from a blackbody of the same temperature. Object materials, surface treatments exhibit emissivity ranging from approximately 0.1 to 0.95 (FLIR Systems Manual 2009, Yogzheng 2006). Emissivity values vary for different wavelengths and they are directly related to the materials surface condition and temperature. Randomly selected emissivity values may lead to incomplete assessment (N. Avdelidis and A. Moropoulou, 2002).

Emissivity value of the common building materials in a range of 0.7 to 0.95, select the suitable emissivity value for the building envelope (Yongzheng et.al 2006). For this study purpose the test wall was painted with white paint of emissivity 0.9 for simplicity in thermography measurements.

I. Reflected apparent temperature (RAF)

It is the general term for the perceived outdoor temperature, caused by the combined effects of air temperature, relative humidity and wind speed. This parameter is used to compensate for the radiation reflected in the object.

RAF is determined by using the thermal imaging camera, to determine the RAF, first crumble a large piece of aluminum foil, uncrumble the aluminum foil and attach it to a piece of the cardboard of same size, now put the piece of the cardboard in front of the object under investigation, and make sure that the side with aluminum foil points to the camera, set emissivity to 1.0 and measure the apparent temperature of the foil

(RAF). (This complies with ASTM 1862-97 and ISO 18434-1 standards), with proper RAF and proper emissivity, obtain the temperatures of other areas of interest.

J. Distance between the object and envelope

Distance between the object and front lens of the camera, is used to compensate for the following two reasons:

- That radiation from the target is absorbed by the atmosphere between the object and the camera.
- The radiation from the atmosphere itself is detected by the camera.

Distance between the object and the camera varies with each building, depends on the free space available around the object/ size of the room for indoor measurements. Once the thermal image of a wall/ roof is captured, if there is any irregularity in the surface temperature is noticed, then a more detailed measurement of that particular area is to be conducted from the nearest location possible.

K. Thermographic image recording

The measurement should be started by performing a preliminary test over the surface of the envelope. Parts of the surface of special interest, or parts exhibiting anomalies, shall be studied in detail. Thermograms shall be taken of selected parts of the envelope under investigation (parts which are free from defects as well as parts where it is suspected that construction defects are present). The positions of the parts represented on the thermogram should be indicated on a plan/sketch of the building.

Deviations and irregularities in the appearance of a thermogram often indicate a defect in the building envelope. The appearance of a thermogram relating to a construction with a defect may vary considerably. Finally, take and IR image of the outside surface and standard target

L. Digital image recording/ photo

The corresponding photo of the same surface for which the thermographic image is taken can be recorded, and the photo can be used for visual localization of defects and analysis. The thermal imaging camera used for the study had the built-in digital camera which allows taking the thermal imaging and digital photo at the same time without changing the position of the camera, so as to have similarity in the images for later reference for exact location of the defects.

A measurement form as shown in **Figure 3.2** is developed based on the literature review for onsite inspections and measurements, to note the environmental conditions and other important factors, the form also points out the various devices and instruments required during thermographic inspection of buildings.

BUILDING ENVELOPE THERMOGRAPHIC ON-SITE INSPECTION AND MEASUREMENTS

Equipments/ Instruments needed for Inspection: ***Date:*** _____ ***Time:*** _____

☐ ThermaCam	☐ LCD monitor	☐ Tripod	☐ Digital Thermometer	☐ Pressure gauge	☐ Air Velocity meter
☐ Digital Camera	☐ Aluminum Foil	☐ Measuring Scale	☐ Double side tape	☐ Compass	☐ Measuring tape/ Ultrasonic (Laser) distance measurer

Thermographer: _____ Building type: _____ Location: _____ Building Reference Number: _____

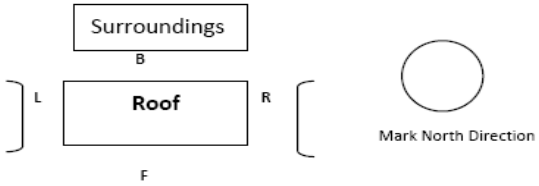

Notes:

INDOOR MEASUREMENTS	T image file, Digital Image file	OUTDOOR MEASUREMENTS	T image file, Digital Image file
Material: _____ F __ °C, ___%, ___ (m/s) ___∈, ___m, ____RTF °C, ___Pa, _____, _____	(____Pa)	F __ °C, ___%, ___ (m/s) ___∈, ___m, ____RTF °C, ___Pa, _____, _____	
Color: _____	**(pressure Difference)**		_____, _____
Material: _____ B __ °C, ___%, ___ (m/s) ___∈, ___m, ____RTF °C, ___Pa, _____, _____	(____Pa)	F __ °C, ___%, ___ (m/s) ___∈, ___m, ____RTF °C, ___Pa, _____, _____	
Color: _____	**(pressure Difference)**		_____, _____
Material: _____ L __ °C, ___%, ___ (m/s) ___∈, ___m, ____RTF °C, ___Pa, _____, _____	(____Pa)	F __ °C, ___%, ___ (m/s) ___∈, ___m, ____RTF °C, ___Pa, _____, _____	
Color: _____	**(pressure Difference)**		_____, _____
Material: _____ R __ °C, ___%, ___ (m/s) ___∈, ___m, ____RTF °C, ___Pa, _____, _____	(____Pa)	F __ °C, ___%, ___ (m/s) ___∈, ___m, ____RTF °C, ___Pa, _____, _____	
Color: _____	**(pressure Difference)**		_____, _____
Material: _____ ROOF __ °C, ___%, ___ (m/s) ___∈, ___m, ____RTF °C, ___Pa, _____, _____	(____Pa)	F __ °C, ___%, ___ (m/s) ___∈, ___m, ____RTF °C, ___Pa, _____, _____	
Color: _____	**(pressure Difference)**		_____, _____

Figure 3.2 Building Envelope Thermographic On-Site Inspection and Measurement form

3.5 Heat Flux Instrument Selection and Characteristics

There are wide ranges of data loggers available for various applications such as buildings, geotechnical, geothermal energy and bridge monitoring etc. However following are the required few characteristics of data loggers with reference to building application.

- Flexible power and communication options, preferably wireless communications
- Large internal memory, and expandable with add-on memory systems
- Software compatibility with Logger Net, PC400, or latest programs
- Communicates via various options: TCP/IP, email, FTP, web server
- Keyboard and display unit with the device for onsite programming and controlling
- Compatibility with sensors
- Scan Rate: once per second
- Long backup battery support

3.6 Data Logger Devices

There are various data loggers available such as CR10, CR10X, CR200, CR 1000, and CR 3000 etc. CR 1000 measures more sensors than any other data logger (http://www.campbellsci.com/dataloggers). **Figure 3.4** illustrates various examples of data logger devices. However for this case study data logger selected is CR 10X, due to its availability within the university.

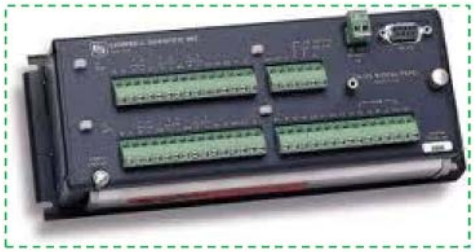

CR 10X Series Data Logger

CR 1000 Series Data Logger

CR 200X Series Data Logger

CR 3000 Micro logger

Figure 3.3Various types of data loggers

A multiplexer AM 16/32 is used to connect more number of sensors, for 3 sets of complete measurements at a time. **Figure 3.4** illustrates the setup of heat flux meter, multiplexer, battery and various sensor connections.

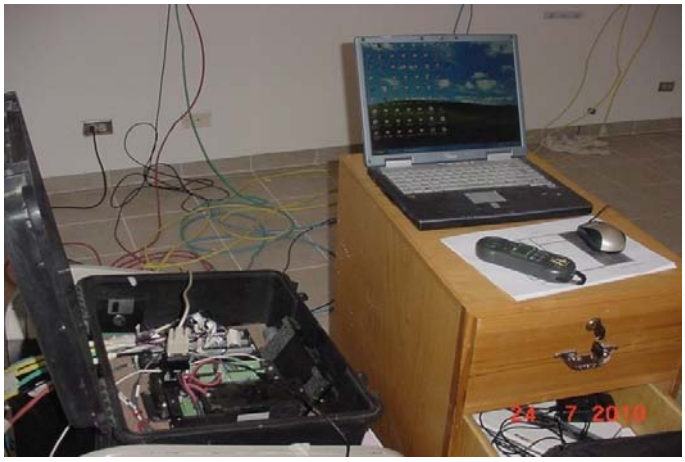

Figure 3.4 Heat flux meter setup

3.7 Heat Flux Sensors

A heat flux sensor is a transducer that generates an electrical signal proportional to the total heat flux over the surface of the sensor. The measured heat flux is divided by the fixed surface area of the sensor to determine the heat flux density. Two types of heat

flux sensors (HFS) used in the study are BF-03 and HFP01 soil heat flux plate, the specifications are mentioned in **Table 3.1**.

Table 3.1 Specifications of the Heat Flux Sensors and Thermocouples ***(http://www.vatell.com/bfsensor.htm, and*** www.campbellsci.com/documents/manuals/**hfp01**.pdf***)***

Heat Flux Transducer Type	***BF-03***
Size	5.1cm x 5.1cm (2inch x 2inch)
Active Area	22.42 cm^2 (4.7cm x 4.77cm)
Sensor Thickness (adhesive tape is 0.127mm thick)	0.2mm
Thermal Resistance	0.0008 $m^2.^oK/W$
Sensitivity	50 mV / (W/cm^2)
Response Time	~ 0.9 sec
Max. Temp. (ºC)	150 (ºC)
Heat Flux Transducer Type	***HFP01***
Size	Dia 80mm (3.15 in)
Measurement range	± 2000 W/ m2
Sensor Thickness	5mm (0.2 in)
Thermal Resistance	<0.00625 m2.ºK/W
Sensitivity	50 µV / (W/m2)
Nominal Resistance	2 W
Max. Temp. (ºC)	70 (ºC)
Thermocouples Type	T type, 0 to 350°C

Figures 3.5 illustrate two types of heat flux sensors, which were used for conducting the measurements.

(a) (b) (c)

Figure 3.5 Heat Flux Sensors

Figure 3.5 (a) illustrates BF-03 senor, (b) illustrates HFP-01 heat flux sensors and (c) illustrates the drawing in which 1 indicates the sensor area, 2 indicates the guard of ceramic-plastic composite, and 3 indicates cable.

3.8 Selection of Residential Building

Building selected is an existing residential building located on KFUPM campus, Dhahran, Saudi Arabia. The building was constructed around 15 years back. The building envelope selected for the study is originally non insulated, but for study purpose and for conducting the measurements of thermal conductivity with various material using heat flux instrument and thermal imaging technique, three types of insulations were installed on the one of the selected wall. The building is centrally air conditioned, to achieve constant and steady state conditions during the measurements.

A. Characteristics of building envelope

- Drawings and other construction related documents relating to the building envelope has been studied to know about the wall, roof construction details and other related information of the building envelope.
- The geographical orientation of the building. The entrance of the selected building is facing south-west Direction.

3.9 Building Description

The total floor area of the building is 71m2, consisting of one living/dining hall, one bedroom, one kitchen, and one washroom, its floor-to-floor height is 2.77m. The walls of the building were composed of 200mm heavy wt hollow, 20mm cement plaster with sand on both sides. The roof consists of 25mm cement mortar, 50mm sand screed sloping, asphalt roofing roll, 200mm heavy wt concrete dried aggregate, and 20mm

cement plaster with sand. The windows are 6 mm single clear glazing with interior shading of venetian blinds. The HVAC system used in the building is packaged constant air volume (CAV) system. **Figure 3.6** illustrates the building layout. **Figure 3.** illustrates the building cross section. **Table 3.2** describes the building characteristics.

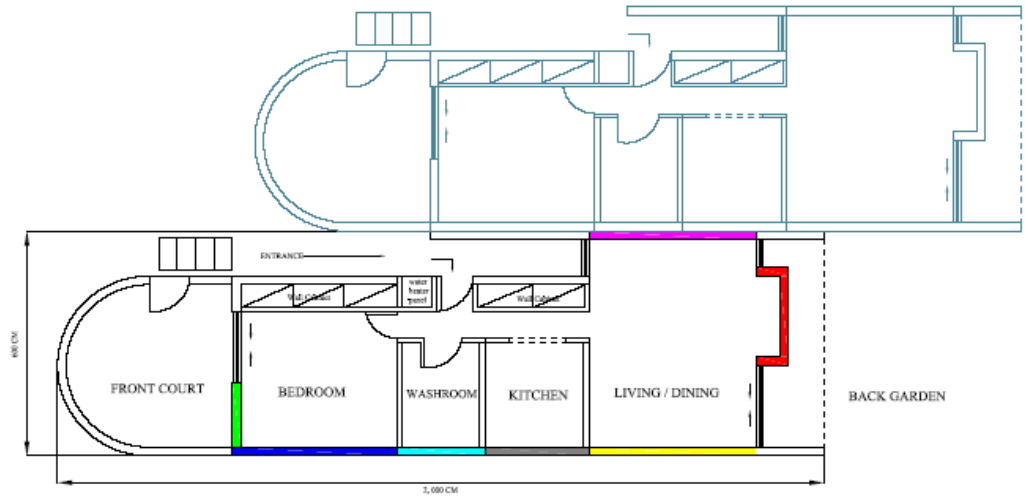

GROUND FLOOR PLAN HOUSE 3401 - FAROOQ COURT

East North

Figure 3.6 Building layout

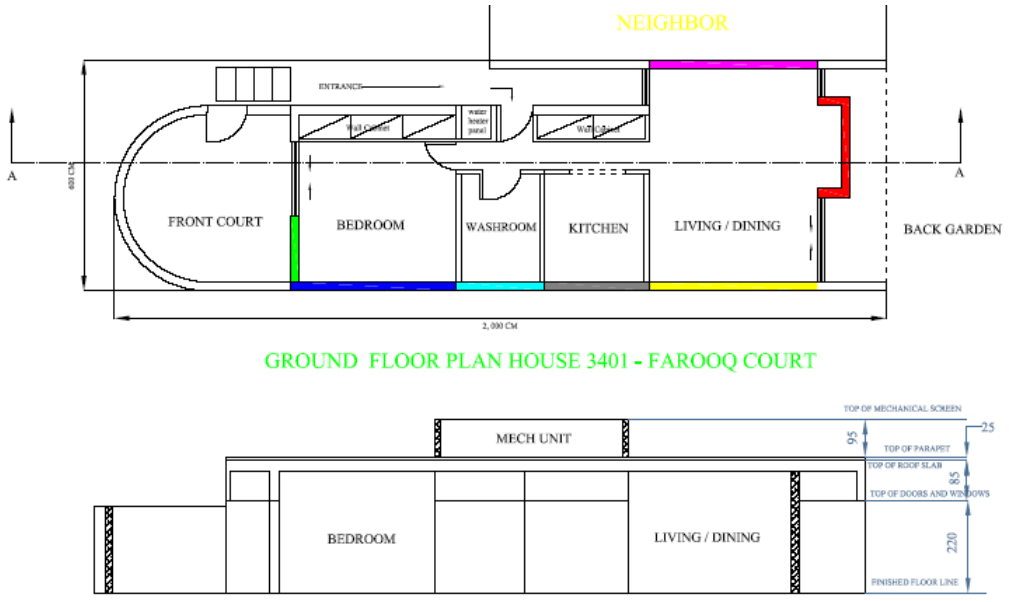

Figure 3.7 Building layout and cross section

Table 3.2 Building Description

Characteristics	Description of the Base Case
Location	Dhahran (26.27 N latitude, 50.15 E longitude, and 17m above sea level)
Orientation	Front Elevation facing South East
Plan Shape	Polygon
Number of floor	One
Floor to Roof Height	2.77 m (Finish floor line)
Conditioned Floor Area	71 m^2 (70.52)
Gross Wall Area	117 m^2
Wall Area	100 m^2
Window Area	17, 14.5%
Type of Glass	6 mm Single Clear glazing + Venetian Blinds
Solar Absorbance (for Exterior Surfaces)	0.7
Exterior Walls	200mm Heavy Wt Hollow + 20mm cement plaster with Sand on both sides
Roof	25mm Cement Mortar+50mm Sand Screed Sloping+ Asphalt Roofing Roll + 200mm Heavy Wt Concrete Dried Aggregate+ 20mm Cement Plaster with Sand
Floor	100mm Heavy Wt Concrete Dried Aggregate + 50mm Sand Screed Sloping+ 25mmCement Mortar +25mm Terrazzo Tile
Occupancy	2 Persons
Lighting Power	780W

Equipment Power	600W
Infiltration	0.5 ACH
System Type	Packaged constant air volume (CAV)
Thermostat Setting	22
Weather File	Dhahran:2002

3.10 Construction of Test Wall

For this study a wall was selected facing North East (to avoid the effect of solar radiation), of Size 4 meters X 2.77 meters, the original composition of the wall was 200mm Heavy Wt Hollow, 20mm cement plaster with sand on both sides. For the study purpose the wall composition is been changed by adding the different insulations and gypsum board. Three different types of insulation have been used namely, expanded polystyrene, extruded polystyrene, and fiber glass to conduct measurements with different wall compositions, and to apply the measurement and analysis to different wall compositions. (Properties of these insulation materials are illustrated in Appendix B. Now the wall has been modified in such a way that, it should represent three different types of wall by adding 50mm insulation of different types for a length of 1.2 meter each approximately, and a gypsum board is being used to cover insulation. The wall was then painted white (0.9 Emissivity) to avoid the difficulty of finding the emissivity of wall surface. **Figure 3.8** illustrates the thermal images and digital photos of the building. **Figure 3.9** illustrates the test wall construction, and **Figure 3.10** illustrates the various measurement points within the test wall.

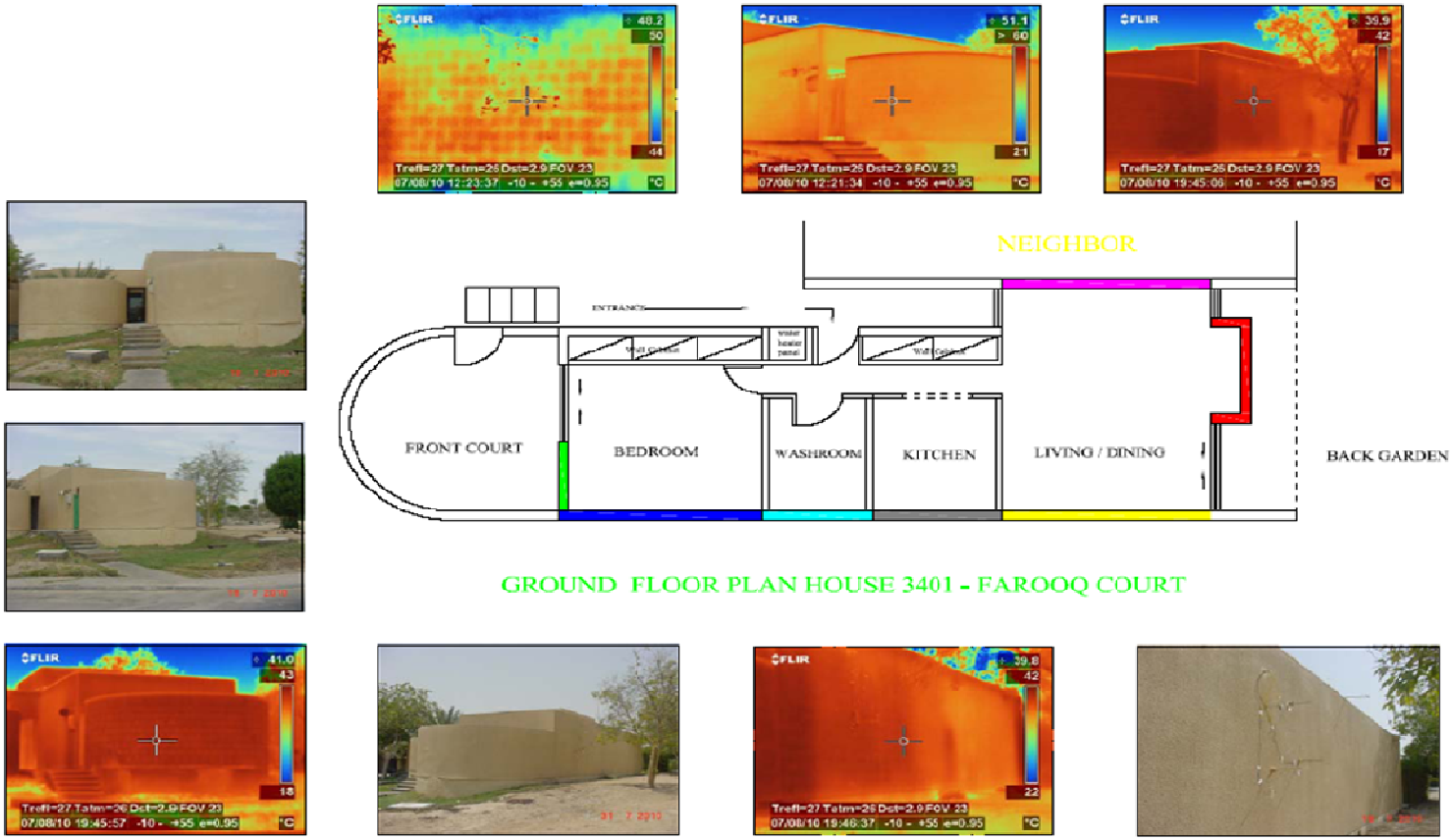

Figure 3.8 Building layout with digital photographs

Figure 3.9 Test wall construction

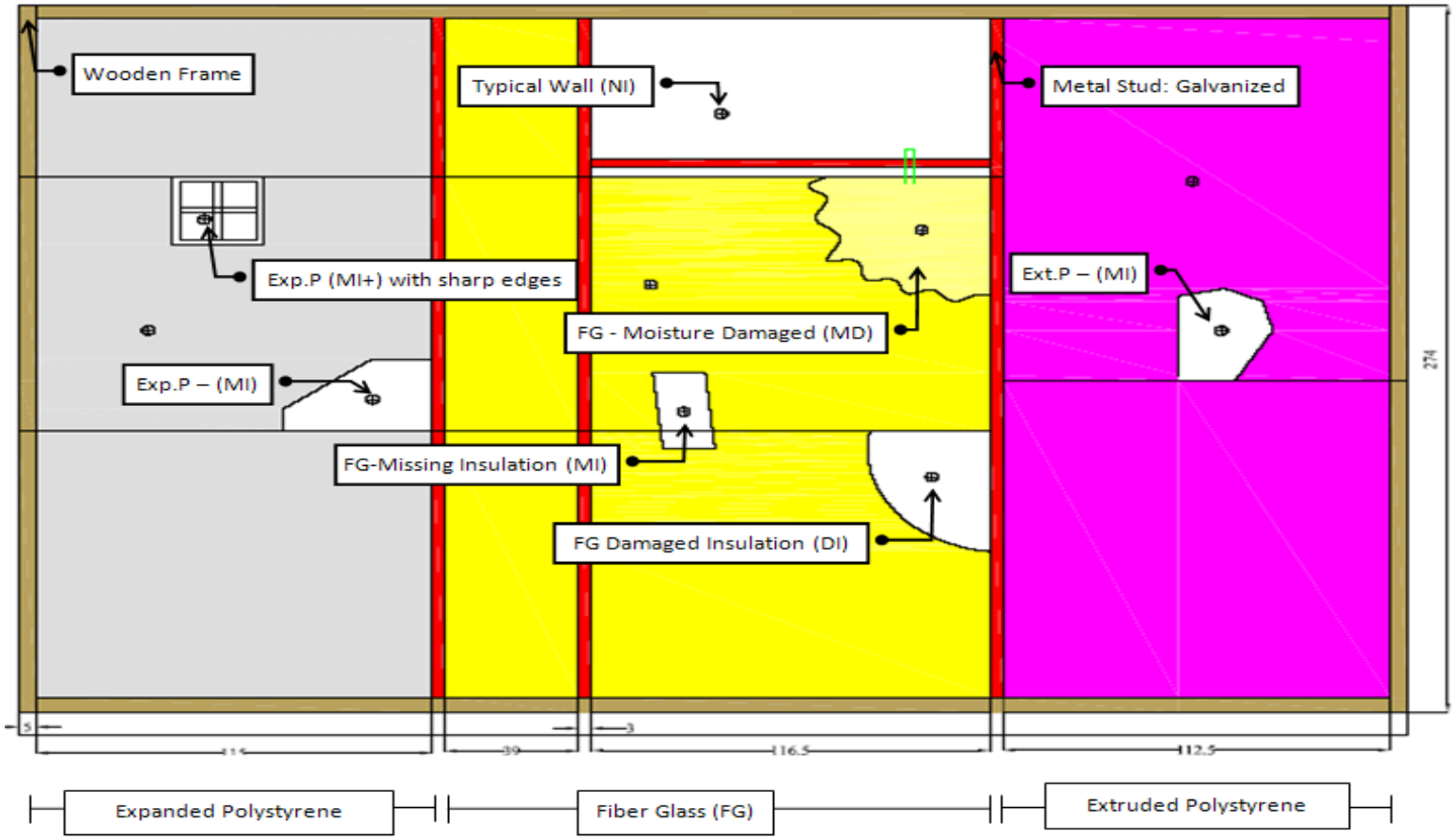

Figure 3.10 Measurement points on test wall

3.11 Measurement of Thermal Conductivity 'K' Using Holometrix

As stated, three different types of insulations and one type of gypsum board have been used for the construction of the wall, the K value for these materials were found using the heat flow meter (Holometrix, Type Lambda 2300V) following the ASTM C518 and ISO 8301 standards.

The maximum dimensions for the specimen is 300mm X 300mm X 100mm. The heat flow meter can test specimen with thermal conductivity range of 0.05 to 0.5 W/m-K, the test specimen must be kept in the normal room temperature (21-23 ^{o}C for at least 24 hours before testing.

A. Procedure for conducting the test

The density of sample insulation material in kg/m^3 is determined by measuring its actual dimensions, (determine its volume accurately). The exact thickness can be obtained by thickness transducer of the lambda instrument, then weigh the sample accurately by using a sensitive digital weighing machine. The specimen (of size 300mm X 300mm X 50mm thick is used in this test), is placed in the test section between two plates and the conditions are set so that the plate will attain different, constant temperatures. Due to the temperature difference across the specimen, heat flows through the specimen from the hotter plate to the cooler plate.

An external PC controls the Lambda heat flow meter. When the instrument reaches thermal equilibrium, the temperature of each plate, temperature gradient across the specimen, heat flow through the specimen are constant, when these values are constant, the specimen determines the thermal conductivity of the test specimen. The

detailed test reports are in presented in Appendix B. **Figure 3.11** illustrates the setup of Holometrix Instrument.

Figure 3.11 Holometrix Instrument and Setup

3.12 Estimated Components of Test Wall

The theoretical values of thermal conductivity, thermal resistance of cement plaster with sand aggregate, 50mm Air gap, and interior and exterior film coefficients are taken from ASHRAE fundamentals 2005. Insulation thermal resistance values were measured utilizing Holometrix instrument. **Table 3.3 to Table 3.9** describes the various compositions of the wall systems considered in the study, roof, and floor systems with their theoretical thermal resistance values.

Table 3.3 The estimated components of the FG-A wall system

Equivalent Wall		**FG-A Wall components**	Thickness (**TH**), mm	**K**, W/m.C	**R**, m^2.C /W	
	Exterior	Exterior Air Film			0.040	
		Cement Plaster w/ Sand	20	0.7200	0.028	**0.246**
WALLs		CMU Heavy Wt. Hollow	200	1.0500	0.190	
		Cement Plaster w/Sand	20	0.7200	0.028	
	Interior	Interior Air Film			0.120	
		Total **TH**	**240**	Total **R**	**0.406**	

Table 3.4 The estimated components of the FG-B wall system

Equivalent Wall		FG-B Wall components	Thickness (**TH**), mm	**K**, W/m.C	**R**, m^2.C /W	
	Exterior	Exterior Air Film			0.040	
		Cement Plaster w/ Sand	20	0.7200	0.028	**0.486**
WALLs		CMU Heavy Wt. **8"** Hollow	200	1.0500	0.190	
		Cement Plaster w/Sand	20	0.7200	0.028	
		Air Gap	50	0.0250	0.160	
		Gypsum Board	13.3	0.1653	0.080	
	Interior	Interior Air Film			0.120	
		Total **TH**	**303.3**	Total **R**	**0.646**	

Table 3.5The estimated components of the FG-D wall system

Equivalent Wall		FG-D Wall components	Thickness (**TH**), mm	**K**, W/m.C	**R**, m^2.C /W	
	Exterior	Exterior Air Film			0.040	
		Cement Plaster w/ Sand	20	0.7200	0.028	**1.826**
WALLs		CMU Heavy Wt. Hollow	200	1.0500	0.190	
		Cement Plaster w/Sand	20	0.7200	0.028	
		Fiber Glass	50	0.0334	1.499	
		Gypsum Board	13.3	0.1653	0.080	
	Interior	Interior Air Film			0.120	
		Total **TH**	**303.3**	Total **R**	**1.986**	

Table 3.6 The estimated components of the Exp-P wall system

Equivalent Wall		Exp.P Wall components	Thickness (**TH**), mm	**K**, W/m.C	**R**, m^2.C /W	
	Exterior	Exterior Air Film			0.040	
		Cement Plaster w/ Sand	20	0.7200	0.028	**1.544**
WALLs		CMU Heavy Wt. Hollow	200	1.0500	0.190	
		Cement Plaster w/Sand	20	0.7200	0.028	
		Expanded Polystyrene (White)	50	0.0411	1.217	
		Gypsum Board	13.3	0.1653	0.080	
	Interior	Interior Air Film			0.120	
		Total **TH**	**303.3**	Total **R**	**1.704**	

Table 3.7 The estimated components of the Ext.P wall system

Equivalent Wall		Ext.P Wall components	Thickness (**TH**), mm	**K**, W/m.C	**R**, m^2.C /W	
	Exterior	Exterior Air Film			0.040	
		Cement Plaster w/ Sand	20	0.7200	0.028	**1.964**
WALLs		CMU Heavy Wt. Hollow	200	1.0500	0.190	
		Cement Plaster w/Sand	20	0.7200	0.028	
		Extruded Polystyrene (Pink)	50	0.0305	1.638	
		Gypsum Board	13.3	0.1653	0.080	
	Interior	Interior Air Film			0.120	
		Total **TH**	**303.3**	Total **R**	**2.124**	

Table 3.8 The estimated components of the Roof system

		Roof Components	Thickness (**TH**), mm	**K**, W/m.C	**R**, m^2.C /W	
	Exterior	Exterior Air Film			0.040	
		Tiles, Terrazzo, 1"	25	1.77	0.014	**0.299**
		Cement Mortar, **1"**	25	0.71	0.035	
ROOF		Sand/ Screed Sloping, **2"**	51	1.35	0.038	
		Asphalt Roofing Roll	-	-	0.026	
		Heavy Wt. Concrete, Dried Aggregate **8"**	203	1.35	0.150	
		Cement Plaster w/Sand, **1"**	25	0.71	0.035	
	Interior	Interior Air Film			0.107	
		Total **TH**	**329**	Total **R**	**0.446**	

Table 3.9 The estimated components of the Floor system

		Floor Components	Thickness (**TH**), mm	**K**, W/m.C	**R**, m^2.C /W	
	Exterior	Exterior Air Film			0.040	
		Heavy Wt. Con, Dried Aggregate 4**"**	152	1.90	0.080	**0.167**
		Sand/Screed Sloping, **2"**	51	1.35	0.038	
FLOOR		Cement Mortar, **1"**	25	0.71	0.035	
		Tiles, Terrazzo **1"**	25	1.77	0.014	
	Interior	Interior Air Film			0.162	
		Total **TH**	**253**	Total **R**	**0.369**	

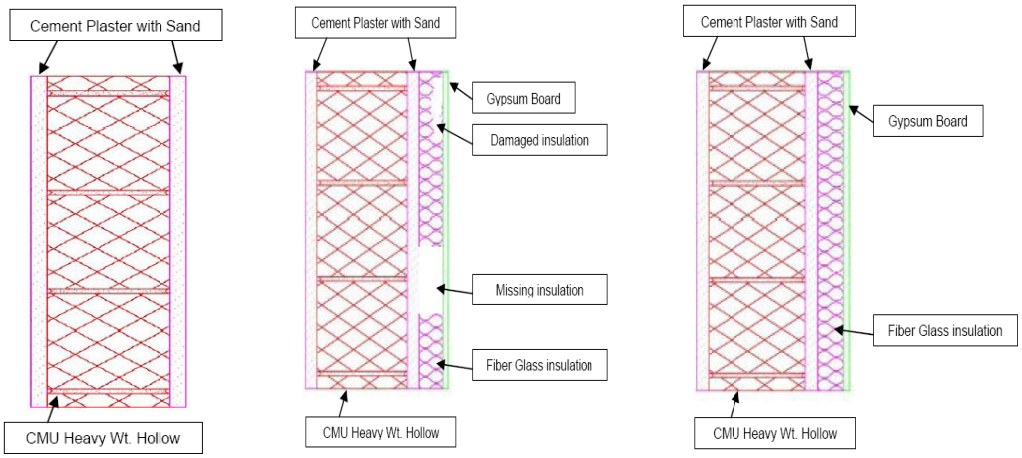

Figure 3.12 Cross section FG wall system

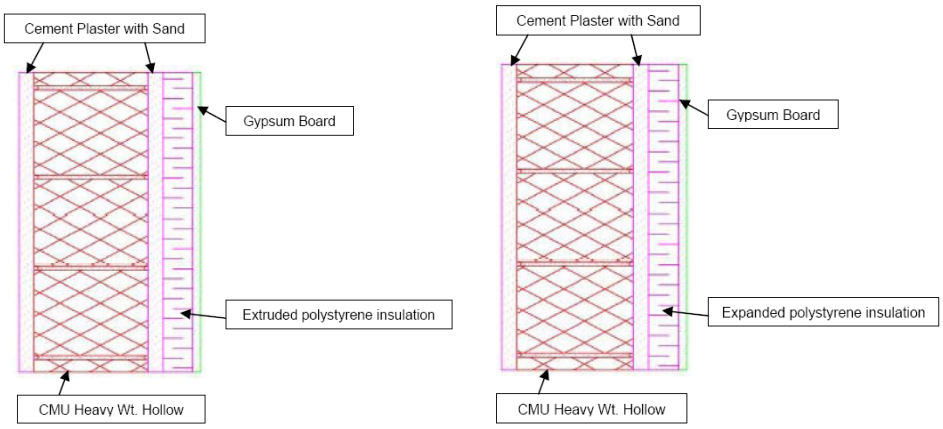

Figure 3.13 Cross section of (a) Ext.P and (b) Exp.P wall system

Figures 3.12 (a) to (c) illustrates the cross sections of FG-A, FG-B, FG-C and FG-D wall systems and **Figure 3.13 (a) and (b)** illustrates the cross sections Ext.P and Exp.P wall systems, constructed within the test wall.

3.13 Measurements: - Heat Flux Instrument

In-situ thermal resistance measurements were conducted following the procedure "In-situ measurement of thermal resistance and thermal transmittance", (IS0 9869: 1994) established by the International Standards Organization. The IS0 9869: 1994 describes the heat flow meter (HFM) method for the measurement of the thermal transmission properties of plane building components, primarily consisting of opaque layers perpendicular to the heat flow and having no significant lateral heat flow. This method is not intended as a high precision method replacing the laboratory instruments. However, this heat flow meter measurement method is suitable for components consisting of quasi-homogeneous layers perpendicular to the heat flow, provided that the dimensions of any in homogeneities in close proximity to the heat flow meter (HFM) are much smaller than its lateral dimensions and are not thermal bridges, which can be detected by infrared thermography. This standard sets the procedure for in-situ measurements of the thermal resistance of building envelope using quantitative

methods for the analysis of the measured data namely the average method and the dynamic method. In principle, the R-value can be obtained by measuring the heat flow rate through an element with a heat flow meter, together with the temperatures on the surfaces of both sides of the element under steady state conditions. However, since steady state conditions are never encountered on a site in practice, such a simple measurement is not possible. But there are several ways of overcoming this difficulty including:

a. Imposing steady-state conditions by the use of a hot and a cold box. This method is commonly used in the laboratory (IS0 8990) but is cumbersome in the field;

b. Assuming that the mean values of the heat flow rate and temperatures over a sufficiently long period of time gives a good estimate of the steady state condition. This method is widely used but may lead to long periods of measurements and may give erroneous results in certain cases;

c. Using a dynamic theory to take into account the fluctuations of the heat flow rate and temperatures in the analysis of the recorded data.

The accuracy of the measurement depends on the accuracy of the calibration of the heat flow meter (HFM) and the temperature sensors used, random variations caused by slight differences in the thermal contact between the sensors and the surface; the operational error of the HFM due to modifications of the isotherms caused by the presence of the HFM. The total uncertainty is expected to be between 14% and 28%. The probability of obtaining a large error is increased when the temperatures (particularly the indoor temperature) show large fluctuations (before or during the test) compared to the temperature difference between both sides of the element.

Subsequently, the measurement procedure requires that the building's indoor temperature is brought to a uniform condition approaching steady state conditions by operating the air-conditioning for a reasonable period of time before as well as during the measurements.

3.14 In-Situ Measurement of Envelope R-Values

For the test wall, a total of ten locations (i.e. nine spots on the test wall and one on the roof – in ten spots, three spots were for three types of insulation, four were of missing insulation, one each for wall without insulation, and moisture damaged.) were selected for measuring the thermal resistances (R-values), of walls and roof. The test was conducted for a span of 25 days, 5 days for each set of measurement with three heat flux sensors. The heat flow and temperature sensors were mounted and connected to the associated data multiplexer and logger. In this test two types of heat flux sensors (HFS) used are BF-03 and HFP01 soil heat flux plate, The HFS is a thin, thermally resistive plate with temperature sensors arranged in such a way that the electrical signal given by the sensors is directly related to the heat flow through the plate. A minimum of two temperature sensors were used, one on each side of the element under investigation. Good temperature sensors have accuracy such that temperature errors are small when compared with the measured temperature difference across the element. Suitable surface temperature sensors (for R or Λ-value measurements) are thin thermocouples and flat resistance thermometers. One sensor is incorporated within one side of the HFM, the side that will be in contact with the surface of the element being measured. The HFM calibration factors were given by the manufacturer and were used for conversions of units.

The HFMs and Thermocouples were connected to a Relay Multiplexer (i.e. AM16/32), and a data logger (i.e. CR10X Measurement and Control Module). A program was developed (see Appendix B) for CR 10X data logger with the help Engr. Aftab Ahmed (Engineer-III, RI KFUPM), to run the data logger and to record the measurement every five minutes at all 15 locations (12 temperature, and 3 heat flux measurements), and to extract all the data from the CR 10X instrument to the computer.

Efforts were made to select the locations (i.e. measurement spots) for mounting the HFMs and temperature sensors for conducting the measurements. Generally, to ensure the integrity of measurements over the measurement period, the locations for equipment installation were selected to ensure:

- Accessibility
- Ease of installation and monitoring of the equipment;
- Protection of the equipment against damage.

A. Location of the measured area (spot)

The measuring equipment (HFMs and thermocouples) was mounted according to the purpose of the measurements which is to determine the total R-value of the walls and roof systems. The visually appropriate location(s) were investigated by thermography. The sensors were then mounted in such a way so as to ensure a result which is representative of the whole element and at the required locations of interest. The HFMs were not installed in the vicinity of thermal bridges, cracks or similar sources of inconsistency as detected from the thermography images for each component. Sensors were placed so that they are not under the direct influence of either a heating or a cooling device or under the draught of a fan.

B. Mounting of the HFMs

The HFMs (with their incorporated surface temperature sensors) were mounted directly on the face of the element adjacent to the more stable temperature. The HFMs were mounted in direct thermal contact with the surface of the element over the whole area of the sensor. A thin layer of thermal contact paste for BF03 sensor/ Vaseline for HFP01 was used for this purpose. Precautions were taken to prevent any air bubbles, dirt, or water from becoming trapped between the HFM and the investigated surface.

C. Mounting of the temperature sensors (Thermocouples)

Since the thermal resistance is to be measured, surface temperature sensors (thermocouples) in the vicinity of the HFM were used. The external surface thermocouples were mounted on the external surface opposite to the HFM. Both surface temperature sensors were mounted so as to achieve good and firm thermal contact with the surface with 10 m length of lead wires.

Data was recorded continuously at 5 minute intervals (which are the average values of several measurements sampled at shorter one minute intervals) over a period of four days. Before and during the recording periods the HFM was kept inside the building to maintain the stable temperature around it. The recorded data were processed so that it can be used for computer analysis. The heat flux measurements were performed during 18th July to 11th August, 2010. The measurements were conducted following ISO 9869:1994 Standard as discussed in a previous chapter. The building air-conditioning system was left operating for a reasonable period of time before measurements were taken in order to reach stability of thermal behavior of the measured components.

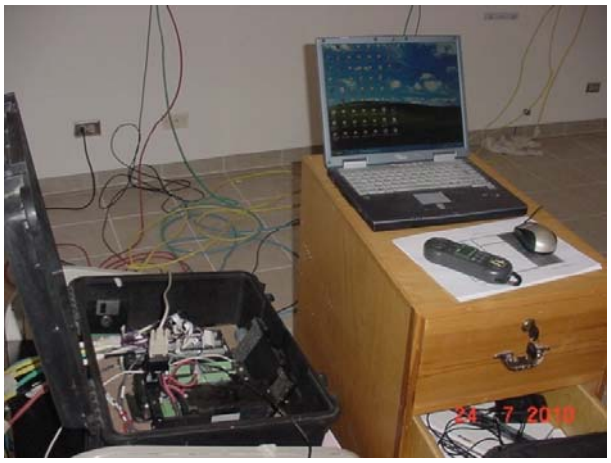

Figure 3.14 Heat flux meter and data logging system setup

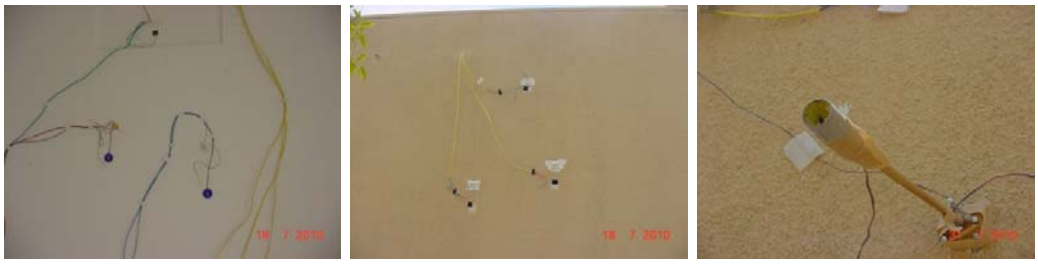

(a) (b) (c)

Figure 3.15 (a) Indoor heat flux sensors, surface and air temperature sensors installed on the wall (b) Outdoor surface and air temperature sensors installed on the wall (c) Outdoor air temperatures sensors installed on the wall

Figure 3.14 illustrates the heat flux meter setup**, Figure 3.15 (a)** illustrates an example of indoor heat flux sensors, surface and air temperature sensors installed on the wall system. **Figure 3.15 (b)** illustrates an example of outdoor surface and air temperature sensors installed on the wall system. **Figure 3.15 (c)** illustrates the protection of air temperature sensor from direct solar radiation using the stainless steel tube.

A. Data collection

The data was retrieved from the heat flux CR 10X instrument using the Campbell Scientific logger Net 2.1 software. The program used for retrieval of data is described in Appendix B.

Example of 5- Min measure temperature of the wall systems and roof systems of the residential building, The 5 min measured surface to surface wall, R_w and R_F are described in **Tables 3.10 (A) to Table 3.10 (C)**.

Table 3.10 Example 5 min Temperature of measurement different wall systems

A. Example 5 min Temperature of FG-A wall System

Time	Air out ^{o}C	Air in ^{o}C	Sur out ^{o}C	Sur in ^{o}C	Q W/m2	So-Si	To-Ti	Resistance m^2.K/W
1900	40.84	25.50	40.58	32.51	58.62	8.07	15.34	0.1377
1905	40.80	25.55	40.53	32.56	61.13	7.97	15.26	0.1304
1910	40.68	25.53	40.41	32.55	52.88	7.86	15.15	0.1486
1915	40.67	25.49	40.37	32.52	62.75	7.85	15.18	0.1251
1920	40.65	25.49	40.28	32.51	58.9	7.77	15.15	0.1319
1925	40.67	25.42	40.23	32.51	59.46	7.72	15.25	0.1298
1930	40.62	25.47	40.12	32.47	57.56	7.65	15.15	0.1329

B. Example 5 min Temperature of FG-B wall system

Time	Air out ^{o}C	Air in ^{o}C	Sur out ^{o}C	Sur in ^{o}C	Q W/m2	So-Si	To-Ti	Resistance m^2.K/W
1900	40.84	25.50	14.52	41.62	27.94	13.68	15.34	0.9421
1905	40.80	25.55	14.68	41.54	27.93	13.61	15.26	0.9271
1910	40.68	25.53	14.57	41.46	27.92	13.54	15.15	0.9293
1915	40.67	25.49	14.79	41.38	27.92	13.46	15.18	0.9101
1920	40.65	25.49	14.71	41.3	27.9	13.4	15.15	0.9109
1925	40.67	25.42	14.75	41.24	27.91	13.33	15.25	0.9037
1930	40.62	25.47	14.75	41.14	27.87	13.27	15.15	0.8997

C. Example 5 min Temperature of FG-D wall system

Time	Air out ^{o}C	Air in ^{o}C	Sur out ^{o}C	Sur in ^{o}C	Q W/m2	So-Si	To-Ti	Resistance m^2.K/W
1900	38.55	25.34	8.87	40.29	27.21	13.08	13.21	1.4746
1905	38.5	24.97	10.25	40.19	27.18	13.01	13.53	1.2693
1910	38.51	25.63	7.5	40.06	27.23	12.83	12.88	1.7107
1915	38.35	25.65	7.78	39.82	27.24	12.58	12.7	1.6170
1920	38.29	25.12	9.95	39.72	27.21	12.51	13.17	1.2573
1925	38.23	24.99	10.27	39.64	27.18	12.46	13.24	1.2132
1930	38.16	24.81	10.84	39.55	27.18	12.37	13.35	1.1411
2000	37.68	25.19	9	38.88	27.17	11.71	12.49	1.3011

Figures 3.16 to 3.18 illustrate Examples of the measured Surface temperature distribution of the various wall and roof systems with time.

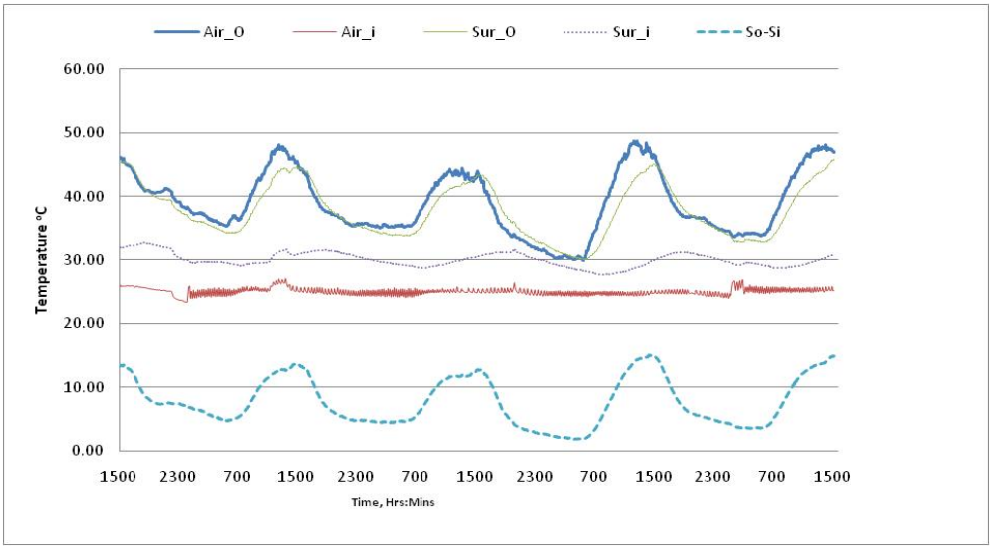

Figure 3.16 Temperature Variations FG-A Wall System

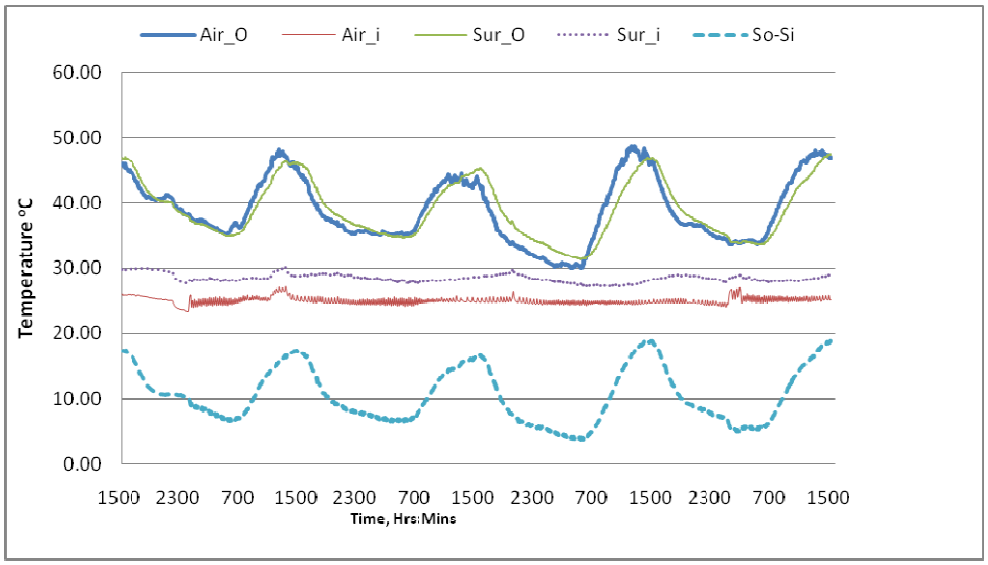

Figure 3.17 Temperature Variations FG-B Wall System

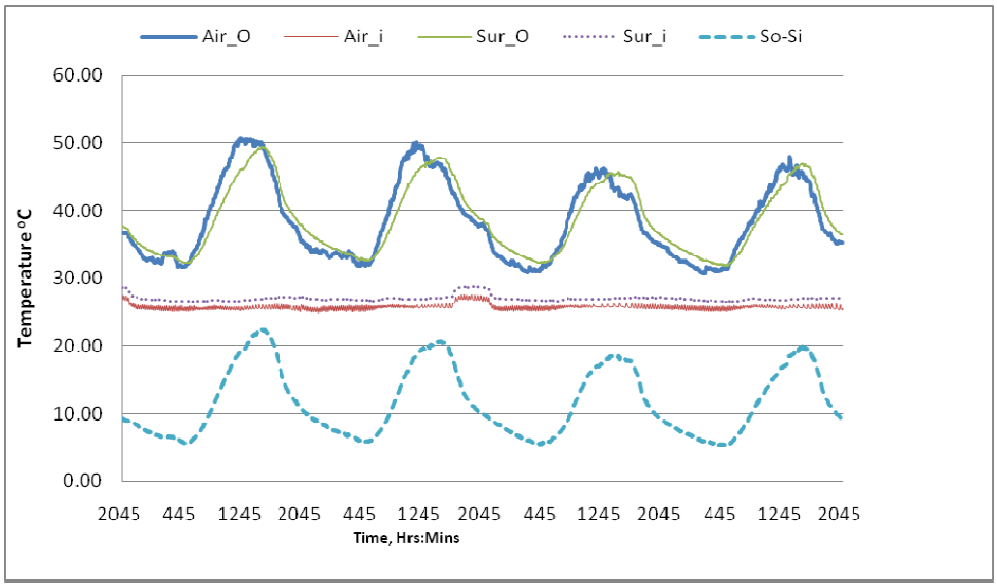

Figure 3.18 Temperature Variations FG-D Wall system

3.15 Infrared Thermography Measurements

The measurements were conducted from 18th July to 11th August, 2010, following the procedure described early in the chapter and by utilizing the developed onsite measurement form.

While conducting the thermal imaging measurements data needs to be collected is, indoor and outdoor temperature, measured using digital thermometers as well with temperature sensors, emissivity of the building envelope materials, relative humidity, also reflective apparent temperature (RAF), distance between object and camera is estimated for each and every measurement, which is used to compensate for the radiation reflected in the object. For convenient purpose the test wall is painted with white color with known emissivity of 0.9, to avoid the calculation of accurate emissivity of building envelope surface. During the investigations a tripod is being utilized to fix the camera, which helps the investigator to take the thermal images with better accuracy. Digital images were taken by a digital camera.

The measurements were usually conducted during the evening time from 17:00 to 24:00, to make sure steady state conditions across the building envelop and to avoid solar radiation. The temperature difference between indoor and outdoor conditions was more than 10^{o}C during the complete measurements, which is an essential condition for thermographic measurements. It is crucial for any prospect of reasonable accuracy that one has as close to steady state conditions as possible for R-value measurements using infrared thermography. **Figure 3.19 and Figure 3.20** illustrates air temperature distribution (outdoor and indoor) and heat flux measurements for 4 days of heat flux measurements, indicating almost constant indoor and outdoor temperature across the building envelope during 18:00 to 5:00, which is essential for IRT measurements and in-situ R-value calculations. **Figure 3.21** illustrates some of the thermal images taken during investigations for the building envelope and test wall.

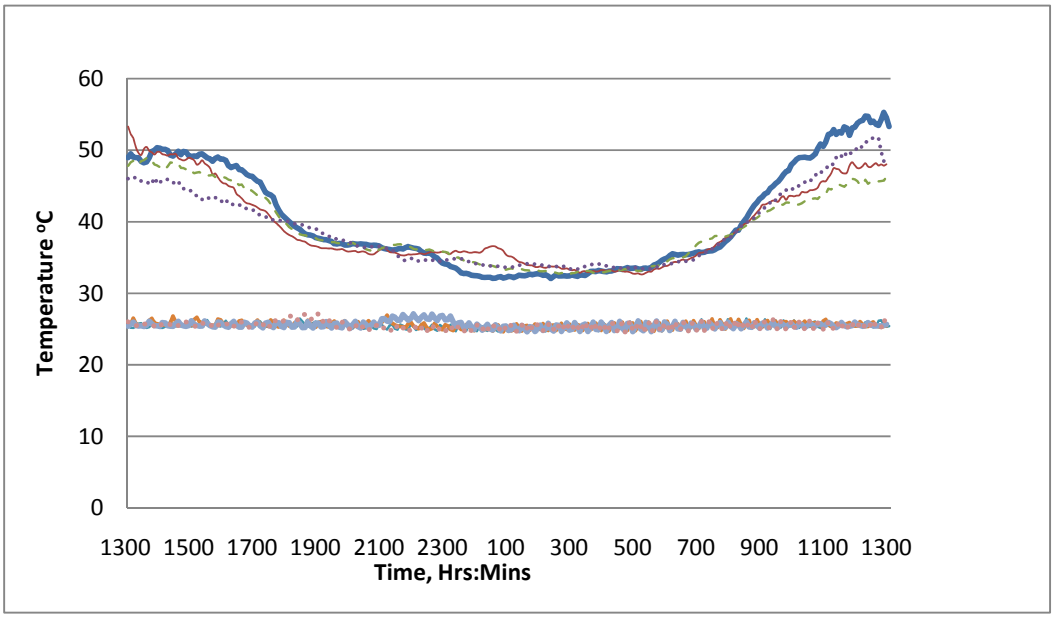

Figure 3.19 Air temperature outdoor, indoor measured over 4 days of heat flux measurements (FG-D wall system).

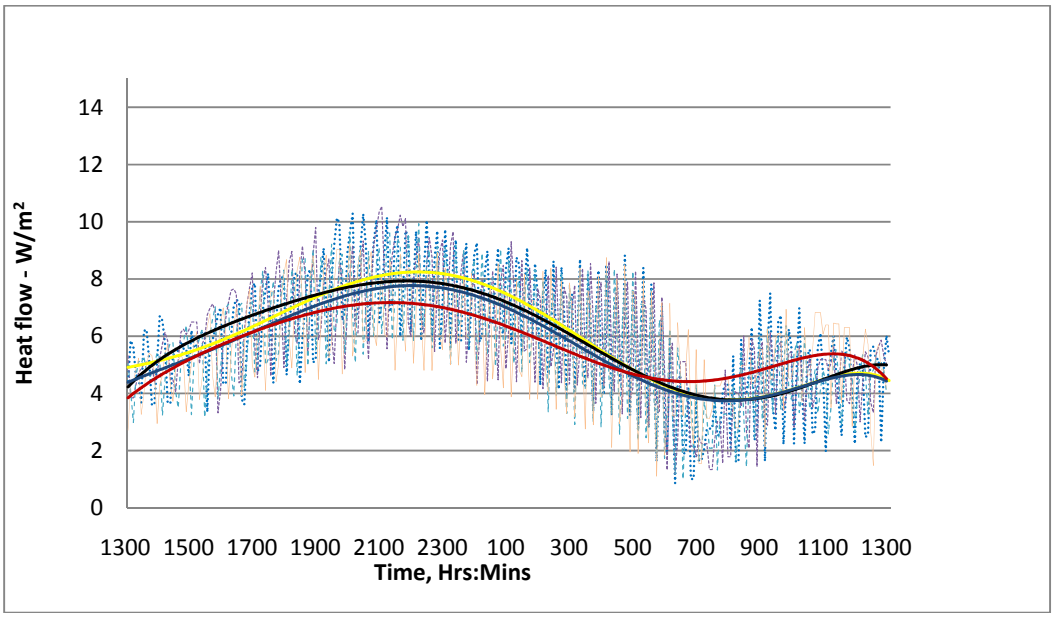

Figure 3.20 Heat flow measured over 4 days of heat flux measurements (FG-D wall system).

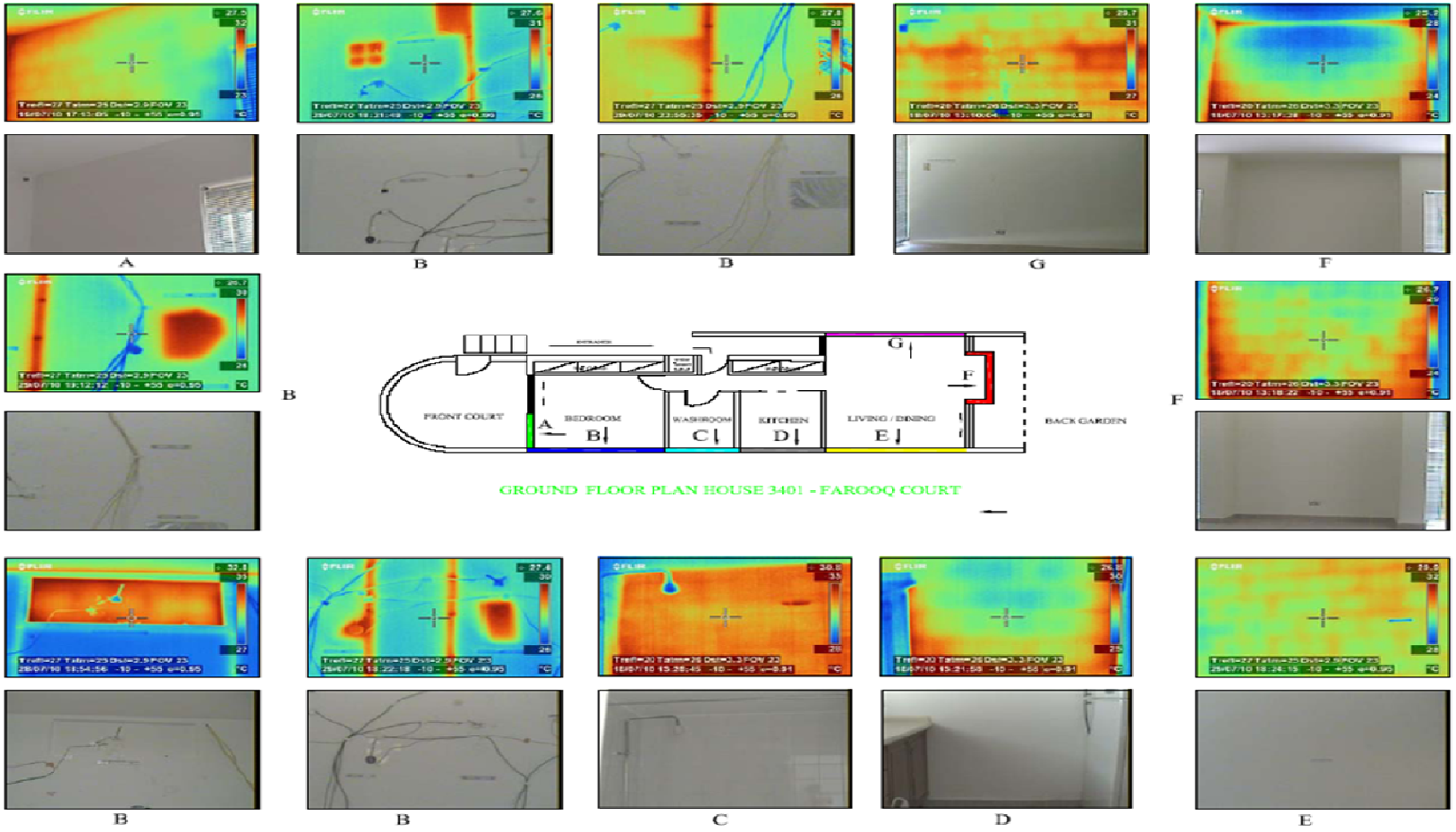

Figure 3.21 Building Layout - Illustrating the thermal images of each wall

CHAPTER FOUR

4 RESULTS AND DISCUSSIONS

4.1 Data Results of Heat Flux Meter

The obtained data is processed using the ISO 9869:1994 standard to determine the in situ R values of the various walls and roof compositions.

A Matlab program (Refer Appendix C) is developed to process the data, by using the simple/ Average Method (with consideration to the storage effects), and Dynamic Method.

The program was developed in such a way that it gives the In Situ R values of average of all 4 days of data collected by using both simple and dynamic method. Program also generates the R values for First 2 Days, Last 2 Days, and First 3 days; in order to verify the conditions of IS 9869:1994 for the accuracy of thermal resistance value. The conditions are mentioned in the description of the simple method. Program also takes into consideration the storage effect, program gives the R value by considering storage effects when the wall composition is known, and also when the wall composition is not known, and shows the change in the R value ($\leq$5%) due to heat storage effect to verify the conditions for accuracy of resistance of the ISO standard.

Program incorporates the code that gives the R value with a more sophisticated dynamic method with consideration of confidence interval. The data has been processed two times by averaging it every 30 min and every 60 min.

The Matlab program is simulated for the various sets of data collected from the Heat Flux (CR 10X) Instrument. **Figure 4.1 and 4.2** illustrates the thermal conductivity values of the test wall at all locations calculated using both simple method and dynamic method. For the test wall the tables shows conductance values for simple method, simple method taking into effect the storage effect when composition is known, simple method taking into effect the storage effect when composition is not known, dynamic method by taking average of the date for every 60 min. the details of the results are present in Appendix D.

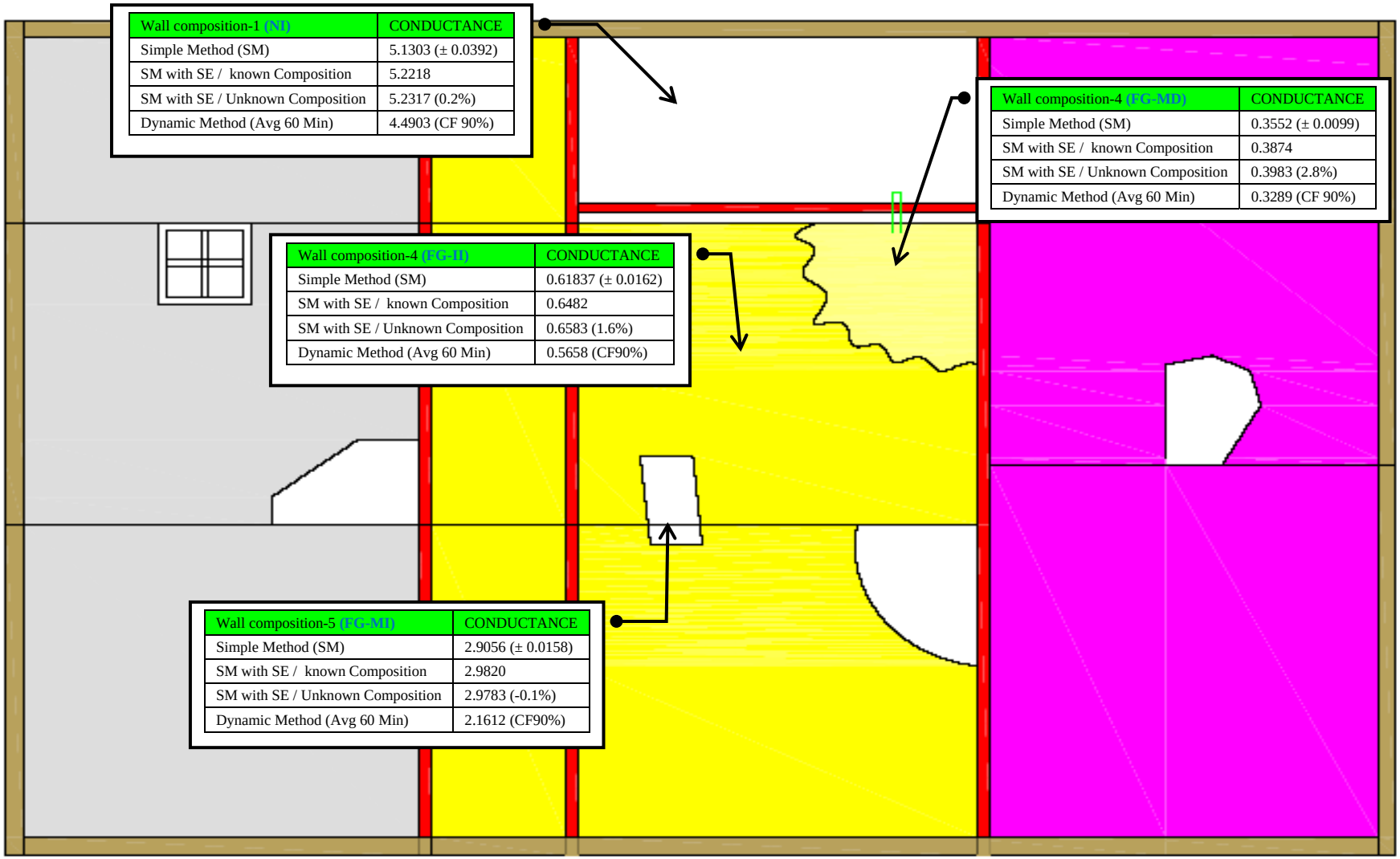

Figure 4.1 Test Wall with Conductance Tables

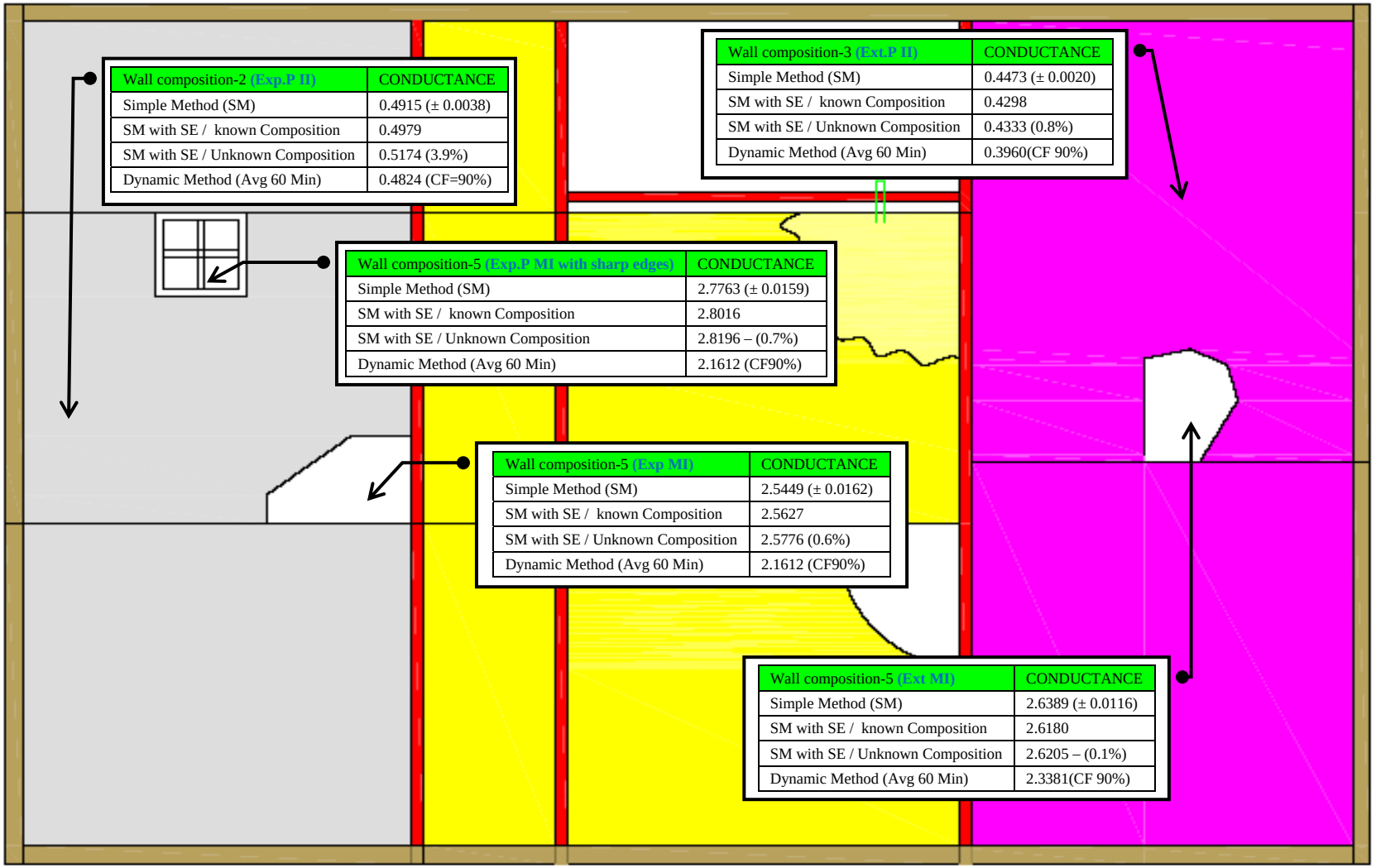

Figure 4.2 Test Wall- Conductance Tables

4.2 Thermographic Image Analysis

The following procedure explains in analyzing the images utilizing various softwares of Flir ThermaCam and image processing, for the quantification of thermal bridging, damaged insulation and missing insulation, to find the insitu thermal resistance of the building envelope.

Once the measurements are finished, the stored images can be reviewed for data accuracy utilizing the Flir ThermaCam software, for any mismatch of data by comparing the emissivity, RH, RAF, distance, temperature with the measurement form. If any of them is not entered properly during the measurements in the camera, it can be inserted in the software. The software takes account of these modified values to produce the image with actual onsite conditions. **Figure 4.3** illustrates the Flir ThermaCam software window. Once this is done the flying spot meter can be used to measure the temperature at any spots within the image, with this tool minimum and maximum temperature in the defective area can be computed just by moving the tool around and in the defective area. A rectangular selection gives an average temperature within that area with indicating the minimum and maximum temperature in the selected area.

The images produced by Flir thermal Imaging camera are of Pixels in size 240X320, producing a total of 76800 Pixels, in turn producing 76800 different areas representing various temperature distribution, which can be produced using the Flir Software It produces this temperature distribution in an excel sheet. The software produces the output, dividing the image into 76800 small areas, hence in various different temperatures representing the surface temperature distribution of wall. An excel function “count if”

was used to find the number of cells representing each temperature, to find the average temperature in the defective area of building envelope.

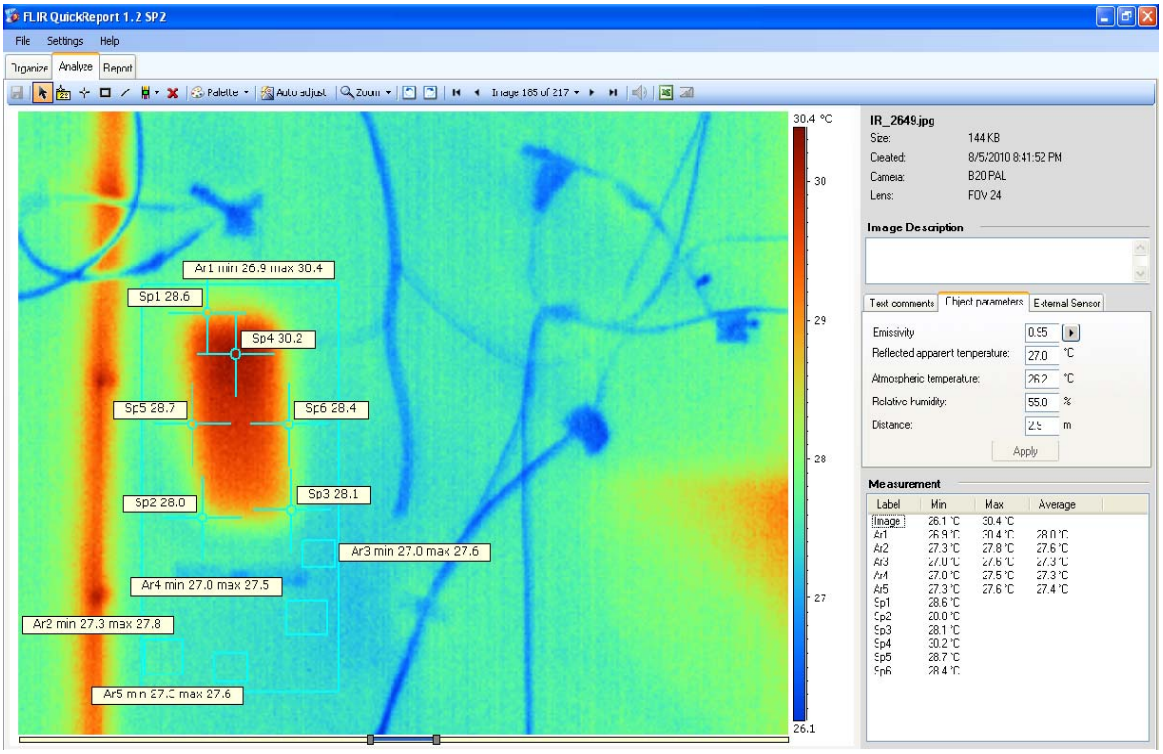

Figure 4.3 Flir ThermaCam software window

While processing the images with various temperature distribution and disturbing lines like in **Figure 4.3**, rectangular selection tool is used to exactly select the area with possible defect. The selection is converted to a temperature distribution matrix with the help of software in the excel spread sheet format, so average temperature distribution of defective and non defective areas can be computed. For the selection of temperature range representing defective and non defective area, spot meter and rectangular tools are utilized as shown in **Figure 4.3**.

Image processing software Image J is used to find the area of the images, utilizes the scale bonded on the wall during the measurements as the reference in calculation of the

area of the image hence area of the each cell is computed. The area of weighted surface temperature distribution is computed for defective and non defective areas. Figure 4.4 illustrates the image processing window with its menu bar, first a scale needed to set with referring to known scale length, area of the whole image can be computed, divided by 76800 to calculate the area of the each cell of the 78600 cell for that particular image. It is to be noted that the area of the each image will vary with regards to the distance of capturing the photo, camera angle and many other factors, area calculated differently for all the images. In the **Figure 4.4** a scale bonded on the test wall can be seen below the missing insulation.

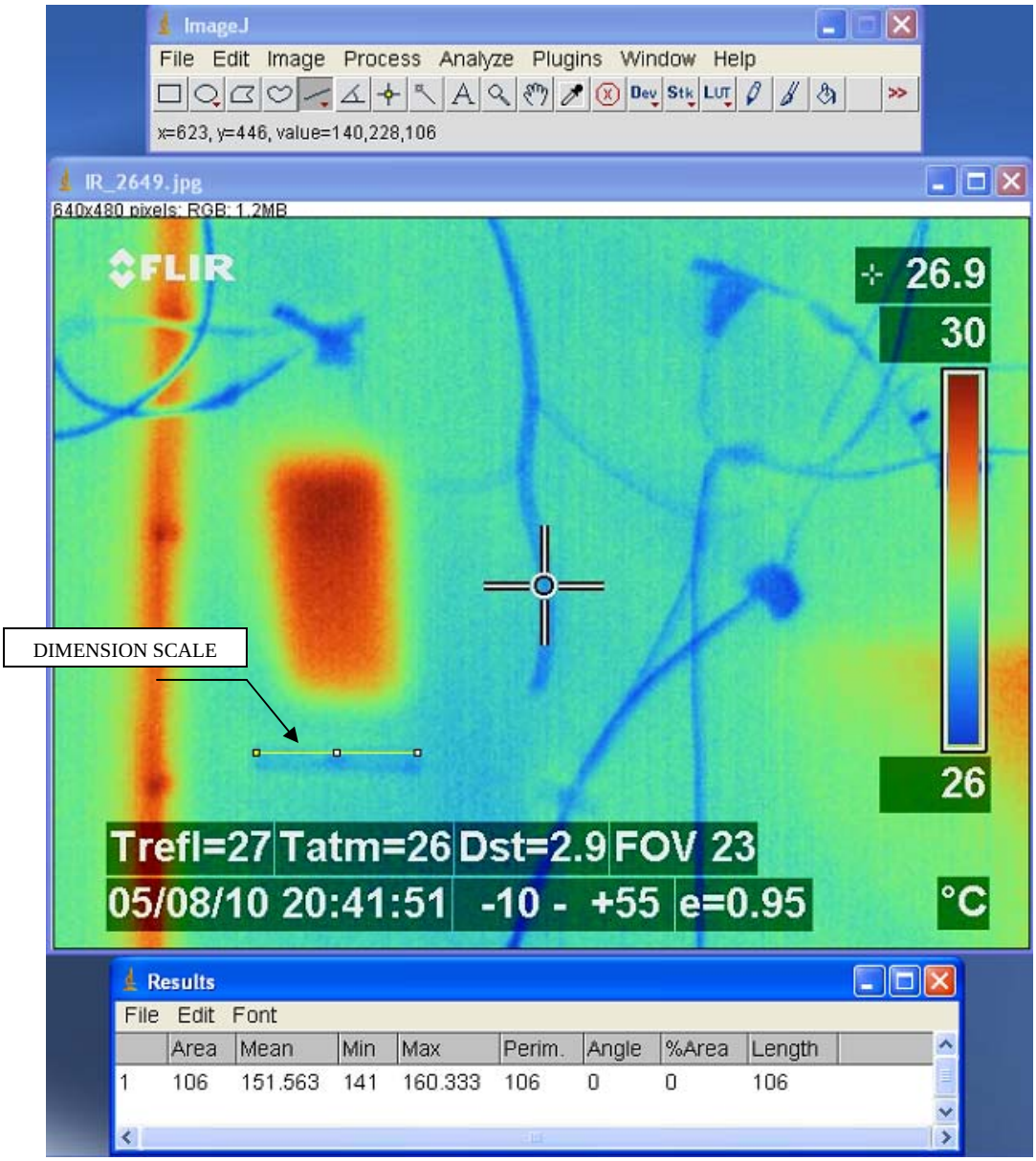

Figure 4.4 ImageJ software window

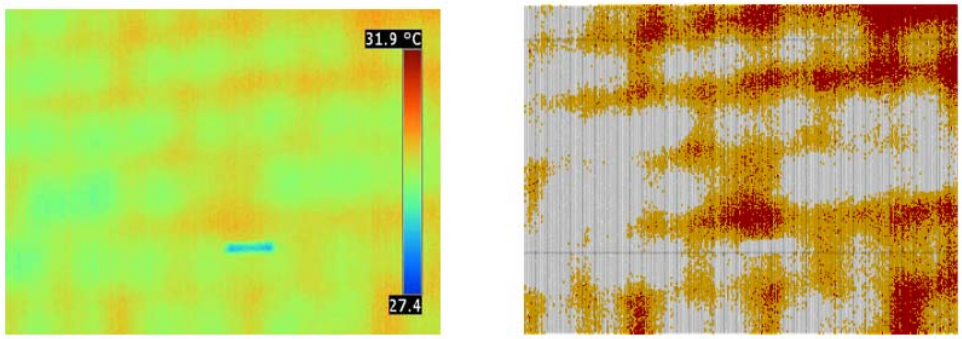

A. Thermal bridging FG-A wall system

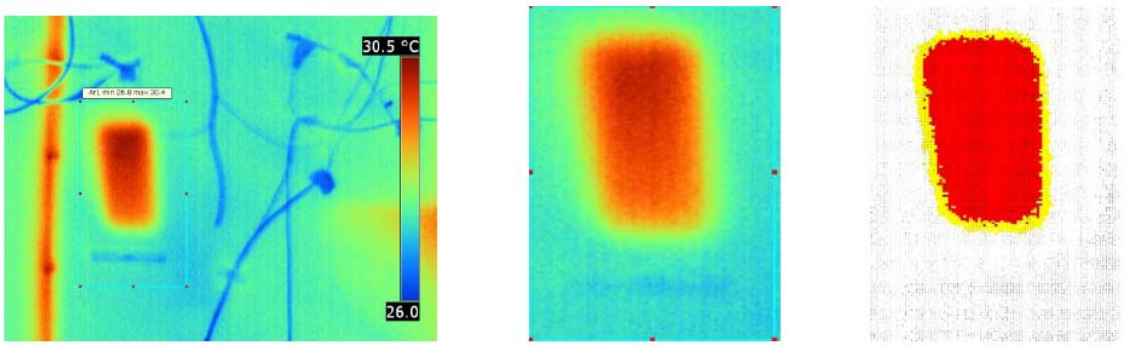

B. Missing insulation FG-B wall system

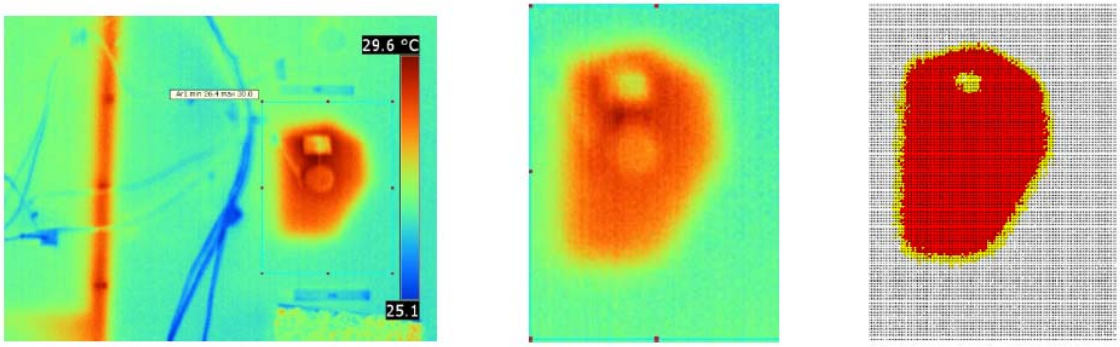

C. Missing insulation Ext.P wall system

Figure 4.5 Analyzed thermal images

Figure 4.5 illustrates the processed images with the procedure described, **Figure 4.5 A** illustrates an example of processed images of the existing wall of the building with thermal bridging due to the presence of mortar between the blocks, with the right side picture showing the processed excel sheet in calculation of the area representing the thermal bridging, areas representing thermal bridging are filled with red and yellow color,

red being filled in the area with higher thermal and yellow in the area with lower thermal leak. **Figure 4.5 B** illustrates an example of missing insulation of FG-B wall system (test wall), and had processed with similar procedure described except selecting a rectangular area, rather than considering the full image. **Figure 4.5 C** illustrates an example of processed image of missing insulation in Ext.P wall system.

4.3 Quantification Procedure

The R-Value of the wall is summation of resistance of the all the material within the wall assembly, as it is calculated for the temperature drop across all of them as shown in **Figure 4.6.** Just as Ohm's law for electrical circuits gives the resistance as the voltage drop divided by the current across a resistor or series of resistors, heat flow gives the R-Value as the temperature drop across a series of thermal resistances divided by the heat flow through those resistances. Under steady state conditions voltage flow across the circuit or single resistor will be the same, thus explaining that heat flow across the wall assembly and heat flow in internal air film will be the same under steady state conditions. This is used as the first assumption in developing the quantification procedure for quantification of thermal defects in the building envelope (Robert Madding Inframation, 2008).

Figure 4.6 Nature of Heat Flow Across a wall Assembly

Quantification method utilizes the following method proposed by Italo M and Valter E (1998)

The thermal power flowing through the wall (Q1) and the defective area (Thermal Leak) of the wall (Q2) can be defined as follows.

$$Q_1 = U_{sr}.\Delta T = \alpha_1 (T_i - T_{sr})$$

$$Q_2 = U_s.\Delta T = \alpha_2 (T_i - T_s)$$

Where,

Q_1, Thermal power flowing through the wall

Q_2, The thermal power flowing through the defective area

U_{sr}, Theoretical thermal transmittance of the wall with known R-value (W/m $^{2^o}C$)

U_s, Thermal transmittance of the unknown composition area in the wall (R-value not known). (W/m $^{2^o}C$)

$\alpha_{1,2}$, Internal laminar coefficients

ΔT, Internal/ external air average temperature difference.

T_i, Average temperature of internal air.

T_{sr}, Average temperature the wall surface (Known R-value)

T_s, Average temperature of the defective area in the wall (ex: missing insulation) or area with unknown R-value.

The Thermal transmittance value can be obtained by following transformations

$$\alpha_1 = U_{sr}.\Delta T /(T_i - T_{sr})$$

$$\alpha_2 = U_s.\Delta T /(T_i - T_s)$$

As a first Approximation, assuming that internal laminar coefficients of the investigative areas to be similar considering the constant steady state indoor conditions (Say $\alpha_1 = \alpha_2$)

$$U_{sr}.\Delta T/(T_i - T_{sr}) = U_s.\Delta T/(T_i - T_s)$$

The temperature difference ΔT int/ext being the same,

$$U_{sr}/(T_i - T_{sr}) = U_s./(T_i - T_s)$$

$$U_{sr}/U_s = (T_i - T_{sr})/(T_i - T_s)$$

Thermal Resistance R ($m^{2^o}C/W$) is given by the reciprocal of Thermal Transmittance. Rearranging the equations to make the thermal resistance of the defective area as the subject of the formula

$$U_s = U_{sr}(T_i - T_s)/(T_i - T_{sr})$$

$$R_s = R_{sr}(T_i - T_{sr})/(T_i - T_s)$$

Where,

R_{sr} , Thermal Resistance of the Wall

R_s, Thermal Resistance of defective area (Thermal Leak) or R-value of unknown composition.

4.4 Validation of quantification procedure

The thermal images were processed for R-value calculations at the point of heat flux measurements to validate the quantification procedure for better prediction of R-value based on IRT measurements. **Table 4.1** refers to wall system abbreviations with their compositions.

Table 4.1 Wall system compositions used in R-value quantification

S No	Wall system-Abbreviation	Composition
1	FG-A	200mm Heavy Wt Hollow + 20mm cement plaster with Sand on both sides
2	FG-B	200mm Heavy Wt Hollow + 20mm cement plaster with Sand on both sides+ 50mm air gap+ 13.3 Gypsum board
3	FG-D	200mm Heavy Wt Hollow + 20mm cement plaster with Sand on both sides+ 50mm fiber glass insulation+ 13.3 Gypsum board
4	Exp.P MI	200mm Heavy Wt Hollow + 20mm cement plaster with Sand on both sides+ 50mm air gap+ 13.3 Gypsum board
5	Exp.P MI+	200mm Heavy Wt Hollow + 20mm cement plaster with Sand on both sides+ 50mm air gap+ 13.3 Gypsum board
6	Exp.P II	200mm Heavy Wt Hollow + 20mm cement plaster with Sand on both sides+ 50mm expanded polystyrene insulation+ 13.3 Gypsum board
7	Ext.P MI	200mm Heavy Wt Hollow + 20mm cement plaster with Sand on both sides+ 50mm air gap+ 13.3 Gypsum board
8	Ext.P II	200mm Heavy Wt Hollow + 20mm cement plaster with Sand on both sides+ 50mm extruded polystyrene insulation+ 13.3 Gypsum board

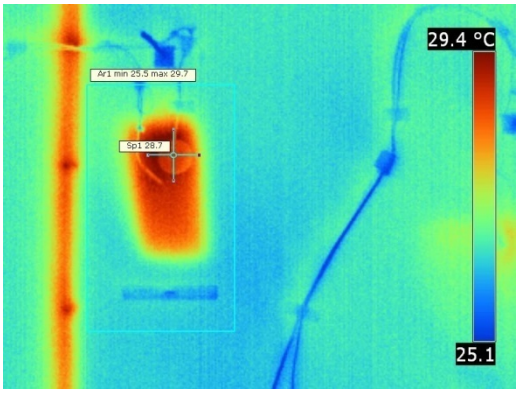

a. FG-B wall system, one point measurement

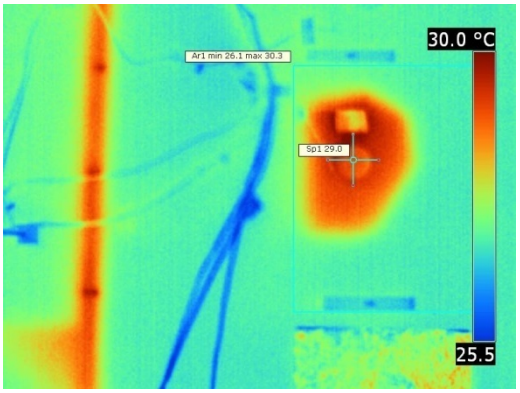

b. Ext.P MI wall system, one point measurement

Figure 4.7 One point selection at sensor location in thermal image

Figure 4.7 illustrates an example of one point selection in the thermal image to find the surface temperature at the sensor location.

Figure 4.8 illustrates temperature distribution during the period of IRT measurements, of the indoor air temperature, reference wall system surface temperature and surface temperature of the wall surfaces for which the R-value is to be calculated using the reference wall system.

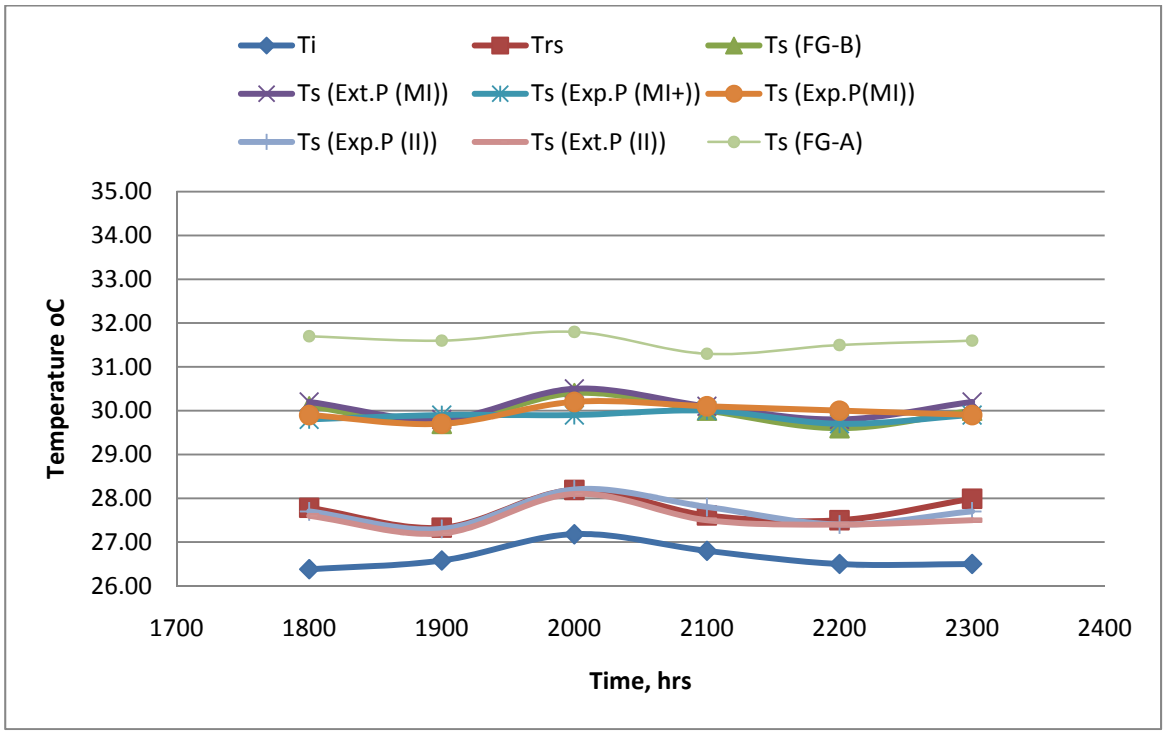

Figure 4.8 Temperature: T_i, T_{rs}, T_s Plot, during IRT measurements

FG-D wall system is used as reference in R-value calculation for the other wall systems. The R- values were calculated by both utilizing the R- value of FG-D wall based on dynamic method (uses heat flux measurements) and its theoretical value. It is to show the applicability of IRT in terms of finding the R-values of non homogeneous wall with one reference point. The R- value of the reference point can be measured using heat flux measurements, but in most situations it is not practical to perform these measurements, because of this theoretical R- value of the reference wall can also be used to find the R-values of other locations. The results of R-value calculations using both R-value based on

dynamic method (R_{DM}) and theoretical R-value (R_T) of the reference point. The R_{DM} value of the reference point is 1.9272 m^2.C /W, and theoretical value is 1.986 m^2.C /W. there is not much significant difference between the two R- values because the theoretical R-values of the fiber glass insulation and gypsum board inn FG-D wall system are measured in the laboratory using heat flow meter as described in chapter 3, and for other materials the R-values are taken from ASHRAE standard. When R_{DM} is used as a reference it has a significant advantage over using the theoretical R-value, because there is no need to know the wall compositions. But when using the theoretical R-value as reference, the composition of wall system must be known. **Table 4.2** shows to R-values of various wall systems calculated using IRT, based on the reference R_{DM} of the FG-D wall system measured using heat flux dynamic method, now on this calculated R-value using IRT is referred to as R-IRT_{DM}. To calculate the R-values first the average surface temperature of the unknown R-value wall system is calculated over the measurements period, average temperature over the measurement time is considered to be more accurate, because heat flow meter measurements analysis also utilize the average temperature in calculating R-value using both simple and dynamic method, rather than calculating R-value at each measurement and taking the average R-value.

Table 4.2 R-values calculated using IRT based on both R_{DM} and R_T

R-value calculated for			FG-A	FG -B	Exp.P (MI)	Exp.P (MI+)	Exp.P (II)	Ext.P (MI)	Ext.P (II)
Point measurement	Ti	Tsr	Ts	Ts	Ts	Ts	Ts	Ts	Ts
1800	26.38	27.78	31.70	30.10	29.90	29.80	27.70	30.20	27.60
1900	26.58	27.33	31.60	29.70	29.70	29.90	27.30	29.80	27.20
2000	27.18	28.19	31.80	30.40	30.20	29.90	28.20	30.50	28.10
2100	26.80	27.61	31.30	30.00	30.10	30.00	27.80	30.10	27.50
2200	26.50	27.50	31.50	29.60	30.00	29.70	27.40	29.80	27.40
2300	26.50	27.99	31.60	30.00	29.90	29.90	27.70	30.20	27.50
Avg Temperature (18:00 to 23:00)	26.66	27.73	31.58	29.97	29.97	29.87	27.68	30.10	27.55
R- value based on R_{DM} (m^2.C /W)	-	-	0.4213	0.6271	0.6271	0.6467	2.0219	0.6029	2.3237
R- value based on R_T (m^2.C /W)	-	-	0.436	0.6463	0.6463	0.6664	2.0836	0.6212	2.3946

Table 4.2 shows to R-values of various wall systems calculated using IRT, based on the theoretical R-value of the FG-D wall system, now on this calculated R-value using IRT is referred to as R-IRT_T. To calculate the R-values first the average surface temperature of the unknown R-value wall system is calculated over the measurements period.

Table 4.3 shows the percentage variation in the R-values calculated using IRT measurements (R-IRT_{DM} and R-IRT_T) with measured R-values using dynamic method. From the table it is observed that the R-values calculated using IRT are within the range of almost within 10% with regards to their true R-value. It is to be noted that R-IRT_{DM} is more accurate method for R-value calculations instead R-IRT_T because it uses a true R-value as a reference, but in cases where conducting heat flux measurements are not possible due to time concerns, practicality, availability of heat flux equipments, extensive calculations, theoretical R-value of the reference wall can be used as the base R-value.

Table 4.3 R-values calculated using IRT, and there percentage variation from true R-value

Point measurement	R_{DM}	R-IRT_{DM}	% Variation, Ref DM	R-IRT_T	% Variation, Ref DM
FG-A	0.387	0.4188	8.2	0.4332	11.9
FG-B	0.672	0.6207	7.6	0.6397	4.8
Exp.P (II)	1.9097	2.0098	5.2	2.0712	8.5
Exp.P (MI)	0.672	0.624	7.1	0.643	4.3
Exp.P (MI+)	0.672	0.646	3.9	0.6657	0.9
Ext.P (II)	2.6852	2.3176	13.7	2.3883	11.1
Ext.P (MI)	0.5648	0.596	5.5	0.6142	8.7
Average % variation	-	-	7.3	-	7.2
Standard deviation	-	-	3.2	-	4.0

Figure 4.9 illustrates graphically the relation between R-values calculated using IRT based on R_{DM} and R_T R-value as reference, with R_{DM} values measured using heat flow

meter. And indicates the calculated R-values are within the 10% range when compared to their true R-values.

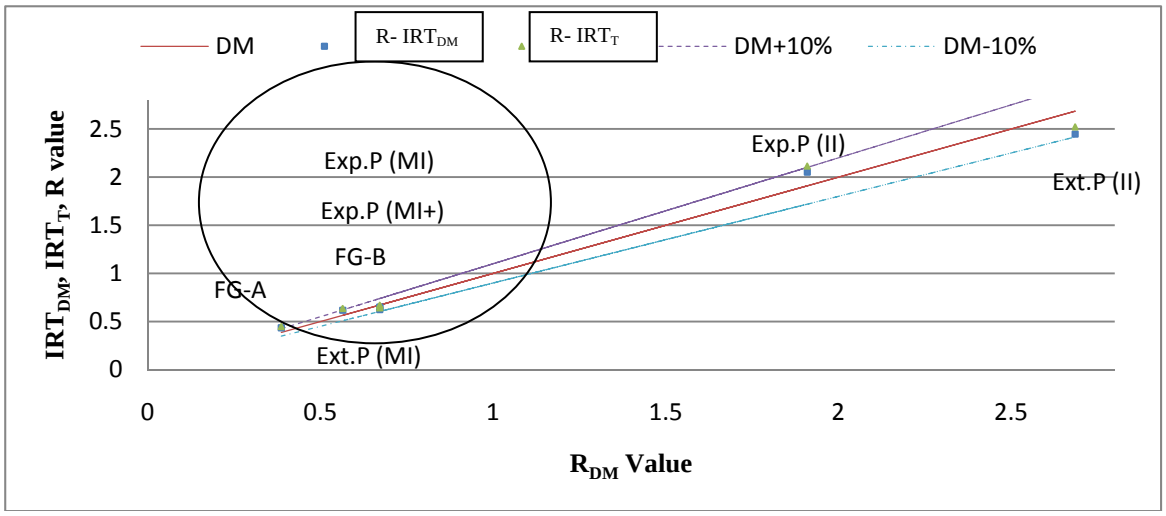

Figure 4.9 R-values using R_{DM} Vs IRT_{DM}, IRT_T

The portion highlighted with circle is enlarged in the **Figure 4.10** for better interpretation of calculated results.

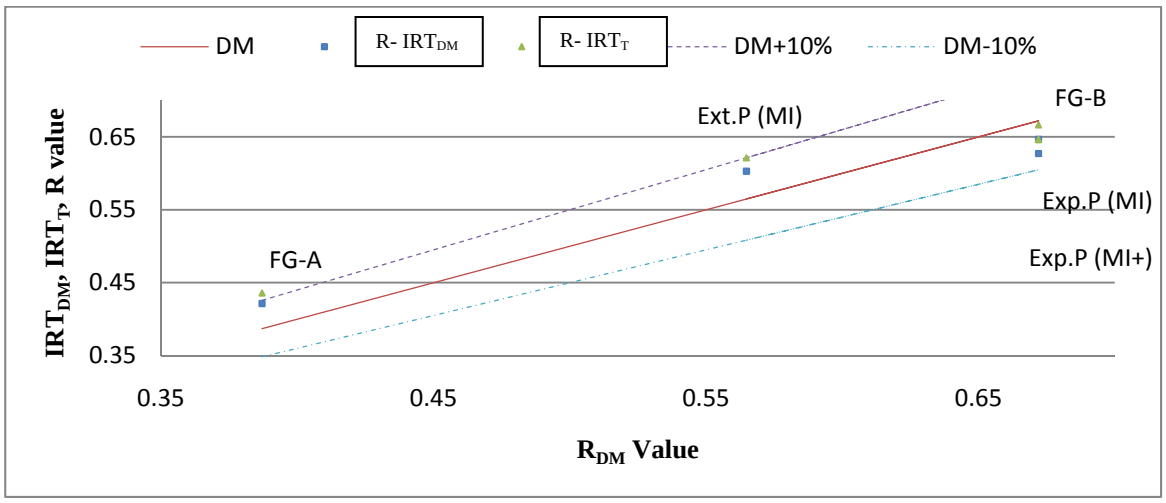

Figure 4.10 R-values using R_{DM} Vs R- IRT_{DM}, R- IRT_T

The results obtained in R-value calculations using IRT is found to be very close to true values obtained through the dynamic method. The IRT measurements are having a significant advantage over the heat flux dynamic method that, it can also calculate the R-

value of the defect by considering the total area of the defect, where as heat flux sensor takes into account only the portion of the defect at the location of the sensor. The following sections show the procedure for better prediction of R-value for defective areas by considering the total area of defect based on IRT measurements. IRT measurements also help in better predicting the area of defect.

4.5 Quantification of Missing Insulation

The images taken for FG-B wall system were analyzed to find the in-situ thermal resistance of area with the missing insulation, **Figure 4.11** illustrates an example of thermal image for FG-B wall system. **Figure 4.11 A** to **4.11C** illustrate the processing of the images with the method described. The images were usually taken with approximate variation of 10 minutes of the mentioned time.

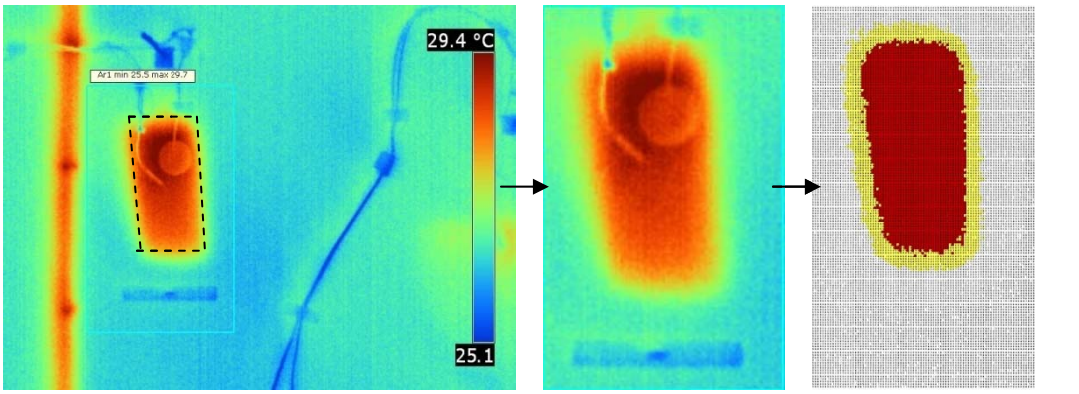

A (Total damage area) B (area to be processed) C (Processed image using Excel)

Figure 4.11 Missing Insulation, FG-B wall system

Table 4.4 Average surface temperature and area of FG-B wall system calculated using IRT

Time	Area of defect cm^2	% Variation determined area/ actual area	Image reference	Surface temperature of defective area
18:00	456	1.3	2568	29.66
19:00	433	3.8	2595	29.34
20:00	459	2	2623	29.91
21:00	472	4.9	2649	29.43
22:00	463	2.9	2677	29.12
23:00	466	3.6	2697	29.17
Avg	458	Max 4.9%, Avg 1.8%, Min 1.3%	Average	29.44
Actual area	450			

Table 4.4 Presents the area and average surface temperature calculated over the measurements period of time, also compares the determined area with actual area using IRT measurements for FG-B wall system. **Table 4.5** shows the true R-value for the FG-B wall system and presents the percentage R-value variation of theoretical and calculated using IRT based on R_{DM}, and R_T as reference to find the R-value of total defective area, for the FG-B wall system with reference to true R-value measured with heat flux dynamic method (DM).

Table 4.5 R-value of FG-B wall system – comparison

Method	Theoretical	SM	R_{DM}	$R\text{-}IRT_{DM}$ – one spot in defective area at	$R\text{-}IRT_T$ - one spot in defective area at sensor	$R\text{-}IRT_{DM}$ - total defective area	$R\text{-}IRT_T$ - total defective area
R, $m^2.C$ /W	0.646	0.46	0.672	0.6271	0.6463	0.7463	0.769
Percentage Variation (Reference – R_{DM})	3.9	31.5	-	6.7	3.9	11	14.4

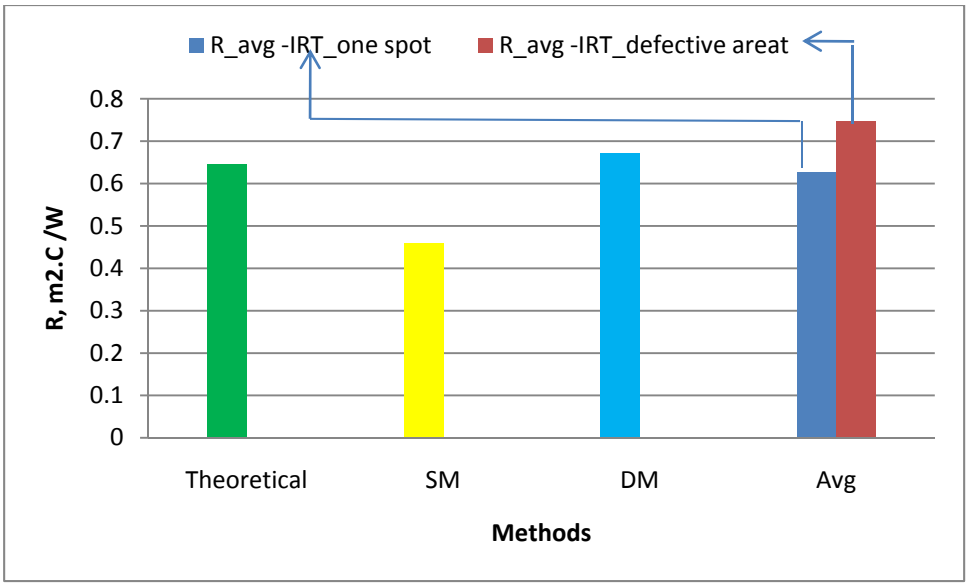

Figure 4.12 R-value comparison- different methods (FG-B wall system) Avg calculate reference to IRT_{DM}

Figure 4.12 illustrates the comparison of R-value with different methods for FG-B wall system. It also indicates the variation in R-value of one spot compared to total defective area. Thus IRT technique can be used for prediction of effective R-value of the total defective area, compared to the heat flux method, which gives the R-value at a particular location only.

Figure 4.13 illustrates an example of thermal image for Ext-P wall system. **Figures 4.13A to 4.13C** illustrate the processing of the images with method described.

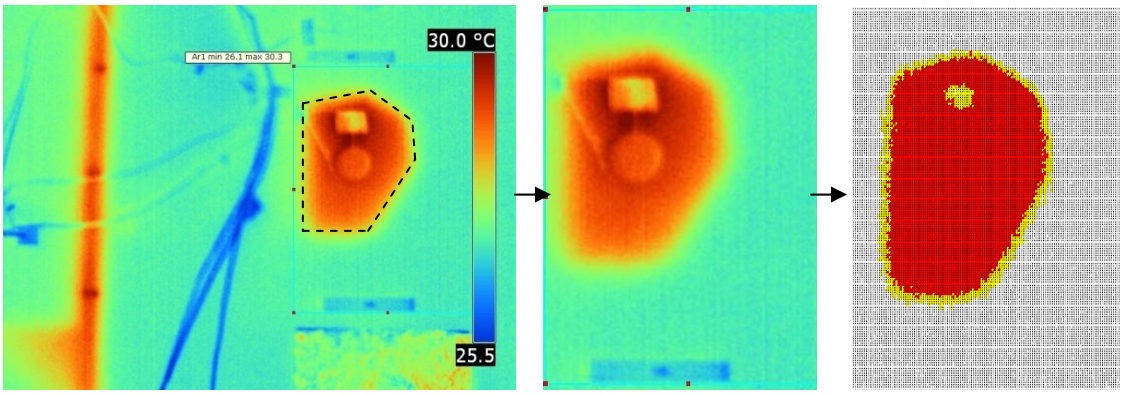

A (Total damage area) B (area to be processed) C (Processed image using Excel)

Figure 4.13 Missing Insulation, Ext.P wall system

Table 4.6 Presents the area and average surface temperature calculated over the measurements period of time, also compares the determined area with actual area using IRT measurements for Ext.P wall system. **Table 4.7** shows the true R-value for the Ext.P MI wall system and presents the percentage R-value variation of theoretical and calculated using IRT based on R_{DM}, and R_T as reference to find the R-value of total defective area, for the FG-B wall system with reference to true R-value measured with heat flux dynamic method (DM).

Table 4.6 Average surface temperature and area of Ext.P (MI) wall system calculated using IRT

Time	Area of defect cm^2	% Variation determined area/ actual area	Image reference	Surface temperature of defective area
18:00	823	2.2	2563	29.72
19:00	820	1.9	2591	29.53
20:00	816	1.4	2617	29.95
21:00	773	4	2645	29.65
22:00	802	0.4	2671	29.43
23:00	770	4.3	2693	29.43
Avg	801	Max 4, Avg 0.5, Min 0.4	Average	29.6
Actual area	805			

Table 4.7 R-value of Ext.P (MI) wall system – comparison

Method	Theoretical	SM	R_{DM}	$R\text{-}IRT_{DM}$ – one spot in defective area at sensor location	$R\text{-}IRT_T$ - one spot in defective area at sensor location	$R\text{-}IRT_{DM}$ - total defective area	$R\text{-}IRT_T$ - total defective area
R, $m^2.C/W$	0.646	0.46	0.5648	0.6029	0.6212	0.7053	0.7268
Percentage Variation (Reference – R_{DM})	12.5	18.5	-	6.7	10	24.8	28.6

Figure 4.14 illustrates an example of thermal image for Exp-P MI wall system. **Figures 4.14 A to 4.14C** illustrate the processing of the images with method described.

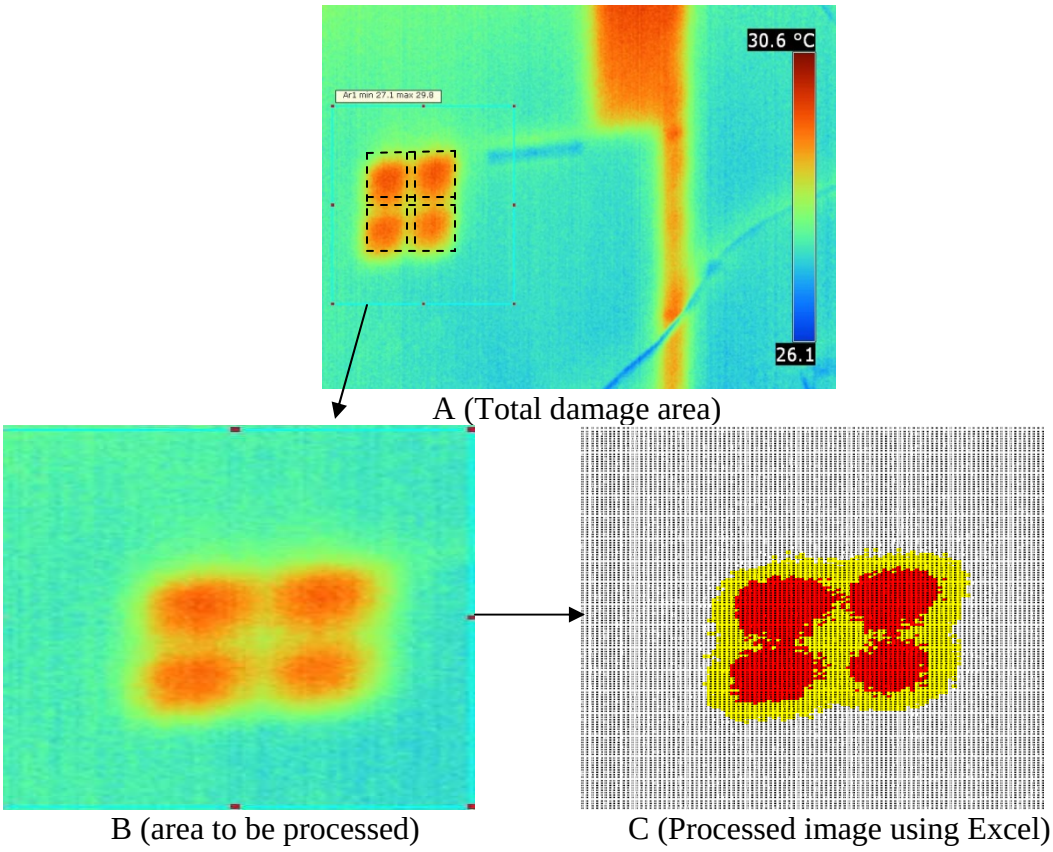

Figure 4.14 Missing Insulation, Exp.P (MI) wall system

Table 4.8 Average surface temperature and area of Exp.P (MI) wall system calculated using IRT

Time	Area of defect cm ^{2}	% Variation determined area/ actual area	Image reference	Surface temperature of defective area
18:00	379	5.3	2575	29.35
19:00	433	8.3	2601	29.2
20:00	420	5	2627	29.41
21:00	410	2.5	2655	29.36
22:00	386	3.5	2681	29.15
23:00	390	4.5	2703	29.17
Avg	403	Max 8.3%, Avg 1%, Min 2.5%	Average	29.27
Actual area	400			

Table 4.8 Presents the area and average surface temperature calculated over the measurements period of time, also compares the determined area with actual area using IRT measurements for Exp.P wall system. **Table 4.9** shows the true R-value for the Exp.P MI wall system and presents the percentage R-value variation of theoretical and calculated using IRT based on R_{DM}, and R_T as reference to find the R-value of total

defective area, for the FG-B wall system with reference to true R-value measured with heat flux dynamic method (DM).

Table 4.9 R-value of Exp.P (MI) wall system – comparison

Method	Theoretical	SM	R_{DM}	R-IRT_{DM} – one spot in defective area at sensor location	R-IRT_T - one spot in defective area at sensor location	R-IRT_{DM} - total defective area	R-IRT_T - total defective area
R, m^2.C /W	0.646	0.46	0.672	0.6467	0.6664	0.7933	0.8175
Percentage Variation (Reference – R_{DM})	3.9	31.5	-	3.8	0.9	18	21.6

4.6 Quantification of Damaged Insulation

The images taken for FG-C wall system were analyzed to find the insitu thermal resistance of the damaged insulation, **Figure 4.15** illustrates an example of a thermal image for FG-C wall system. **Figures 4.15A to 4.15C** illustrate the processing of the images with method described.

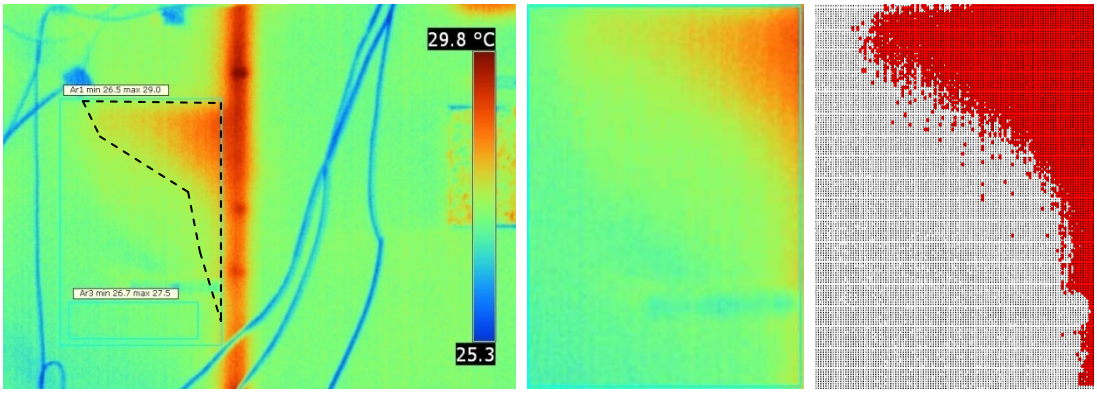

A (Total damage area) B (area to be processed) C (Processed image using Excel)

Figure 4.15 Damaged Insulation, FG-C wall system

Table 4.10 Average surface temperature and area of Exp.P (MI) wall system calculated using IRT

Time	Area of defect cm^2	Image reference	Surface temperature of defective area
18:00	486	2567	28.3
19:00	495	2593	27.92
20:00	-	2619*	-
21:00	493	2647	28.01
22:00	-	2673*	-
23:00	491	2695	28.17
Average	491	Average	28.1

*Measurements error: the images were not processed, because the measuring scale in the images was not clear.

Table 4.10 Presents the area and average surface temperature calculated over the measurements period of time for FG-C wall system. **Table 4.11** shows the true R-value for the FG-C wall system in case of no defects (FG-D wall system), and presents the R-value calculated using IRT based on R_{DM}, and R_T as reference to find the R-value of total defective area,

Table 4.11 R-value of FG-C wall system – comparison

Method	Theoretical- considering no defect	R-IRT_{DM} - total defective area	R-IRT_T - total defective area
R, m^2.C /W	1.986	1.4407	1.4847

*No heat flux measurements are available for this damaged insulation area.

It is observed from the results that the infrared images can be used to better predict the in-situ R values of wall system in a quick time comparing with other time consuming methods utilizing the heat flux instruments, and the results obtained were comparable with the most sophisticated dynamic method. It is found through the results that the simple method is the least accurate method for determination of in-situ thermal resistance of wall systems.

4.7 Quantification of Thermal Bridging

Thermal image of the FG-A wall system, representing the whole envelop is processed using the described procedure. The thermal image of the wall is illustrated in **Figure 4.16** the area of thermal bridging can be seen in slight red color in the image. A graph has been plotted between the magnitude of temperature and percentage of area is shown in **Figure 4.17**. Percentage areas representing thermal bridging, computed utilizing the stated procedures is marked with red color in the graph.

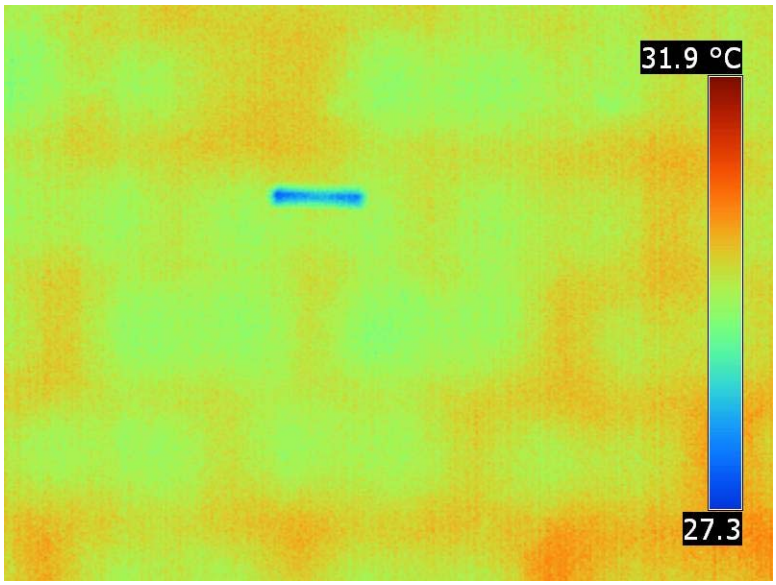

Figure 4.16 Thermal bridges in a FG-A Wall system

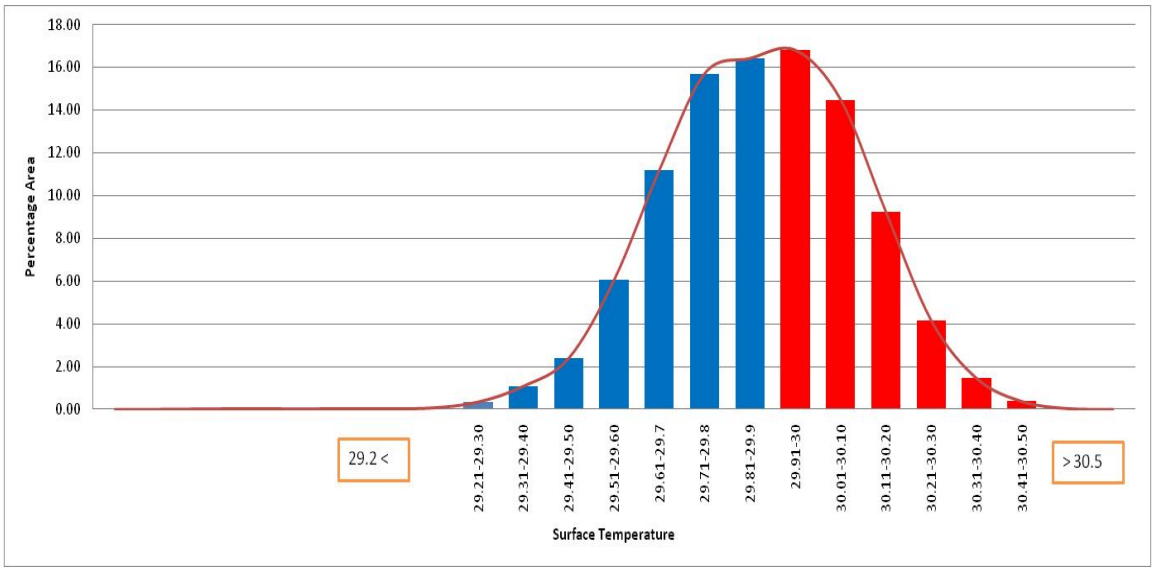

Figure 4.17 Surface temperature distribution of the wall representing the wall total area

Figure 4.18 illustrates the surface temperature variation over the FG-A wall, during the measurements time with its variation to surface area of the wall.

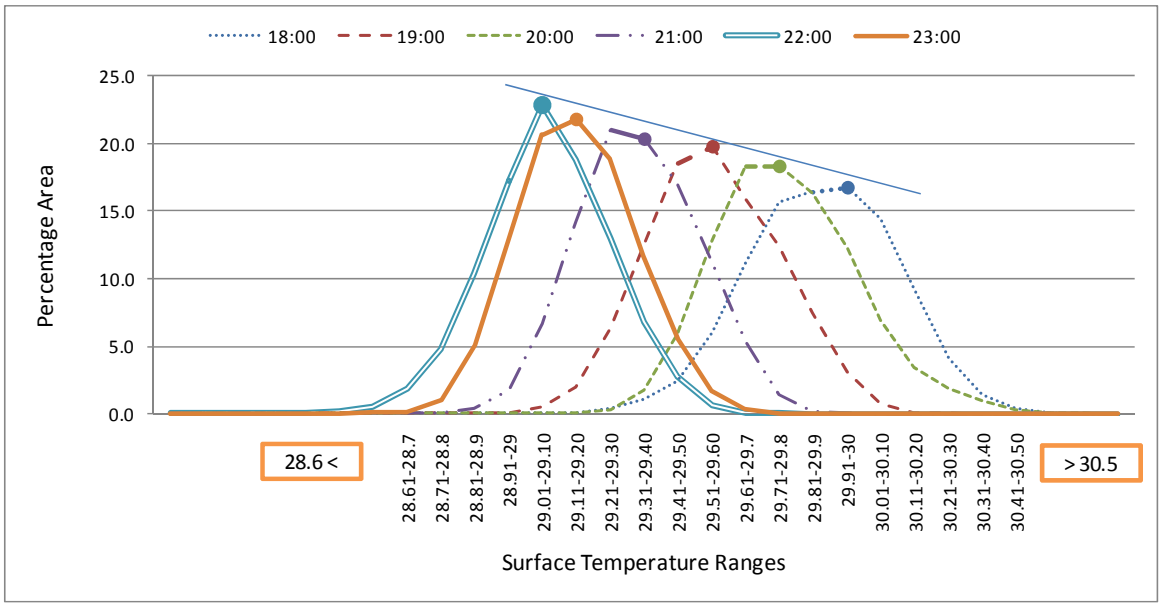

Figure 4.18 Comparative Chart- Temperature distribution curve (% Area) at various times

The detailed result with percentage difference in the normal wall area and thermal bridging area is illustrated in **Figure 4.18**. The curve trend can be observed that as the time making progress in the night the surface temperature is decreasing.

Figure 4.19 also illustrates graphically the percentage area representing normal area and thermal bridging of the FG-A wall system.

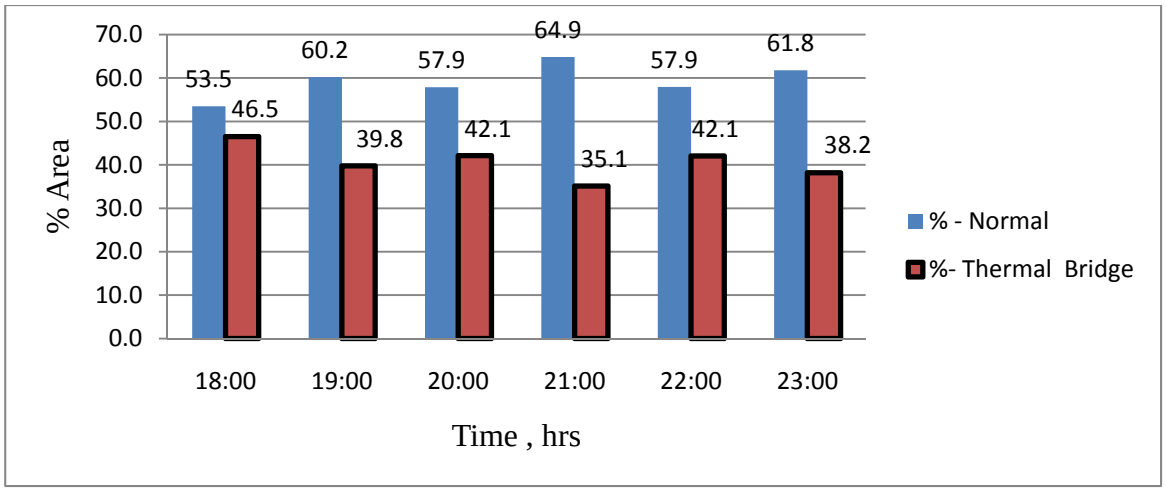

Figure 4.19 Comparison between Percentage, Normal area and Thermal Bridging area

Thermal Bridging area represents the area of the wall where the composition of wall changes from CMU Hollow block to Cement Mortar and the change in theoretical thermal resistance value at the mortar area is presented in the **Table 4.12.**

Table 4.12 The estimated components of the FG-A wall system with cement mortar instead CMU heavy wt block

Theoretical						
Equivalent Wall		**Wall-1 Components**	Thickness (**TH**), mm	**K**, W/m.C	**R**, m^2.C /W	
	Exterior	Exterior Air Film			0.040	
		Cement Plaster w/ Sand	20	0.7200	0.028	**0.171**
WALLs		Cement mortar: Bed/Vertical joints	200	1.7300	0.116	
		Cement Plaster w/Sand	20	0.7200	0.028	
	Interior	Interior Air Film			0.120	
		Total **TH**	**240**	Total **R**	**0.331**	

The results of the image processing and quantification procedure are used to find the area weighted thermal resistance of the wall as shown in **Table 4.13** with listing percentage variation reference to dynamic method. The change in the thermal resistance (R) value of the wall due to thermal bridging is found to be around 4.8% comparing with results obtained through dynamic method utilizing heat flux instrument, when the FG-A wall composition is known, the R value is found based on the area weighted average. Calculations were also performed to find the Insitu R value of the FG-A wall system, based on the quantification procedure describe by finding the average surface temperature distribution of the defective and normal area, the results obtained through this calculation is deviating by 1.4% from the dynamic method.

Table 4.13 Thermal Resistance of FG-A wall system- comparison

Methods	Theoretical	SM	DM	IRT- Area Weighted average -Known composition	IRT- Area Weighted average –Unknown Composition
R, m^2.C /W	0.246	0.1949	0.227	0.2160	0.2239
Percentage Variation (Reference DM)	8.4	14.14	-	4.8	1.4

4.8 Impact of Thermal Bridging on Energy Consumption

The building has been simulated with Visual DOE Simulation Software to find the impact of thermal bridging on the cooling energy consumption.

The base case model was developed using Visual DOE 4.1 hourly energy simulation program, which uses DOE-2.1 as its calculation engine. The Visual DOE 4.1 was selected as simulation tool in this study for the following reasons:

- It is a detailed hourly energy simulation program using hourly weather data.
- It covers all major building components, including building envelope, lighting, day lighting, water heating, HVAC and central plant, and is especially useful for studies of envelope and HVAC design alternatives.

It uses DOE-2.1E simulation tool as its calculation engine, which is one of the most widely used simulation tool that has been validated in several studies, Neymark. J et.al (2002) and Pasqualetto. L, Zmeureanu. R, Fazio. P, (1998).

- It is easily available commercially, supported by graphical Windows interface allowing easy geometric modeling.

The base model was developed from data accumulated in earlier stages through review of design drawings, and observations in the house.

- The weather file used for performing the simulations was for the city of 'Dhahran',
- The weather file for the year 2002 was used due to unavailability of the latest weather files.

The annual energy use of the building, obtained from initial simulation run, was found to be 30, 246 kWh. **Figure 4.20** illustrates the Base case energy consumption in KW- hr for each alternative simultaneously.

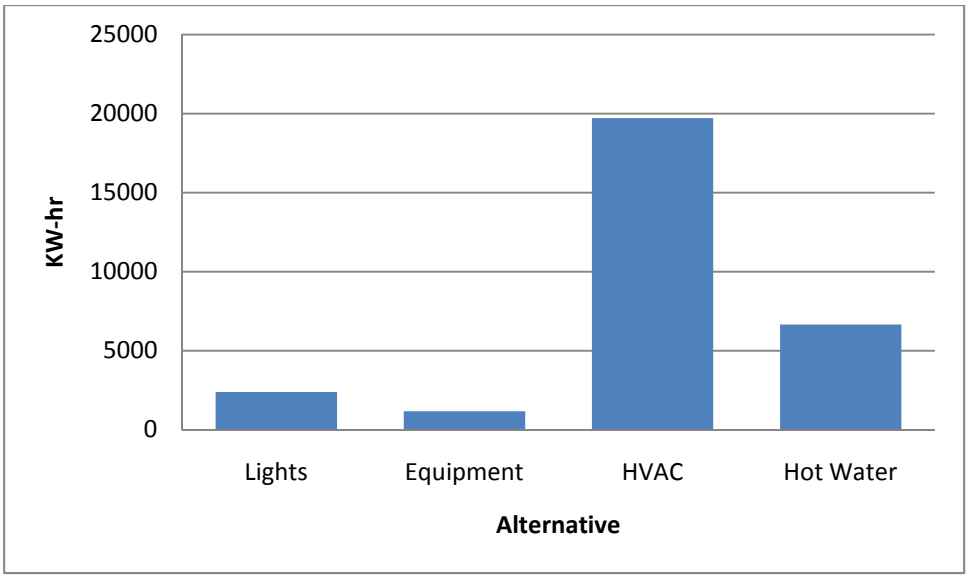

Figure 4.20 Base case energy consumption in Kwh

Simulations were performed with considering the effect of thermal bridging on the thermal resistance value of the wall, to find the impact of the thermal bridging on HVAC energy consumption It is observed that the thermal bridging has increased the HVAC energy consumption by 4.3%., detailed result is shown in **Table 4.14**.

Table 4.14 Effect of Thermal Bridging on HVAC Energy Consumption

Type of load	Energy-Kwh (Base case)	Energy-KWh Effect of thermal bridging	% Increase in energy consumption
HVAC	19716	20572	4.3
Total	29942	30798	2.9

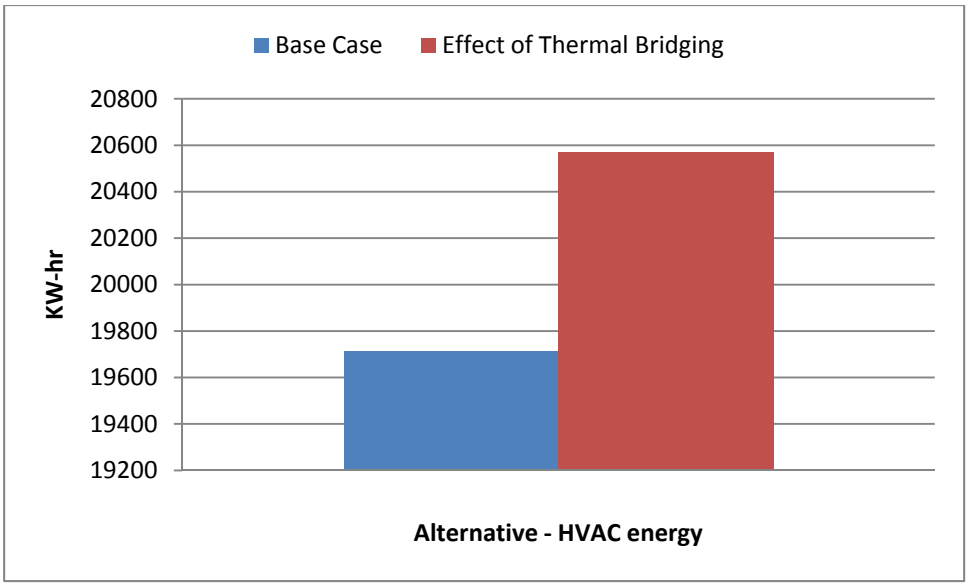

Figure 4.21 Effect of Thermal Bridging on HVAC Energy Consumption

Figure 4.22 illustrates a comparison of the impact on energy consumption on HVAC energy of the case study building due to the presence of thermal bridging in the Envelope.

In the case study building, building envelope is composed of 38% of the wall component (100 m^2 of total 259 m^2), which is contributing to 48.6% in cooling energy. And on segregation of the results in Visual DOE it is obtained that, the wall with thermal bridging is contributing 4.6% increase in total cooling energy. However the magnitude of increase in cooling energy due to thermal defects would vary with size of building and also depends on the type and magnitude of the defect in the building envelope.

CHAPTER FIVE

5 Systematic procedure for assessing the R-value of building envelope using infrared thermography IRT

5.1 Pre Measurements

A. Factors Affecting IRT Measurements

To measure surface temperature variation precisely, it is necessary to compensate for the effect of number of different radiation sources. This is done automatically by the camera, by providing following information:

- The emissivity of object
- The reflected apparent temperature (using a pre described procedure)
- The distance between the object and the camera
- The relative humidity and air temperature of indoor and outdoor environment.

Factors affecting the IR thermography inspection of a Wall System

- Climate/ Weather: wind, rain, ambient temperature
- Wetting of wall surface or moisture content within the wall
- Building: Orientation to the path of sunshine during the survey, existence of any heat generating equipment inside the building.
- Wall Surface: - emissivity, dryness, reflectivity, texture, roughness, color, stains, wall finish.

- Angle of vision and survey distance
- Building in shade of eaves or adjacent building, or screening objects (e.g. trees).

B. Infrared Device Selection and Characteristics

Few essential and basic characteristics need to be considered for the selection of the infrared device suitable for building envelope IR investigations, these are

- High resolution/ Image quality
- Wide temperature range (-10 to +55 ^{o}C) with sensitivity less the 0.1^{o}C
- Intelligent battery system, easily chargeable and long life battery
- Built in laser pointer
- Incorporated emissivity tables
- Large LCD screen, see chapter 3 for details.

C. Infrared Device Settings

Following are basic camera settings need to be performed before conducting the measurements.

- The camera on a tripod need to be fixed for better and accurate measurement, when the display provided with the camera is very small and not enough for normal human eyes to find tiny defect in the envelope, an LCD monitor is preferably required to be connected to the camera for large display, it also provides better and accurate measurement of defective areas. For long time measurements an extra battery of the camera is required.
- Temperature range settings: the cameras usually will have the option in selection of temperature range setting, for building envelope inspections temperature range of -10 to +55 ^{o}C is recommended.

- Focus control settings: auto focusing the camera, the camera needs to be kept steady while auto focusing.
- Emissivity settings: the appropriate emissivity value for the building surface is to be selected based on the color and surface finish.
- When conducting measurements for same building, the camera settings need not to be change, as this makes comparison easier for the various similar surfaces.

D. Criteria for Measurements

- The measurement should not be carried out when the outside or inside air temperature is liable to vary considerably
- The measurement should not be carried when the wall/roof system is exposed to direct solar radiation
- The measurement should not be carried when the wind varies noticeably (ISO 6781- 1983).
- For at least 24 hrs before the start of the thermographic measurements the indoor conditions are to be constantly maintained at suitable temperature. During the measurements, the air temperature drop across the building envelope is required to be at least 10^{o}C.
- The recommended negative pressure across the building for thermographic measurement is 10-50 Pa.
- Under the climatic conditions of Saudi Arabia, recommended measurements time during July and August is between 18:00 and 24:00

5.2 During Measurements

- Measurements should be carried during study state conditions, recommended time for Dhahran climate during the month of July and August is 18:00 to 24:00, minimum 4 to 6 measurements should be taken, that is one at the start of each hour.
- Information concerning environmental conditions such as outside air temperature, relative humidity, cloudiness and any moisture on the outside of the building, together with wind conditions, shall be recorded. A described Building Envelope Thermographic On-Site Inspection and Measurement form for recording of environmental and other parameters can be utilized.
- The inside and outside air temperature is to be measured preferably using temperature sensors, or also can be measured using digital or ordinary thermometers, to an accuracy of $\pm 1^{O}C$.
- Measurement scale: the measurement scale to be used in all the thermographic measurements, it can be utilize to obtain the area of the defects, during the thermal image processing stage.
- For indoor measurements the direct flow of air from the A/C duct on the measurement wall is to avoided for better and reliable measurements.
- Determination of reflective apparent temperature using thermal imaging camera.
- Distance between the object and front lens of the camera is to be measured, to compensate for the reason that radiation from the target is absorbed by the atmosphere between the object and the camera.
- Thermographic image recording

- Digital photo recording (Refer chapter 3 for details)

- R-value for reference wall can be measured using heat flow meter, to be used in quantification of defective areas in the wall system. If it is not possible due to any reasons such as time concerns, practicality, or due to availability of equipments, then theoretical R value can be used in determination of affective R-value of non homogeneous wall system using IRT. But the theoretical R-value of the reference wall must be taken from the standards (ASHRAE).

- Heat flux measurements

Conduct measurement as per ISO 9869 standard (Dynamic Method)

Table 5.1 Comparison between R-value obtained using dynamic method and theoretical R-value

Criteria/ Item	Dynamic Method	Theoretical
Compositions of wall	R-values can be computed with unknown composition	Must be known to find R-value
Time duration	Long	Short
Practicability	Difficult/ Not practical	Easy (ASHRAE Standard)
Age of construction	Takes into account	Does not take into account
Construction defect	Takes into account	Does not take into account
Equipments	Must be available	No need
Cost	High	Low
Calculation	Extensive	Simple
R-value correctness	High. Close to actual	Low

5.3 Data Analysis

- Once the measurements are finished, the stored images are to be reviewed for data accuracy utilizing the Flir ThermaCam software, for any mismatch of data by comparing the emissivity, RH, RAF, distance, and temperature with the measurement form.

- Utilizing various software's of Flir ThermaCam and image processing, for the quantification of thermal bridging, damaged insulation and missing insulation, to find the insitu thermal resistance of the building envelope.
- The flying spot meter (ThermaCam software) can be used to measure the temperature at any spots within the image. Also it is used to find the surface temperature range within the defective area. A rectangular selection gives an average temperature within that area with indicating the minimum and maximum temperature in the selected area.
- The software produces the output, dividing the image into 76800 small areas (240X320 Matrix) hence in various different temperatures representing the surface temperature distribution of wall.
- An excel function "count if" can be used to find the number of cells representing each temperature, to find the average temperature in the defective and non defective area of building envelope.
- Image processing software Image J is used to find the area of the images, the scale bonded on the wall during the measurements is utilized as the reference in calculation of the area of the image hence area of the each cell is computed.
- The area weighted surface temperature distribution is computed for defective and non defective area.
- Proposed quantification procedure is then utilized for the calculation of in-situ thermal resistance.

Figure 5.1 illustrates graphically the proposed systematic procedure for assessing R-Value of building envelope using IRT

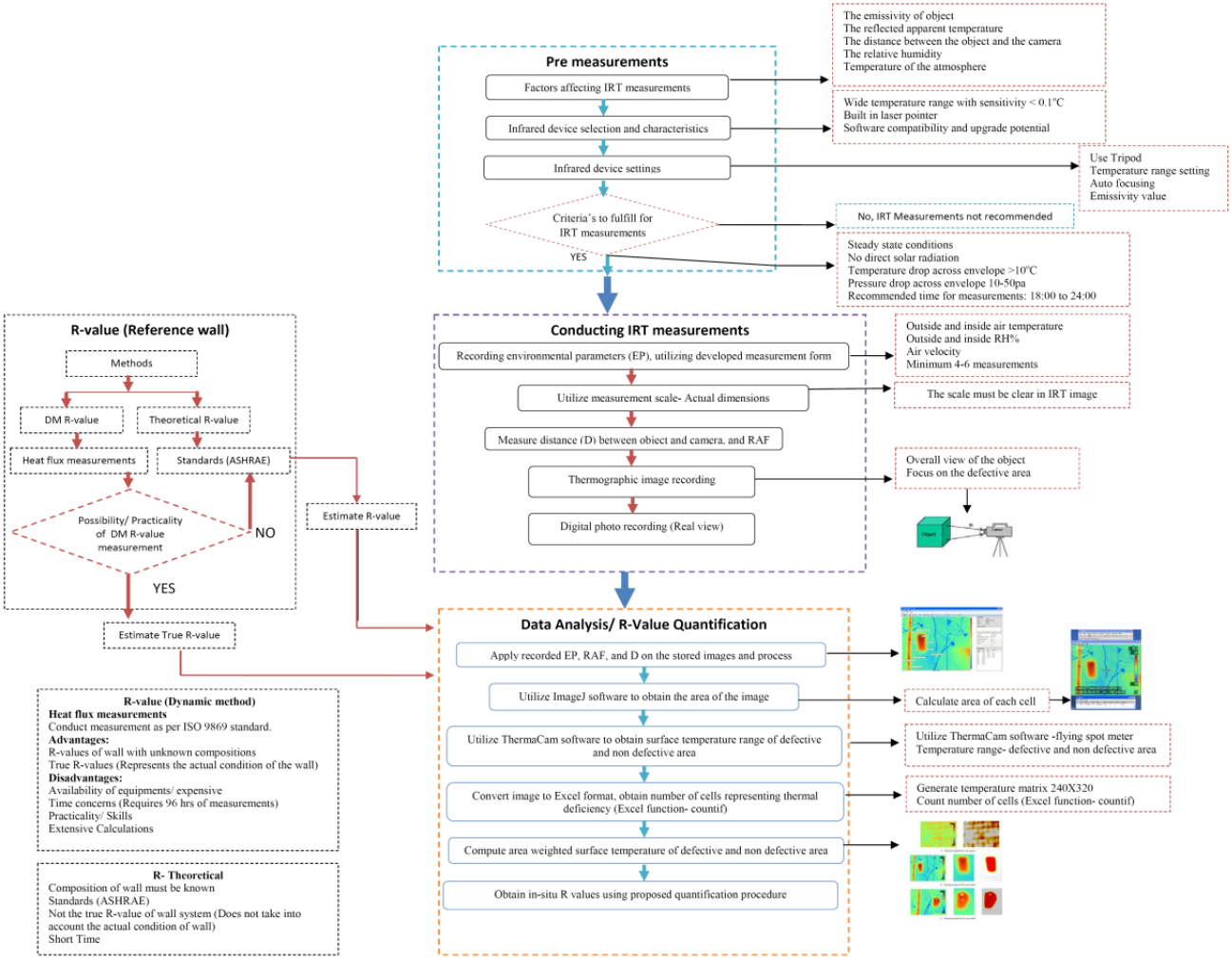

Figure 5.1 Systematic procedure for assessing R-Value of building envelope using IRT

CHAPTER SIX

6 Summary, Conclusions and Recommendations

This chapter concludes the thesis by outlining the contributions achieved, and the scope of future work.

6.1 Summary

The present study is aimed at assessing the thermal energy performance of envelope design. Infrared thermography can easily detect building abnormalities that result in energy losses. An infra red (IR) camera is a device that makes an image of the thermal pattern and is calibrated to measure the emissive power of the surface in an area at various temperatures. It uses a lens to focus the emitted IR radiation on to a detector and the electrical response signal is converted into visual display in which the different colors correspond to various temperatures. The surface temperature distribution can be used to detect thermal irregularities due to thermal bridging, insulation defects, and moisture or air leakage. An increase in temperature causing an increase in heat transfer is directly proportional to the surface temperature differences between the defective and non-defective areas. The application of infrared thermography has provided a reliable and accurate assessment method for the inspection of buildings and structures. The main

factors effecting the infrared measurements are the emissivity of object, reflected apparent temperature, distance between the object and the camera, and the relative humidity. The temperature drop across the building envelope should be sufficiently large to permit the detection of thermal irregularities. For ease of interpretation the thermographic examination should preferably be carried out with constant temperature- and pressure drops across the envelope.

For the study a residential building on KFUPM campus is selected to conduct both thermographic and heat flux measurements. The building envelope is modified by installing three different types of insulation layers (i.e. Fiber Glass, Extruded Polystyrene, and Expanded Polystyrene). Data obtained by heat flux measurements about the building envelope thermal characteristics has been processed following the ISO standard 9869:1994. To solve the required algorithm a MATLAB Program was developed. Simultaneously thermal imaging technique is used to record the surface temperature variation in the building envelope. Recorded thermal images are analyzed using Flir, Excel and ImageJ software's to detect damaged thermal insulation, missing insulation and thermal bridging, and the area of the defects with weighted surface temperature distribution is computed. A method for quantification of missing thermal insulation, damaged insulation and thermal bridging is developed to improve the prediction of actual thermal resistance of building envelope using infrared thermography. As a result of analysis of R-value calculation for the test wall it is found that R-values calculated using R-IRT_{DM} on average are varying by 7.3% when R-value is calculated referenced to R_{DM}, and R-IRT_T on average are varying by 7.2 % when R-value is calculated referenced to R_T of the wall. However reference R-value, measured using dynamic method value is more

accurate and reliable compared to theoretical R- because it takes into account the age of the construction and other factors as described in the study. IRT method described in the study can be used to obtain the effective R-value of the envelope by considering total thermal behavior of the envelope considering the total defective area rather than measuring the R-values at a single point using the dynamic method.

Energy simulation program Visual DOE is used to evaluate the impact of thermal bridging on cooling energy, compared to when building envelope is properly designed and well constructed. It is observed that the thermal bridging has increased the HVAC energy consumption by around 4% in this particular case.

6.2 Conclusions

The present study was aimed at predicting of actual R-value of building envelope using high definition thermal imaging technique. Essential features and characteristics required of the thermal imaging device, various available ThermaCam, essential features and characteristics and the various heat flux measurement instruments are described in the study.

During thermographic measurements the indoor conditions are to be maintained at suitable temperature, and during the measurements the air temperature drop across the building envelope shall be at least 10^{o}C. For better and accurate results during the measurement period, the air temperature drop shall not vary more than 30 % from its value at the start of the measurements. During the investigations, the indoor air temperature shall not vary by more than 2^{O}C. The measurements were conducted from 18^{th} July to 11^{th} August, 2010 as per the described procedure. The measurements were

usually conducted during the evening time from 18:00 to 24:00, to make of sure steady state conditions across the building envelop and to avoid the effect of solar radiation.

The building selected for the study is an existing residential building located on KFUPM campus, Dhahran, Saudi Arabia. The building envelope of the selected building is originally non insulated. For this study a wall was selected facing North East of Size 4 meters length X 2.77 meters height, the original composition of the wall was 200mm heavy weight hollow, 20mm cement plaster on both sides. The wall composition has been changed by adding different types of insulation and gypsum boards. Three different types of insulation have been used, namely expanded polystyrene, extruded polystyrene, and fiberglass to conduct measurements with different wall compositions, and to apply the measurement and analysis to different wall systems. K value for the used insulation materials were measured using the heat flow meter (Holometrix, Type Lambda 2300V) following the ASTM C518 and ISO 8301 standards.

In-situ thermal resistance measurements were conducted following the procedure “in-situ measurement of thermal resistance and thermal transmittance”, (IS0 9869: 1994) established by the International Standards Organization. For the test wall, a total of ten locations (i.e. nine spots on the test wall and one on the roof – in ten spots, three spots were for three types of insulation, four were of missing insulation, one spot for wall without insulation, and moisture damaged were selected for measuring the thermal resistances (R-values), of walls and roof. The test was conducted from 18th July-11 August 2010, for 5 days for each set of measurement with three heat flux sensors. A program was developed for CR 10Xmulti-channel data logger to setup the data logger and to record the measurement every five minutes at the investigated locations (12

temperature, and 3 heat flux measurements), and to retrieve/ download all the data from the CR 10X instrument to the computer.

A Matlab program is developed to process the heat flux data, by using the simple method without and with consideration to the storage effects (when the wall composition is known and not known), and the dynamic method, which is more sophisticated but gives a quality criterion of the measurement and may shorten the test duration for medium to heavy elements exposed to variable indoor and outdoor temperatures.

The stored images are reviewed for data accuracy utilizing the Flir ThermaCam software, for any mismatch of data by comparing the emissivity, RH, RAF, distance, temperature with the measurement form. Any of them not entered properly during of the measurements in the camera, can be inserted in the software. The software takes account these modified values to produce the image with actual onsite conditions. Once this is done the flying spot meter can be used to measure the temperature at any spots within the image. A rectangular selection gives an average temperature within that area with indicating the minimum and maximum temperature in the selected area.

The images produced by Flir thermal imaging camera are of 240 X 320 pixels in size, producing a total of 76800 pixels, in turn producing 76800 different areas representing various temperature distributions. The temperature distribution can be retrieved in an excel sheet. An excel function “count if” is used to find the number of cells representing each temperature, to find the average temperature in the defective area of building envelope. Image processing software ImageJ is used to find the area of the images,

utilizes the scale bonded on the wall during the measurements as the reference in calculation of the area of the image.

A quantification procedure is developed to find the in-situ thermal resistance of missing insulation and thermal bridging. For the case study building it is found that, 40% of the envelope wall area is effected by the thermal bridging, it is mainly due to mortar between the concrete masonry units heavy weight blocks. The R-value found for wall using IRT is varying by 8.2% when R-value is determined referenced to R_{DM}, and 11.9% when R-value is determined based on referenced to R_T compared to the results obtained via dynamic method.

The quantification procedure is also applied to find the in-situ R-value of missing insulation. R-values obtained using R-IRT_{DM} for missing insulation is varying from R_{DM} by 6% on average, and R-IRT_T for missing insulation is varying from R_{DM} by 6.5% on average compared to the results obtained with R_{DM}. R-values for properly insulated areas calculated using R-IRT_{DM} are on average varying from R_{DM} by 9.4% , and R-IRT_T are varying from R_{DM} by 9.8% compared to the results obtained with R_{DM}. Based on analysis of R-value calculation for the test wall it is found that R-values determined using R-IRT_{DM} are varying from R_{DM} by 7.3% and R-IRT_T are varying from R_{DM} by 7.2 %. However reference R-value, measured using dynamic method value is more accurate and reliable compared to theoretical R- value because it takes into account the age of the construction and other factors as described in the study.

Theoretical R-value and R-value measured using dynamic method gives the R-values of the wall at a particular point on the wall envelope, rather than considering the total

thermal behavior of the wall envelope. IRT method described in the study can be used to obtain the effective R-value of the envelope by considering total thermal behavior of the envelope and with respect to total defective area. The proposed method in the study is applied to obtain the effective R-value of the total damaged insulation area rather than measuring the R-value at one point using the dynamic method. R-values obtained using R-IRT_{DM} for total defective area in the FG-B wall system was varying by 6.7% compared to R_{DM}, and it is varying by 3.9% when calculated using R-IRT_{DM} at the same location measured using the dynamic method, which shows that there is different type of thermal behavior within the missing insulation, and proves the effectiveness of IRT technique in determination of effective R-value of the building envelope.

Simulations using Visual DOE software were performed to find the impact of thermal bridging on HVAC energy consumption. It is observed that the thermal bridging has increased the HVAC energy consumption by around 4% in this particular case. However, the magnitude of variation could vary depending on the type and magnitude of the defects existing in the building envelope.

The methods proposed in the study for quantification of thermal deficiency in building envelop can be used for better prediction of actual thermal resistance value of the building envelope. However heat flux measurements at one point in a non homogeneous wall can be utilized to better predict the overall effective R-value of the wall using IRT with more reliable results, rather than using Theoretical R-value of the wall.

6.3 Recommendations for Future Work

The study has highlighted many findings that may lead to future potential research. The followings are potential extensions of this research.

- Developing a computer program to estimate the Insitu R-values from IR Images, to automate the procedure described for the quantification.

- Moisture damage in thermal insulation was not considered in this study, developing a method for quantification of R-values due to moisture damage using IR images is recommended for future investigations.

- Integration of three software programs (Flir, ImageJ, and Excel) into one program for speeding the process of R-value quantification.

REFERENCES

1. ASHRAE Fundamentals “The ASHRAE Hand Book of Fundamentals”, 2005.
2. Al-ajmi Farraj F, V.I. Hanby. (2008). “Simulation of energy consumption for Kuwaiti domestic buildings”, Elsevier, Energy and Buildings 40, pp. 1101–1109.
3. Al-Homoud MS (2005) “Performance characteristics and practical applications of common building thermal insulation materials”, Elsevier, Building and Environment 40, 353–366.
4. Antonio Colantonio (1998). “The use of infrared thermography in detection, remediation and commissioning of thermal comfort problems in office buildings”, Public Works and Government Services Canada, Technology Directorate.
5. Academy of infrared thermography, (1990). “Infrared thermography and predictive building maintenance”, B.C. Canada.
6. Ananthanarayanan P N. (2007) “Basic Refrigeration and Air conditioning” Tata McGraw Hill, Third Edition, pp. 369-370.
7. Avdelidis N.P and Moropoulou A. (2002). “Emissivity considerations in building thermography”, Elsevier, Energy and Buildings 35, pp. 663–667.
8. B. Drury Crawley, Linda K. Lawrie, Frederick C. Winkelmann, W.F. Buhl, Y. Joe Huang, Curtis O. Pedersen, Richard K. Strand, Richard J. Liesen, Daniel E. Fisher, Michael J. Witte, Jason Glazer (2001). “Energy plus: creating a new generation building energy simulation program”, Elsevier, Energy and Buildings 33, pp. 319-331.
9. Barreira E and Vasco P. de Freitas. (2005). “Evaluation of building materials using infrared thermography”, Elsevier, Construction and Building Materials 21 (2007) pp. 218–224.
10. Balaras C A and Arguiriou A. (2002). “Infrared thermography for building diagnostics. Energy and Buildings”, Elsevier, Energy and buildings 34, pp. 171-183.
11. Changhai Peng, Zhishen Wua (2008), “In situ measuring and evaluating the thermal resistance of building construction”, Energy and Buildings vol. 40, 2076–2082
12. Chew M.Y.L (1998). “Assessing building facades using Infra-red Thermography”, MCB University Press, Structural Survey, Volume 16 · Number 2 · 1998 · pp. 81–86.
13. Christopher J.P. (2009). “The Complete Guide to Exterior Wall Insulation” well Garth Publishing Limited, pp 5.
14. David L. Jakovac (2010), “How Infrared Thermography Drives Building Energy Conservation Retrofit Techniques - FDJ Engineering & Construction”, InfraMation 2010 Proceedings.
15. Dufour Marianne Bérubé, Dominique Derome, Radu Zmeureanu (2009). “Analysis of thermograms for the estimation of dimensions of cracks in building envelope, Elsevier”, Infrared Physics & Technology 52, pp. 70–78
16. FLIR SYSTEMS, 2004. FLIR System manual, 2004
17. FLIR Systems (2009). Users Manual, Thermo Cam B 20
18. Gul Oral Koclar, Alpin K'oknel Yener, Nurg'un Tamer Bayazit. (2004). “Building envelope design with the objective to ensure thermal, visual and acoustic comfort conditions”, Elsevier, Building and Environment 39, pp.281 – 287.
19. G.Fivos sargentis , A. Chatzimpiros and N. Symeonidis (2009), “ Determination method of thermal conductivity of building parts in situ through IR imaging by minimizing the influence of environmental parameters”, Proceedings of the 11th International Conference on Environmental Science and Technology Chania, Crete, Greece.
20. Hatice Sozer (2010). “ Improving energy efficiency through the design of the building envelope” Energy and Buildings 35, 327–336

21. Juha Jokisalo, Jarek Kurnitski, Minna Korpi, Targo Kalamees, JuhaVinha (2009). “Building leakage, infiltration, and energy performance analyses for Finnish detached houses”, Elsevier, Building and Environment44, pp. 377–387.
22. K.S. Al-Jabri, A.W. Hago, A.S. Al-Nuaimi, A.H. Al-Saidy (2005), “Concrete blocks for thermal insulation in hot climate”, Cement and Concrete Research 35 (2005) 1472– 1479
23. Robert madding (2008). “Finding R-values of stud frame constructed houses with IR thermography”, Inframation 2008 proceedings.
24. Jinghua. Y (2009). “Evaluation on energy and thermal performance for residential envelopes in hot summer and cold winter zone of China”, Elsevier, Applied Energy 86.
25. Luai M. Al-Hadhrami, A. Ahmad, 2009, “Assessment of thermal performance of different types of masonry bricks used in Saudi Arabia”, Elsevier, Applied Thermal Engineering 29, pp- 1123–1130.
26. Lyberg M.D (1990). “Detection of moisture damage in buildings using thermography”, SPIE Vol. 1313 Thermo sense XII.
27. Mohamed A. Elhadidy, Manzoor-ul-Haq, and Aftab Ahmad (2000), “Electric Energy Consumption in Selected Residential Buildings at KFUPM, Dhahran, Saudi Arabia”, IEEE, KFUPM/RI project No. 12031.
28. Meroni and Valter (1998). “Energy assessment of building envelopes through NDT methods”, Proceeding of SPIE, Vol 3056, pp. 50-58.
29. Neymark. J et.al (2002). “Applying the building energy simulation test (BESTEST) diagnostic method to verification of space conditioning equipment models used in whole-building energy simulation programs”, Energy and Buildings 34, Pg. 917–931
30. Mao. G and Johannesson. G, (1997). “Dynamic calculation of thermal bridges”, Elsevier, Energy and Buildings 26 (1997) 233-240.
31. Neto Luı´s P.C, Gameiro Silva M.C, Jose J Costa. (2006). “On the use of infrared thermography in studies with air curtain devices”, Elsevier, Energy and Buildings 38, pp. 1194–1199.
32. Tuomaala .P and Rahola. (1995). “Combined Air Flow and Thermal Simulation of Buildings”, Elsevier, Building and Environmen1, Vol. 30, No. 2, pp. 255-265, 1995.
33. Pasqualetto. L, Zmeureanu. R, Fazio. P, (1998). “A Case Study of Validation of an Energy Analysis Program: MICRO-DOE2.1 E, Building and Environment. Vol. 33, No. I, pp. 2141
34. Raj Baldev, Jaya Kumar T and Thavasimuthu M. (2007).”Practical Non Destructive Testing”, Alpha Science International Ltd, pp. 125-129.
35. Saudi Electricity Company (SEC), Annual Report, 2008.
36. Saleh Al Saadi. N (2006). “Envelope design for thermal comfort and reducing energy consumption in residential buildings”, KFUPM, a Master Thesis.
37. Theodosiou T.G and Papadopoulos A.M. (2008). “The impact of thermal bridges on the energy demand of buildings with double brick wall constructions”, Elsevier, Energy and Buildings 40. Pp.2083–2089.
38. Titman DJ, (2001). “Applications of thermography in non-destructive testing of structures”, Elsevier, NDT&E International 34, pp.149–154.
39. Tommy Lo Y. and Choi. K.T.W. (2004). “Building defects diagnosis by infrared thermography”, Emerald Group Publishing Limited, Structural Survey Volume 22 · Number 5 · 2004 · pp. 259–263.
40. Will Decker (2009), “Evaluation of Residential Masonry Buildings”, InfraMation 2009 Proceedings
41. Wiggenhauser. H (2002). “Active IR-applications in civil engineering”, Elsevier, Infrared Physics & Technology 43, pp. 233–238.
42. Yin Pan Yiqun, Rongxin, and Zhizhong Huang. (2008). “Energy modeling of two office buildings with data center for green building design”, Elsevier, Energy and Buildings 40, pp.1145–1152.
43. Xavier P.V. Maldague. (2001). “Theory and Practice of Infrared technology for Non Destructive Testing”, John Wiley & Sons.

44. Yilmaz. Z (2006). “Evaluation of energy efficient design strategies for different climatic zones: Comparison of thermal performance of buildings in temperate-humid and hot-dry climate”, Elsevier, Energy and Buildings 39, pp. 306–316.
45. ISO standard 6781-1983, Thermal Insulation- Qualitative detection of thermal irregularities in building envelopes- Infrared method.
46. Yongzheng Shi, Hongbing Chen, Qi Xu, Deying Li, Zhonghua Wang, and Xiumu Fang (2006). “Application of Infrared Thermography in Building Energy Efficiency”, ICEBO2006, Building Commissioning for Energy Efficiency and Comfort, Vol. VI-5-3.
47. http://apps1.eere.energy.gov/buildings/energyplus/energyplus_about.cfm, accessed January 2011.
48. http://www.campbellsci.com/dataloggers, accessed January 2011.

APPENDECES

APPENDIX A: Test reports of thermal conductivity of various insulation materials used in the case study, measured using Holometrix

APPENDIX B: Developed data logging program to retrieve measurements from heat flux instrument

APPENDIX C: Program developed to calculate R-value using the algorithm of simple and dynamic method

APPENDIX D: Thermal Conductance measurement of the Test Wall

APPENDIX A: Test reports of thermal conductivity of various insulation materials used in the case study, measured using Holometrix

TEST REPORT : Thermal Insulation

Date	:	Sunday, July 25, 2010	
Material Type	:	Expanded Polystyrene , Styrofoam	
Specimen Identification	:	EP-2, D32.27	
Color	:	White	
Trade Mark	:	EP-2	
Supplied by **(Applicant)**	:	EP-2	
Manufactured by	:	EP-2	
Specimen Thickness	:	5.00	cm (Transducer sensed)
Specimen Density	:	32.27	Kg/m^3 , (as measured)
Number of Setpoints	:	3	
Mean Temperature Range	:	20 To 35	^oC
Setpoint Temperatures	:	20, 24, 35	^oC
Delta Temperature	:	21	^oC

NOTE: TEST IS CONDUCTED ACCORDING TO : **ASTM C 518 - 91, ISO 8301**

TEST RESULTS : (SI Units)

Mean Temperature (T), ^oC	Thermal Conductivity (*k*), W / m. ^oK	Thermal Resistance (*R*), $m^2.{}^oK$ / W
19.38	0.040345	1.23981
24.1	0.041055	1.21837
35.34	0.042921	1.16540

k , T Correlation =	k = 0.0001622 (T) + 0.037178
k @ 24 ^oC, (W / m.^oK)	0.04107

Accuracy = +/- 1.0% - 3.0%

Repeatability = +/- 0.1% - 0.3%

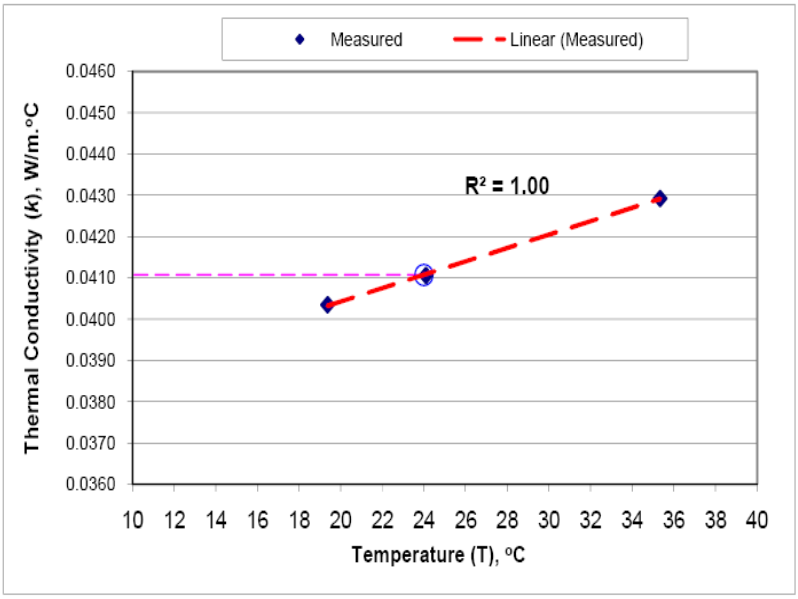

Note : This report concerns the test specimen described above and received by the ARE LAB is CONFIDENTIAL
* It should therefore be used by the applicant only, and should not be used for the product advertisement

TEST REPORT : Thermal Insulation

Date	:	Monday, July 26, 2010	
Material Type	:	Extruded Polystyrene , Styrofoam	
Specimen Identification	:	E-1, D32.27	
Color	:	Pink	
Trade Mark	:	E-1	
Supplied by **(Applicant)**	:	E-1	
Manufactured by	:	E-1	
Specimen Thickness	:	5.03	cm (Transducer sensed)
Specimen Density	:	32.27	Kg/m^3 , (as measured)
Number of Setpoints	:	3	
Mean Temperature Range	:	20 To 35	^oC
Setpoint Temperatures	:	20, 24, 35	^oC
Delta Temperature	:	21	^oC

NOTE: TEST IS CONDUCTED ACCORDING TO : **ASTM C 518 - 91, ISO 8301**

TEST RESULTS : (SI Units)

Mean Temperature (T)	Thermal Conductivity (*k*)	Thermal Resistance ®
^oC	W / m. ^oK	$m^2.^oK$ / W
19.31	0.03	1.67733
24.15	0.030462	1.65189
35.29	0.03198	1.57348

k , T Correlation =	k = 0.0001261 (T) + 0.027505
k @ 24 ^oC, (W / m.^oK)	0.03053

Accuracy = +/- 1.0% - 3.0%

Repeatability = +/- 0.1% - 0.3%

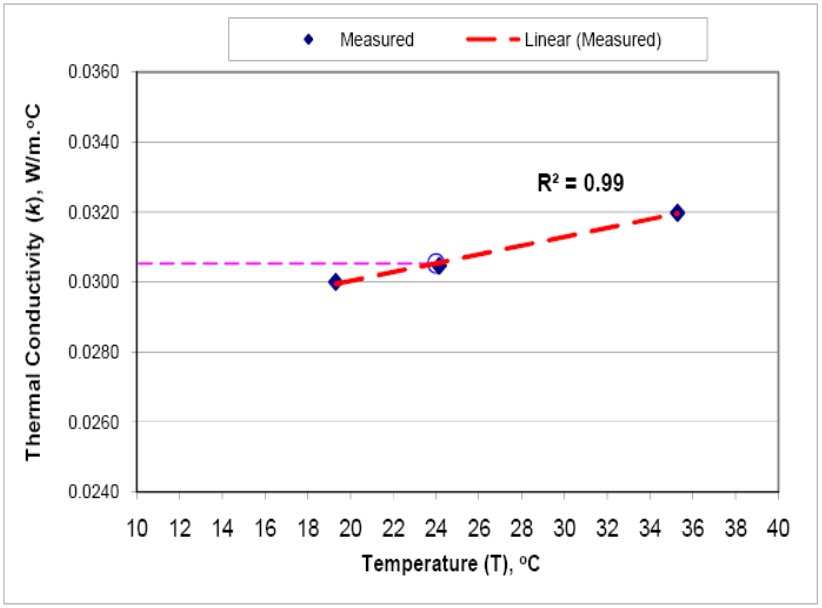

Note : This report concerns the test specimen described above and received by the ARE LAB is CONFIDENTIAL

* It should therefore be used by the applicant only, and should not be used for the product advertisement

TEST REPORT : Thermal Insulation

Date	:	Tuesday, July 27, 2010	
Material Type	:	Fiberglass (Sides: Aluminum and Wooven Mat)	
Specimen Identification	:	F1, D114.65	
Color	:	Yellow	
Trade Mark	:	F-1	
Supplied by **(Applicant)**	:	F-1	
Manufactured by	:	F-1	
Specimen Thickness	:	5.090	cm (Transducer sensed)
Specimen Density	:	114.65	Kg/m^3, (as measured)
Number of Setpoints	:	3	
Mean Temperature Range	:	20 To 35	^oC
Setpoint Temperatures	:	20, 24, 35	^oC
Delta Temperature	:	21	^oC

NOTE: TEST IS CONDUCTED ACCORDING TO : **ASTM C 518 - 91, ISO 8301**

TEST RESULTS : (SI Units)

Mean Temperature (T)	Thermal Conductivity (*k*)	Thermal Resistance ®
^oC	W / m. ^oK	$m^2.^oK$ / W
19.39	0.033028	1.54112
23.96	0.033422	1.52295
35.29	0.033999	1.49710

k , T Correlation =	k = 0.0000591 (T) + 0.031933
k @ 24 ^oC, (W / m.^oK)	0.03335

Accuracy = +/- 1.0% - 3.0%

Repeatability = +/- 0.1% - 0.3%

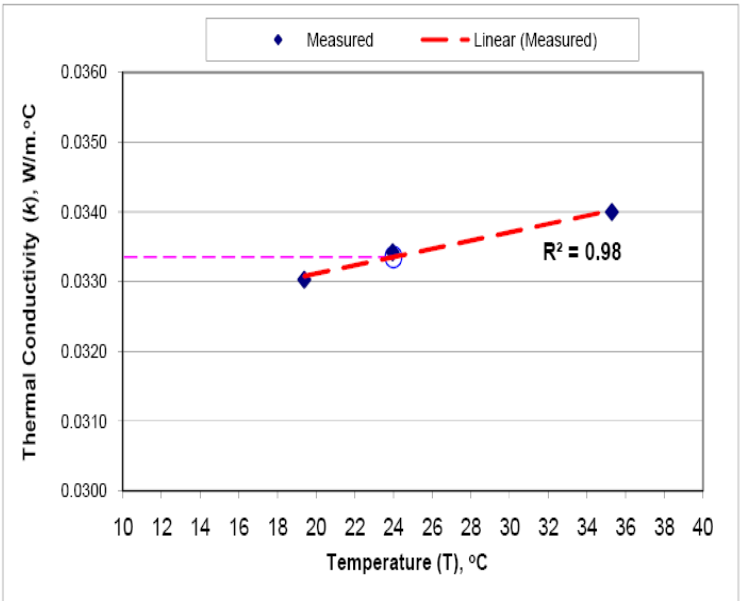

Note : This report concerns the test specimen described above and received by the ARE LAB is CONFIDENTIAL

* It should therefore be used by the applicant only, and should not be used for the product advertisement

TEST REPORT : Thermal Insulation

Date	:	Wednesday, July 28, 2010	
Material Type	:	Gypsum Board	
Specimen Identification	:	G-1, D654.42	
Color	:	White	
Trade Mark	:	G-1	
Supplied by **(Applicant)**	:	G-1	
Manufactured by	:	G-1	
Specimen Thickness	:	1.330	cm (Transducer sensed)
Specimen Density	:	654.42	Kg/m^3, (as measured)
Number of Setpoints	:	3	
Mean Temperature Range	:	20 To 35	^oC
Setpoint Temperatures	:	20, 24, 35	^oC
Delta Temperature	:	21	^oC

NOTE: TEST IS CONDUCTED ACCORDING TO : **ASTM C 518 - 91, ISO 8301**

TEST RESULTS : (SI Units)

Mean Temperature (T)	Thermal Conductivity (*k*)	Thermal Resistance ®
^oC	W / m. ^oK	$m^2.^oK$ / W
19.14	0.164944	0.08063
24.56	0.165542	0.08034
35.08	0.165868	0.08018

k , T Correlation =	k = 0.0000543 (T) + 0.164026
k @ 24 ^oC, (W / m.^oK)	0.16533

Accuracy = +/- 1.0% - 3.0%

Repeatability = +/- 0.1% - 0.3%

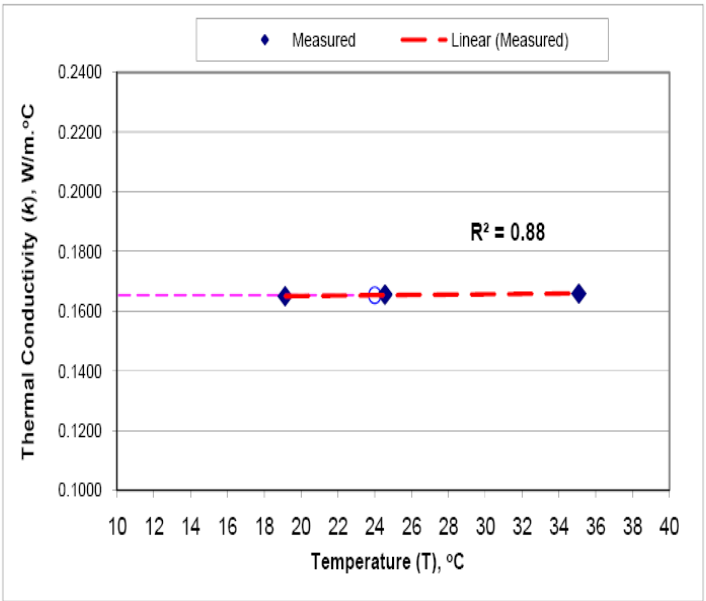

Note : This report concerns the test specimen described above and received by the ARE LAB is CONFIDENTIAL

* It should therefore be used by the applicant only, and should not be used for the product advertisement

APPENDIX B: Developed data logging program to retrieve measurements from heat flux instrument

Program Documentations

```
};CR10X
MODE 1
SCAN RATE 60 : SCANNING EVERY MINUTE
1:P10                   : BATTERY VOLTS
1:26

2:P17                   : INTERNAL TEMPERATURE
1:27                    : LOCATION

3:P86                   : DO LOOP
1:41                    : PART 1, 41 TO ENABLE MULTIPLEXER SET POINT HIGH

4:P87                   : LOOP
1:0                     : DELAY
2:6                     : LOOP COUNT

5:P90                   : STEP LOOP INDEX
1:2                     : INCREAMENT FOR THE LOOP INDEX COUNTER (6X2=12-TEMP) ONE
                          LOOP MEASURES 2

6:P86                   : DO
1:72                    : PULSE PORT 2. (TO PASS THE PULSE)

7:P22                   : EXCITATION WITH DELAY
1:1                     : EXCITATION CHANNEL NUMBER
2:0                     : DELAY TIME
3:1                     : DELAY TIME WHEN EXCITATION IS TURNED OFF
4:0

8:P14                   : THERMOCOUPLE DIFFERENCE TEMP MEASUREMENT
1:2                     : REPITITION
2:22                    : RANGE
3:3                     : CHANNEL LOCATION (DATA LOGGER)
4:1                     : TC TYPE- T-TYPE
5:27                    : REFERENCE THERMISTER
6:1                     : INPUT LOCATION (1,2,3,4,5,6,7,8,9,10,11,12)
7:1                     : MULTIPLIER
8:0                     : OFFSET

9:P95                   : END

10:P87                  : LOOP
1:0                     : DELAY
2:2                     : ITERATION COUNT

11:P90                  : STEP LOOP INDEX
1:2                     : INCREAMENT FOR THE LOOP INDEX COUNTER (6X2=12-TEMP) ONE
                          LOOP MEASURES 2

12:P86                  : DO
1:72                    : PULSE PORT

13:P22                  : EXCITATION WITH DELAY
```

```
1:1                 : EXCITATION CHANNEL NUMBER
2:0                 : DELAY TIME
3:1                 : DELAY TIME WHEN EXCITATION IS TURNED OFF
4:0

14:P2               : VOLTAGE DIFFERENTIAL MEASUREMENT
1:2                 : REPETITIONS
2:23                : RANGE CODE (AUTO RANGE)
3:3                 : DIFFERENTIAL CHANNEL NUMBER FOR FIRST   MEASUREMENT
4:13                : LOCATION FOR HEAT FLUX 13, 14, 15
5:1                 : MULTIPLIER
6:0                 : OFFSET

15:P95              : END

16:P86              : SET PORT LOW (DISCONNECT MULTIPLXER)
1:51                : CONTROL PORT NO.1 (CHANNEL 3)

17:P53
1:13                : FIRST INPUT LOCATION (HFT)
2:169.52        : MULTIPLIER CONSTANT
3:0                 : OFFSET
4:183.84        : MULTIPLIER CONSTANT
5:0                 : OFFSET
6:168.58        : MULTIPLIER CONSTANT
7:0                 : OFFSET
8:0                 : MULTIPLIER CONSTANT
9:0                 : OFFSET

18:P92              : IF TIME - OUT DATA INSTRUCTIONS
1:0                 : FLAG SET
2:5                 : TIME DURATION 5 MIN
3:10                : COMMAND
19:P77              : RECORD REAL TIME
1:120               : 0120 DAY HOUR MIN-DISPLAY
20:P78              : DATA STORAGE FORMAT
1:0
21:P71              : AVERAGING
1:15                : 15 CHANNELS AVERAGING
2:1                 : STARTING FROM LOCATION 1
22:P71              : AVERAGING
1:3                 : REPITITIONS
2:26                : STARTING INPUT LOCATION NO
23:P0
```

APPENDIX C: MATLAB Program developed to calculate R-value using the algorithm of simple and dynamic method

```
%clear;
clc;
close all;
format short g

% Data set = 96, 192, 384, 576, 1152 + 1
 % provide the mat file name.
load Wall-1.mat
 % Assign AA to the data "variable" you needto process
AA= SW1P1NI;
 [rows,columns]= size(AA); clear columns
 %---------- Simple Method
 deltat=300;
w = fix(rows/24)*24; AA=AA(1:w,:);
NumD= 4;
Num = w/NumD;
SD1 = 1      ; ED1= Num;
SD2 = ED1+1  ; ED2= Num * 2;
SD3 = ED2 + 1; ED3 = Num * 3;
SD4 = ED3 + 1; ED4  = Num * 4;
Days = [SD1 SD2 SD3 SD4
       ED1 ED2 ED3 ED4]
 q12 =sum(AA(SD1:ED2,3));
C12 = q12/sum(AA(SD1:ED2,1)- AA(SD1:ED2,2));
R12 = 1/C12;
 q34 = sum(AA(SD3:ED4,3));
C34 = q34/sum(AA(SD3:ED4,1)- AA(SD3:ED4,2));
R34 = 1/C34;

 q123 = sum(AA(SD1:ED3,3));
C123 = q123/sum(AA(SD1:ED3,1)- AA(SD1:ED3,2));
R123 = 1/C123;

 q234= sum(AA(SD2:ED4,3));
C234 = q234/sum(AA(SD2:ED4,1)- AA(SD2:ED4,2));
R234 = 1/C234;

 q1234=sum(AA(SD1:ED4,3));
C1234 = q1234/sum(AA(SD1:ED4,1)- AA(SD1:ED4,2));
R1234 = 1/C1234;

 SM= [C12 R12
    C34 R34
    C123 R123
    C234 R234
    C1234 R1234];

 SMNC = [[12 34 123 234 1234]' SM]

% Check applicable conditions
disp('Change(%)     R1324-R123/R1234 (%) =     R34-R12/R34 (%)=')
SMNCC = [abs((R1234-R123)/R1234*100) abs((R34-R12)/R34*100)]

 %pause

% THERMAL RESISTANCE FOR EACH LAYER OF WALL
```

```
% 1 = CEMENT PLASTER WITH SAND 20 mm, 2= CMU HEAVY WT 200 mm, 3= CEMENT
PLASTER WITH SAND 20 mm

 % wall thickness (Tt) = 0.24 m, Sp Heat Capacity (SH) = 1000 (j/kgK), Density (WD) = 2200 kg/m3 (say)
SH = 1000;
WD = 2200;

 R(1) = 0.035;
R(2) = 0.194;
R(3) = 0.035;
R(4)= 0;
R(5)= 0;
Rt = sum(R);

 % SPECIFIC HEAT FOR EACH LAYER
SH1 = 1000;
SH2 = 1000;
SH3 = 1000;
SH4 = 1000;
SH5 = 1000;

 % DENSITY OF LAYER
D1 = 1300;
D2 = 2300;
D3 = 1300;
D4 = 0;
D5 = 0;

% THICKNESS OF EACH LAYER
T(1) = 0.02;
T(2) = 0.20;
T(3) = 0.02;
T(4) = 0;
T(5) = 0;
Tt = sum(T);

 % CALCULATION OF FACTOR C

C(1) = SH1 *D1 *T(1);
C(2) = SH2 *D2 *T(2);
C(3) = SH3 *D3 *T(3);
C(4) = SH4 *D4 *T(4);
C(5) = SH5 *D5 *T(5);
Ct = sum(C);

 % Calaculation of Rik

 Rik(1)=0;
for j=1:3
    Rik(j+1)=Rik(j)+R(j);
end

 % Calaculation of Rek, Change Rek(3) =0, 3 change to number of layers 3,4,5.

Rek(3) = 0;
```

```
for k=1:3-1
    Rek(3-k)=Rek(3-k+1)+R(3-k+1);
end

 % Calaculation of Fik when the wall composition is known

for k=1:3
    Fik(k)=C(k)*((Rek(k)/Rt)+(R(k)^2/(3*(Rt^2))-(Rik(k)*Rek(k)/Rt^2)));
end

 % Calaculation of Fek when the wall composition is known

for k=1:3
    Fek(k)=C(k)*((R(k)/Rt)*(0.167+(Rik(k)+Rek(k)/3*Rt))+(Rik(k)*Rek(k))/Rt^2);
end

% Thermal mass factors of the structures when the wall composition is known

Fi = sum(Fik);
Fe = sum(Fek);

 % Calculation of Avg Temp for Last 24 Hours and First 24 Hours

avif24 = mean(AA(SD1:ED1,2));
avil24 = mean(AA(SD4:ED4,2));
deltaTi = avil24 - avif24;
 avef24 = mean(AA(SD1:ED1,1));
avel24 = mean(AA(SD4:ED4,1));;
deltaTe = avel24 - avef24;

% CF1 is the correction factor to the heat flux when composition of wall is known
CF1=(Fi*deltaTi + Fe*deltaTe)/deltat;
q1234CF1  = q1234 - CF1;

 % Thermal mass factors of the structures when the wall composition is not known

Ca = SH * WD *Tt;
Fin = Ca/3;
Fen = Ca/6;

 % CF2 is the correction factor to the heat flux when composition of wall is Not known

CF2=(Fin*deltaTi + Fen*deltaTe)/deltat;
q1234CF2 = q1234 - CF2;
 E1= abs(q1234CF1 - q1234)/q1234 *100;
E2= abs(q1234CF2 - q1234)/q1234 *100;
Q1234 = [0   q1234   0
        CF1 q1234CF1 E1
        CF2 q1234CF2 E2]
C1234CF1 = q1234CF1/sum(AA(SD1:ED4,1)- AA(SD1:ED4,2));
R1234CF1 = 1/C1234CF1;

display('C , R Corrected with CF1 when composition of wall is known')
[C1234CF1  R1234CF1  abs(C1234CF1-C1234)/C1234*100 abs(R1234CF1-R1234)/R1234*100]
 C1234CF2 = q1234CF2/sum(AA(SD1:ED4,1)- AA(SD1:ED4,2));
```

```
R1234CF2 = 1/C1234CF2;
display('C , R Corrected with CF2, when composition of wall is Not known')
[C1234CF2  R1234CF2 abs(C1234CF2-C1234)/C1234*100 abs(R1234CF2-R1234)/R1234*100]

 % pause
% Prepare Data for using the Dynamic Method
% Do average as per required number of samples AVRI
 % AVRI = 2, 3, 4, 6, 12
% 10 mintues = 2  (576 hr),
% 15 minutes = 3  (384 hr),
% 20 minutes = 4  (288 hr),
% 30 minutes = 6  (192 hr),
% 60 minutes = 12 (96 hr)

 AVRI = 12;
 RSe = mean(reshape(AA(:,1),AVRI,w/AVRI))';
RSi = mean(reshape(AA(:,2),AVRI,w/AVRI))';
RSH = mean(reshape(AA(:,3),AVRI,w/AVRI))';
A=[RSe RSi RSH];
[rows,columns]= size(A); clear columns

% Dynamic Method

deltat= (AVRI * 300)/2;

m=3;
r=3;             %(Constant Ratio between Time constants ususlly between 3 to 10 such that
tow1=r*tow2=r*r*tow3)
N=rows-1;        % number of data points
M=40;            %(15 to 40)
p=N-M;
 Count =0;

 % counts the number of times while tow1 value changes to find the Square Deviation value.

tow1    = deltat/10;
towINTV = 1800;

% Start of Loop to get Minimum Sqaure Deviation

 [Loop,c]= size([deltat/10:towINTV:p*(deltat/2)]'); clear c
 disp('Rrogram is Running, Please Wait Looping for')
disp (Loop);
pause
for tow = deltat/10:towINTV:p*(deltat/2)   % it is best to choose the largest time constant lying in this
range.
 Count=Count+1

 % GET X MATRIX

tow2 = tow/r;
tow3 = tow/(r*r);
beta1= exp(-deltat/tow);  % beta1 is the exponential functions of the time constant tow1.
beta2= exp(-deltat/tow2);
beta3= exp(-deltat/tow3);
```

```
 % Get Xi1, (Te-Ti), A(c1)-A(c2), Done for the last M points of the data set

for i=N-M+1:N
   Xi1(i-N+M)=A(i,1)-A(i,2);
end

 % finds the derivative of N number of data sets for derte = [(Te - Te-1)/deltat ,(A(Rn,C1)-A(Rn-
1,C1)/deltat]

% derti= [(Ti - Ti-1)/deltat, (A(Rn,C2)-A(Rn-1,C2)/deltat]
for i=2:rows
   derte(i-1)=(A(i,1)-A(i-1,1))/deltat;
   derti(i-1)=(A(i,2)-A(i-1,2))/deltat;
end

 % Get Xi2 and Xi3, takes the last M (40) data from the derti and derti array.

for i=N-M+1:N
   Xi2(i-N+M)=derti(i);
   Xi3(i-N+M)=derte(i);
end

 % i varies from N-M+1 to N
% Get Xi4 sigma(j=i-p to i-1) dertj*(1-beta1)*beta1*(i-j) such that gets an array of M elements,
% dertj is derivative of Inside surface temperatures.


Xi4 = zeros(1,M); Xi5 = zeros(1,M);
Xi6 = zeros(1,M); Xi7 = zeros(1,M);
Xi8 = zeros(1,M); Xi9 = zeros(1,M);

for h=1:M
   for i=N-M+1:N
      for j=h:h+(N-M-1)
         var=derti(j)*(1-beta1)*beta1*(i-j);
         Xi4(h)=Xi4(h)+var;

         var=derte(j)*(1-beta1)*beta1*(i-j);
         Xi5(h)=Xi5(h)+var;

         var=derti(j)*(1-beta2)*beta2*(i-j);
         Xi6(h)=Xi6(h)+var;

         var=derte(j)*(1-beta2)*beta2*(i-j);
         Xi7(h)=Xi7(h)+var;

         var=derti(j)*(1-beta3)*beta3*(i-j);
         Xi8(h)=Xi8(h)+var;

         var=derte(j)*(1-beta3)*beta3*(i-j);
         Xi9(h)=Xi9(h)+var;
       end
   end
end

X=[Xi1' Xi2' Xi3' Xi4' Xi5' Xi6' Xi7' Xi8' Xi9'];
```

```
 % Transposing the arrays to get the required X matrix  clear var Xi*

 % Storing the Last M values of the measured Heat flow data A(:,3)

Q  = A(N-M+1:N,3);
 Y  = inv(X'* X);
Zstar  = Y * X'* Q ;
Qstar = X * Zstar;
S2= sum((Q(:,1)-Qstar(:,1)).^2);
%plot([Q Qstar]); pause(1);
RV(Count,:)= [Count S2 tow Zstar'];
QStarall(:,Count)= Qstar;
 F= 1.669127;  % Student t-distribution at P = 0.9, Degree of freedom = 29
%Im = sqrt( (S2 * Y(1,1))/(M-2*m-4) ) * F;
I(Count) = sqrt( (S2 * Y(1,1))/(M-2*m-4) )* F;
 end
 [VV,II] =min(RV(:,2)); clear VV
RR = [RV(II,:)];
CONF= [I(II)];
 Display Results
display('Simple Method')
 Days
SMNC
 % Check applicable conditions
display('Check conditions < 5%     R1324-R123/R1234 (%) =     R34-R12/R34 (%)=')
 SMNCC
display('Q   Q-Corrected and Error%')
Q1234 = [0   q1234   0
        CF1 q1234CF1 E1
        CF2 q1234CF2 E2]
 display('C , R Corrected with CF1 when composition of wall is known and % change')

 [C1234CF1  R1234CF1  abs(C1234CF1-C1234)/C1234*100 abs(R1234CF1-R1234)/R1234*100]
 display('C , R Corrected with CF2 when composition of wall is NOT known and % change')

[C1234CF2  R1234CF2 abs(C1234CF2-C1234)/C1234*100 abs(R1234CF2-R1234)/R1234*100]

 DM = [RV(II,1:4) 1/RV(II,4) CONF]
QStarBest = QStarall(:,II);
clear rows r towINTV h i j II derte derti Count D E F TX S2
disp('Program Ended')
```

APPENDIX D: Thermal Conductance measurement of the Test Wall

Wall composition-1 (FG-A)	CONDUCTANCE
Simple Method (SM)	5.1303 (± 0.0392)
SM with SE / known Composition	5.2218
SM with SE / Unknown Composition	5.2317 (0.2%)
Dynamic Method (Avg 60 Min)	4.4903 (CF 90%)
Time Constant (Avg 60 Min)	10 hr

Wall composition-2 (Exp.P II)	CONDUCTANCE
Simple Method (SM)	0.4915 (± 0.0038)
SM with SE / known Composition	0.4979
SM with SE / Unknown Composition	0.5174 (3.9%)
Dynamic Method (Avg 60 Min)	0.4824 (CF=90%)
Time Constant (Avg 60 Min)	8.6 hr

Wall composition-3 (Ext.P II)	CONDUCTANCE
Simple Method (SM)	0.4473 (± 0.0020)
SM with SE / known Composition	0.4298
SM with SE / Unknown Composition	0.4333 (0.8%)
Dynamic Method (Avg 60 Min)	0.3960(CF 90%)
Time Constant (Avg 60 Min)	12.6 hr

Wall composition-4 (FG-D)	CONDUCTANCE
Simple Method (SM)	0.6184 (± 0.0162)
SM with SE / known Composition	0.6482
SM with SE / Unknown Composition	0.6583 (1.6%)
Dynamic Method (Avg 60 Min)	0.5658 (CF90%)
Time Constant (Avg 60 Min)	8.6 hr

Wall composition-5 (FG-B)	CONDUCTANCE
Simple Method (SM)	2.9056 (± 0.0158)
SM with SE / known Composition	2.9820
SM with SE / Unknown Composition	2.9783 (-0.1%)
Dynamic Method (Avg 60 Min)	2.1612 (CF90%)
Time Constant (Avg 60 Min)	13 hr

Wall composition-4 (FG-MD)	CONDUCTANCE
Simple Method (SM)	0.3552 (± 0.0099)
SM with SE / known Composition	0.3874
SM with SE / Unknown Composition	0.3983 (2.8%)
Dynamic Method (Avg 60 Min)	0.3289 (CF 90%)
Time Constant (Avg 60 Min)	2 hr

Wall composition-5 (Exp.P MI)	CONDUCTANCE
Simple Method (SM)	2.5449 (± 0.0162)
SM with SE / known Composition	2.5627
SM with SE / Unknown Composition	2.5776 (0.6%)
Dynamic Method (Avg 60 Min)	2.1612 (CF90%)
Time Constant (Avg 60 Min)	12 hr

Wall composition-5 (Exp.P MI+)	CONDUCTANCE
Simple Method (SM)	2.7763 (± 0.0159)
SM with SE / known Composition	2.8016
SM with SE / Unknown Composition	2.8196 (0.7%)
Dynamic Method (Avg 60 Min)	2.1612 (CF90%)
Time Constant (Avg 60 Min)	13 hr

Wall composition-5 (Ext.P MI)	CONDUCTANCE
Simple Method (SM)	2.6389 (± 0.0116)
SM with SE / known Composition	2.6180
SM with SE / Unknown Composition	2.6205 (0.1%)
Dynamic Method (Avg 60 Min)	2.3381(CF 90%)
Time Constant (Avg 60 Min)	14.5 hr

Roof	CONDUCTANCE
Simple Method (SM)	0.9949 (± 0.015)
SM with SE / known Composition	0.9926
SM with SE / Unknown Composition	0.9911(-0.2%)
Dynamic Method (Avg 60 Min)	0.6580(CF90%)
Time Constant (Avg 60 Min)	12 hr

VITAE

- Mohammed Abdul Waheed Khan
- Nationality: Indian
- Date of birth: 26th July 1986, Hyderabad, India.
- Received BE (Bachelor of Engineering) Degree in Mechanical Engineering from Osmania University (OU), Hyderabad, India in May 2007.
- Joined Architectural Engineering Department at KFUPM, Saudi Arabia as a Research Assistant in October 2008.
- Completed MS Degree Requirements in Architectural Engineering Departments at KFUPM in May, 2011.
- Email: mawaheedkhan@gmail.com (or) waheed@kfupm.edu.sa
- Mobile: (00966)-530058904 or (0091)- 9963626667
- Present Address: P.O. Box: 8586, Dhahran, KFUPM 31261, Saudi Arabia.
- Permanent Address: 12-2-831/405, Peace Plaza, Mehdipatnam, Hyderabad, Andhra Pradesh, India-500028.